Obsercontii Esten J mc K.H.T. circulate as appropriate H.S.

NASA Technical Memorandum 86662

ESEARCH AND TECHNOLOGY

NUAL REPORT 1984

Comp. Aero Group
Applied Aero Tech.

es Research Center
ett Field, California

luation of the Tilt Rotor Concept: The XV-15's Role. Future Requirements and Roles of Computers in Aerodynamic
puting Viscous Flows. A Simple Method for Estimating Minimum Autorotative Descent Rate of Single Rotor Helic
and Dynamic Stability Analysis of the Space Shuttle Vehicle-Orbiter. Comparison of Measured and Calculated Helic
npulsive Noise. Effect of High Lift Flap Systems on the Conceptual Design of a 1985 Short-Haul Commercial STO
on Multicyclic Control by Swashplate Oscillation. Low-Speed Aerodynamic Characteristics of
Model at High Angles of Attack and Sideslip. Generalization of Huffman Coding to Minimize
w. Optimum Horizontal Guidance Techniques for Aircraft. Quasi-Optimal Control of a Moving-
ce and Control for Investigating Aircraft Noise-Impact Reduction. Trajectory Module of the N
Aircraft Synthesis Program ACSYNT. A Flight Investigation of the Stability, Control, and Handli
Augmented Jet Flap STOL Airplane. G-Seat System Step Input and Sinusoidal Response Characteristic
Cost/Performance Measurement System on a Research Aircraft Project. Application of Special-Purpose D
ircraft Real-Time Simulation. Wing Analysis Using a Transonic Potential Flow Compu
Hardware Analysis. Phenomenological Aspects of Quasi-Stationary Controlled and U
low Separations. A Method for the Analysis of the Benefits and Costs for Aeronau
CTOL Aircraft Research. Closed-Form Equations for the Lift, Drag, and Pitching-M
ng Schemes. High Angle of Inc
Maneuverable Transonic
from Four Helicopt
nalysis. Multi-Calculation Rate
he Three Stage Compressor
-Ratio Propulsion System
a Harrier V/STOL Resea
tersection Problem. Roto
Model Volume 2: Compu
Rotor in a Wind Tunnel. Fa
s of Advanced Turboprop Trans
, Applied to a Helicopter in the Hov
Automatic and Manual Flight Director Land
V-15 Tilt Rotor Aircraft in Helicopter Mode. Application of Advanced Technologies to Small Short-Haul A
Large Scale Swivel Nozzle Thrust Deflector. High Angle Canard Missile Test in the Ames 11-Foot Tra
Study of Commuter Airplane Design Optimization. Application of Second-Order Turbulent Modeling to
Radiated Aerodynamic Sound. Infrastructure Dynamics: A Selected Bibliography. The Effect of Tip Vorte
Helicopter Noise Due to Blade/Vortex Interaction. A Study of Test Section Configuration for Shock Tube Testi
Airfoils. A Mach Line Panel Method for Computing the Linearized Supersonic Flow Over Planar Wings. An A
on of Short Haul Air Transportation in the Southeastern United States. Development and Flight Tests of a Ka
Navigation During Terminal Area and Landing Operations. Prop-Fan Data Support Study. Study to Determine
onal and Performance Criteria for STOL Aircraft Operating in Low Visibility Conditions. Executive Summary: Re
of an Intra-Regional Air Service in the Bay Area and a Technology Assessment of Transportati
hnology Assessment of Transportation System Investments. Requirements for Regional Short
on of a Flight Program to Determine Neighborhood Reactions to Small Transport Aircraft. A
ing Response at Subsonic and Transonic Speeds: Phase 1: F-111A Flight Data Analysis. Volu
pproach, Results and Conclusions. An Investigation of Wing Buffeting Response at Subsonic
Flight Data Analysis. Volume 2: Plotted Power Spectra. An Investigation of Wing Buffeting Flow over D
ic Speeds. Phase 2: F-111A Flight Data Analysis. Volume 3: Tabulated Power Spectra. Wings with Sha
eared Flow. Pioneer Venus Spacecraft Charging Model. Abstracts for the P... Experiment f
ses. Effects of Mass Addition on Blunt-Body Boundary-Layer Transition and Heat Transfer. Semi-Span W
tudy. Part 2: Broadband Antenna Techniques Survey. Cable Strumming Suppression. Superso
merical Methods to Study Complex Flows at High Reynolds Numbers. ... Correcting Approx
Venus. The Role of Time-History Effects in the Formulation of the Aerodynamics of Aircraft Finite Differe
ements for Computational Aerodynamics. Computational Aerodynamics and the Numerical Effects on C
hree-Dimensional Computational Aerodynamics in the 1980's. Numerical A... ual. Torqu
y, Executive Summary. Preliminary Study for a Numerical Aerodynamic Simula... NASA/ESA C
Fluid Interaction with Spinning Toroidal Tanks. Theoretical Contamination of Cryogenic Preload in a L
y and Toxicity Studies of Candidate Aircraft Passenger Seat Materials. Calculated Rate the Iterative Co
Yields Cl + O 2 Between 220 and 1000 Deg K. On the Period of the Coherent Structure in Sulfur. Status
ers at ... Numbers. Simple Torsion Test for Shear Moduli Determination of Orthotropic Composites. Future Prosp
of an ... oil. A Review of NASA-Sponsored Technology Assessment Projects. Lagrangian Bimolecular Reaction
of Invis... ble Flows. Engineering Tests of the C-141 Telescope. Calculation of Supersonic Viscous Properties of
acteristics of an 0.075-Scale F-15 Airplane Model at High Angles of Attack and Sideslip. Response at Subsonic and Transoni
sting with Splitter Plates. Phenomenological Aspects of Quasi-Stationary Controlled and An Investigation of Wing Buffeti

NASA

This annual report illustrates selected achievements at the Ames-Moffett and Ames-Dryden sites of Ames Research Center. The contents illustrate the challenging work that has been accomplished in the past year in the areas of Aeronautics, Life Science, and Space Science.

If you desire further information on any of the Ames research and technology programs, please write to the Chief Scientist, Dr. Jack Nielsen, MS 200-1A, NASA Ames Research Center, Moffett Field, CA 94035, or call the investigator listed in the report.

Wm F. Ballhaus, Jr.

W. F. Ballhaus, Jr.
Director

Page intentionally left blank

Page intentionally left blank

Table of Contents

NOTE: For additional information on any item, the Ames Staff member(s) named at the end of each item may be contacted. To call Ames Moffett staff (where a four-digit extension number is indicated), commercial telephone users should dial 415-694- followed by the extension number (users with access to the Federal Telecommunications System (FTS) should dial 464- followed by the extension number). To call Ames Dryden staff (where a four-digit extension number is indicated), commercial telephone users should dial 805-258-3311 and ask for the extension (dial directly on FTS, 961- followed by the extension number).

Page intentionally left blank

Page intentionally left blank

Index

Aeronautics

Title	Author	Ames Moffett/ Ames Dryden	Organizational Division	Headquarters Program Office
Automatic Flight Control	S. Sastry M. Athans R. Su L. Hunt G. Meyer	Ames Moffett	Flight Systems and Simulation Research	OAST—RC
Motion and Visual Cue Requirements in Flight Simulation	R. Bray	Ames Moffett	Flight Systems and Simulation Research	OAST—RC
Certification Criteria for VTOL Aircraft	J. Lebacqz	Ames Moffett	Flight Systems and Simulation Research	OAST—RF,RC
VTOL Controls and Displays for Shipboard Operations	G. Farris V. Merrick	Ames Moffett	Flight Systems and Simulation Research	OAST—RC,RF
A Model-Following Control System for Helicopters	K. Hilbert	Ames Moffett	Flight Systems and Simulation Research	OAST—RF
Helicopter Air Combat Simulation	M. Lewis	Ames Moffett	Flight Systems and Simulation Research	OAST—RF
Modern Design Methods for Rotorcraft Flight Control	W. Hindson	Ames Moffett	Flight Systems and Simulation Research	OAST—RF
Ultrareliable Fault-Tolerant Control Systems (UFTCS)	L. Webster	Ames Moffett	Flight Systems and Simulation Research	OAST—RC
Development of Computer-Generated Imagery for Flight Simulation	L. Tweten	Ames Moffett	Flight Systems and Simulation Research	OAST—RC
Air Traffic Flow Management	H. Erzberger L. Tobias	Ames Moffett	Flight Systems and Simulation Research	OAST—RC
Digital Flight Control System Verification Laboratory (DFCSVL)	D. Doane J. Saito	Ames Moffett	Flight Systems and Simulation Research	OAST—RC
Severe Turbulence Encounters	R. Wingrove	Ames Moffett	Flight Systems and Simulation Research	OAST—RC
Rotorcraft Cockpit Intelligence Laboratory	G. Callas B. Nedell	Ames Moffett	Flight Systems and Simulation Research	OAST—RC
Helicopter Satellite-Based Navigation	F. Edwards	Ames Moffett	Flight Systems and Simulation Research	OAST—RC
NASA/FAA Helicopter Microwave Landing System Curved Path Flight Investigation	H. Swenson	Ames Moffett	Flight Systems and Simulation Research	OAST—RC
Helicopter Airborne Radar Landing Guidance	G. Clary T. Davis	Ames Moffett	Flight Systems and Simulation Research	OAST—RC
Lull/Swell Guidance for Shipboard Landing Operations	C. Paulk, Jr.	Ames Moffett	Flight Systems and Simulation Research	OAST—RC,RF
A New Family of Composite Matrix Resins	D. Kourtides	Ames Moffett	Chemical Research Projects Office	OAST—RM
Fire Resistant Insulation	R. Altman	Ames Moffett	Chemical Research Projects Office	OAST—RC
Computer Code for Processing Control of Filament Wound Case	D. Cagliostro	Ames Moffett	Thermo- and Gas-Dynamics	OSF—M
Measurements of Fluctuating Temperatures in a Turbulent Flow Using Laser-Induced Fluorescence	R. McKenzie	Ames Moffett	Thermo- and Gas-Dynamics	OAST—RC
Three-Dimensional Turbulent Flows with Massive Separation	M. Kussoy	Ames Moffett	Thermo- and Gas-Dynamics	OAST—RF
Airfoil Measurements in the New Test Leg (HRC-II) of the High Reynolds Number Facility	J. McDevitt	Ames Moffett	Thermo- and Gas-Dynamics	OAST—RF
Application of a Three-Dimensional LDV to Turbulent Flow	D. Driver	Ames Moffett	Thermo- and Gas-Dynamics	OAST—RF
Computer Simulation of Rotating Stall	P. Spalart	Ames Moffett	Thermo- and Gas-Dynamics	OAST—RF
Adaptive-Grid Method for Fluid-Flow Problems	G. Deiwert	Ames Moffett	Thermo- and Gas-Dynamics	OAST—RF
Design of Diagnostic Probes for Combustion	R. Jaffe	Ames Moffett	Thermo- and Gas-Dynamics	OAST—RF

Title	Author	Ames Moffett/ Ames Dryden	Organizational Division	Headquarters Program Office
Numerical Solution of the Navier-Stokes Equations for Transonic Wing Flow Fields	T. Holst	Ames Moffett	Thermo- and Gas-Dynamics	OAST–RF
Numerical Minimization of Drag for Wings in the Transonic Speed Regime	T. Holst G. Cosentino	Ames Moffett	Thermo- and Gas-Dynamics	OAST–RF
Fast Simulation of Separated Transonic Airfoil Flow	W. Van Dalsem	Ames Moffett	Thermo- and Gas-Dynamics	OAST–RF
Computational Aerothermodynamics	D. Chaussee	Ames Moffett	Thermo- and Gas-Dynamics	OAST–RF
Space Shuttle Main Engine Flow Analysis	D. Kwak	Ames Moffett	Thermo- and Gas-Dynamics	OAST–RF
Transonic Aeroelastic Analysis	P. Goorjian P. Guruswamy	Ames Moffett	Thermo- and Gas-Dynamics	OAST–RF
Atomistic Simulation of Materials	D. Cooper	Ames Moffett	Thermo- and Gas-Dynamics	OAST–RM
Properties of Molecules and Atomic Clusters	D. Cooper R. Jaffe	Ames Moffett	Thermo- and Gas-Dynamics	OAST–RM
Aero-Assisted Orbital Transfer Vehicles	J. Howe	Ames Moffett	Thermo- and Gas-Dynamics	OAST–RF
Space Shuttle Thermal Protection System	H. Goldstein	Ames Moffett	Thermo- and Gas-Dynamics	OAST–RM
Use of Concurrent Computer Architectures to Solve Computational Fluid Dynamics Problems	K. Stevens, Jr.	Ames Moffett	Computer Systems	OAST–RC
An Aero De-icing Device Using Electro-Expulsive Forces	R. Lee L. Haslim	Ames Moffett	Systems Engineering	OAST–RF
Accelerated Characterizing of the Long-Term Mechanical Behavior of Fiber Reinforced Plastics	H. Nelson	Ames Moffett	Systems Engineering	OAST–RM
Three-Dimensional Adaptive Wall Wind Tunnel	P. Luna	Ames Moffett	Systems Engineering	OAST–RF
Dynamic Stall on Airfoils Oscillating in Pitch	C. Sticht	Ames Moffett	Systems Engineering	OAST–RF
Circulation Control Lift Generation Experiment Hardware	T. Panontin	Ames Moffett	Systems Engineering	OAST–RF
Surface Reaction Kinetics: Hydrogen on Iron	M. Shanabarger H. Nelson	Ames Moffett	Systems Engineering	OAST–RM
Aviation Safety Reporting System	W. Reynard	Ames Moffett	Aero-Space Human Factors Research	OAST–RC
JetStar Laminar Flow Control-Leading Edge Flight Test	D. Fisher	Ames Dryden	Research Engineering	OAST–RX
Axisymmetric Base Drag Reduction Study	S. Powers	Ames Dryden	Research Engineering	OAST–RF
Airdata Enhancement via State Reconstruction Techniques	S. Whitmore	Ames Dryden	Research Engineering	OAST–RX
F-14 Variable Sweep Transition Flight Experiment (VSTFE) Basic Wing Pressure Distributions	B. Meyer	Ames Dryden	Research Engineering	OAST–RF
Laser-Enhanced, Water-Tunnel Flow Visualization	C. Beckner R. Curry	Ames Dryden	Research Engineering	OAST–RX
Airplane Performance Modeling	P. Redin	Ames Dryden	Research Engineering	OAST–RX
Adaptive Engine Control System Research	F. Burcham	Ames Dryden	Research Engineering	OAST–RX
Flight Investigation of Digital Engine Control Fault Detection and Accommodation	L. Myers	Ames Dryden	Research Engineering	OAST–RX
Integrated Sensor System	D. Wilner	Ames Dryden	Research Engineering	OAST–RF
HiMAT Composite Structural Analysis	W. Lokos	Ames Dryden	Research Engineering	OAST–RM
Hot Structures Research	W. L. Ko	Ames Dryden	Research Engineering	OAST–RM
Numerical Methods Development in Structures and Dynamics Analysis	K. Gupta	Ames Dryden	Research Engineering	OAST–RM

Life Science

Preliminary Experiment Results from US/USSR Biosatellite	E. Gomersall	Ames Moffett	Biosystems	OSSA–EB
Vestibular Research Facility	R. Mah	Ames Moffett	Biosystems	OSSA–EB
Stereotaxic Microelectrode Drive	J. Kishiyama	Ames Moffett	Biosystems	OSSA–EB
Spacelab 3	C. Schatte	Ames Moffett	Biosystems	OSSA–EB

Title	Author	Ames Moffett/ Ames Dryden	Organizational Division	Headquarters Program Office
Man-Vehicle Systems Research Facility	F. Styles	Ames Moffett	Aero-Space Human Factors Research	OAST—RC
Human Motion Sensor	A. Watson A. Ahumada	Ames Moffett	Aero-Space Human Factors Research	OAST—RC
Investigating Growth Factors to Alleviate Muscle Atrophy in Spaceflight	S. Ellis	Ames Moffett	Biomedical Research	OSSA—EB
Simulated Weightlessness and Female Astronauts	J. Danellis	Ames Moffett	Biomedical Research	OSSA—EB
Psychophysiology Facility for Biofeedback Training and the Study of Motion Sickness	P. Cowings	Ames Moffett	Biomedical Research	OSSA—EB
Echocardiography for Shuttle Crews	D. Goldwater	Ames Moffett	Biomedical Research	OSSA—EB
Student Shuttle Involvement Project (SSIP)	E. Holton	Ames Moffett	Biomedical Research	OSF—MC
Hot Atom Chemistry and the Production of Organic Compounds in Planetary Atmospheres	S. Chang T. Scattergood	Ames Moffett	Extraterrestrial Research	OSSA—EB
Satellite Estimation of Forest-Leaf Area	D. Peterson	Ames Moffett	Extraterrestrial Research	OSSA—EB
Remote Sensing Techniques for Waste Disposal Impact Assessment	E. Horn	Ames Moffett	Extraterrestrial Research	OSSA—EE
Gas Chromatographic Separations of Atmospheric Gases Using Custom-Made Porous Polymers	G. Pollack	Ames Moffett	Extraterrestrial Research	OSSA—EB
Simple and Effective Modulator for Multiplex Gas Chromatography	J. Phillips	Ames Moffett	Extraterrestrial Research	OSSA—EB
The Multichannel Spectrum Analyzer	B. Oliver	Ames Moffett	Extraterrestrial Research	OSSA—EB

Space Science and Applications

Testing of Cryogenically Cooled Silica Mirror Mounts	R. Melugin	Ames Moffett	Space Sciences	OAST—RM
Development of Lightweight Mirrors for Space	R. Melugin	Ames Moffett	Space Sciences	OAST—RM
Bolometers Cooled by Adiabatic Demagnetization	T. Roellig	Ames Moffett	Space Sciences	OAST—RM
Passive Orbital Disconnect Strut	P. Kittel	Ames Moffett	Space Sciences	OAST—RC
Astronomical Demonstration of Infrared CID Technology	J. Goebel C. McCreight	Ames Moffett	Space Sciences	OAST—RC
Optical Information Processing	J. Goebel	Ames Moffett	Space Sciences	OAST—RC
Study of the Radiative Effects of the Arctic Haze	F. Valero T. Ackerman	Ames Moffett	Space Sciences	OSSA—EE
El Chichon Aerosol Evolution	K. Snetsinger	Ames Moffett	Space Sciences	OSSA—EE
Models of Venus' Atmosphere Structure from the Surface to 100 Kilometers Altitude	A. Seiff	Ames Moffett	Space Sciences	OSSA—EL
Dynamics of the Venus Ionosphere	R. Whitten	Ames Moffett	Space Sciences	OSSA—EL
Planetary Lightning Studies	W. Borucki	Ames Moffett	Space Sciences	OSSA—EL,EB
Photometric Search for Other Solar Systems	W. Borucki J. Scargle D. Black	Ames Moffett	Space Sciences	OSSA—EL
Atmospheric Evolution Studies	J. Kasting	Ames Moffett	Space Sciences	OSSA—EL,EB
Cryogenic Grating Spectrometer	E. Erickson	Ames Moffett	Space Sciences	OSSA—EZ
Reflecting-Layer Model of Thick Rough Films Developed for SIRTF	S. Smith	Ames Moffett	Space Sciences	OSSA—EZ
Planetary Detection Studies	J. Scargle	Ames Moffett	Space Sciences	OSSA—EL
Secondary Mirror Chopper for the Space Infrared Telescope Facility (SIRTF)	M. Dix L. Salerno	Ames Moffett	Space Sciences	OSSA—EZ
Future Data Systems Concepts (Network Simulation and Analysis)	T. Grant	Ames Moffett	Information Sciences	OAST—RC
Spatial, Spectral and Radiometric Resolution Affect Classification Accuracy of Satellite Imagery	R. Wrigley	Ames Moffett	Extraterrestrial Research	OSSA—EE

Aeronautics

PAN AIR Development and Applications

PAN AIR currently solves the linear Prandtl-Glauert equation for subsonic or supersonic flow about complete configurations. As part of the PAN AIR improvements contract with the Boeing Company, streamline tracing and a more robust implementation of the Kutta condition were incorporated in the code during FY84.

Applications in FY84 included the proposed F-8/oblique-wing demonstrator aircraft, a high-lift transport wing with 5-element partial-span flaps, and the B-1 bomber.

It was discovered that nonlinear vortex lift generated at high angles of attack by strake-like, low-aspect wings can be estimated with PAN AIR. Shown in figure 1 is an aspect ratio 0.2 rectangular wing at 20° angle of attack. The PAN AIR model has vorticity being shed from the wing side edges, as well as from the trailing edge. The side-edge vorticity shedding causes the spiraling streamline pattern and the nonlinear vortex lift. For the model shown, PAN AIR predicts a nonlinear lift increment that is 2.9 times the linear value (obtained without the side-edge vorticity shedding). Experimental results give a nonlinear lift increment that is 3.6 times the linear value. Thus, the PAN AIR model is picking up about 80% of the large nonlinear lift increment.

Combining PAN AIR's higher-order source and doublet panels with a rectangular field grid allows transonic flow with shocks to be calculated. This has been demonstrated previously in two dimensions. The approach eliminates the body-fitted grid problem, and is now being extended to three dimensions through a two-year contract with the Boeing Company. The goal is to demonstrate a test-bed version of PAN AIR that will solve the nonlinear full-potential equation for transonic flow about complete, realistic aircraft. The initial 3-D transonic result, shown in figure 2, is for an AR-6 rectangular wing having a 12% thick biconvex airfoil. The somewhat distorted upper-surface pressure near the leading edge is due to modeling the surface with linearized boundary conditions.

(L. Erickson, Ext. 6216)

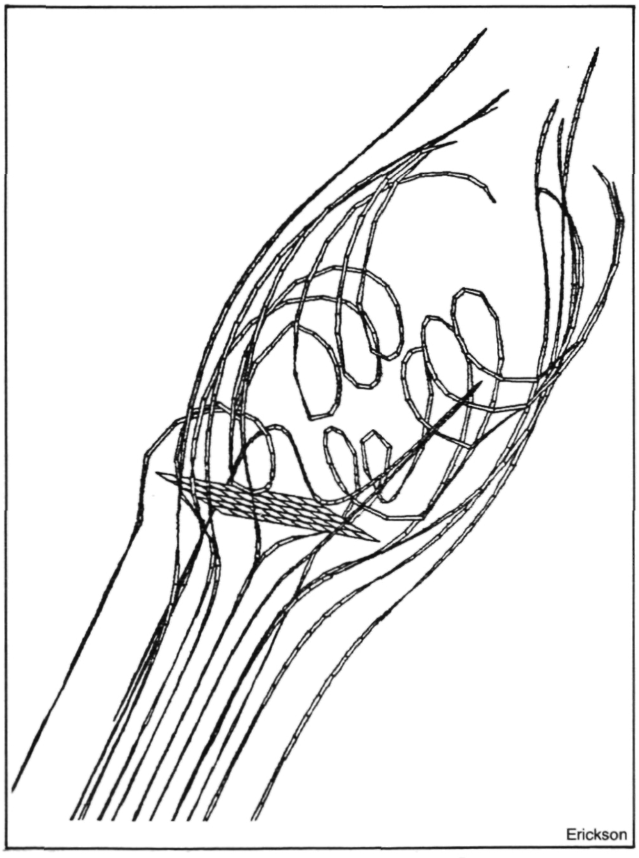

AR = 0.2 rectangular wing at α = 20°, M_∞ = 0.2

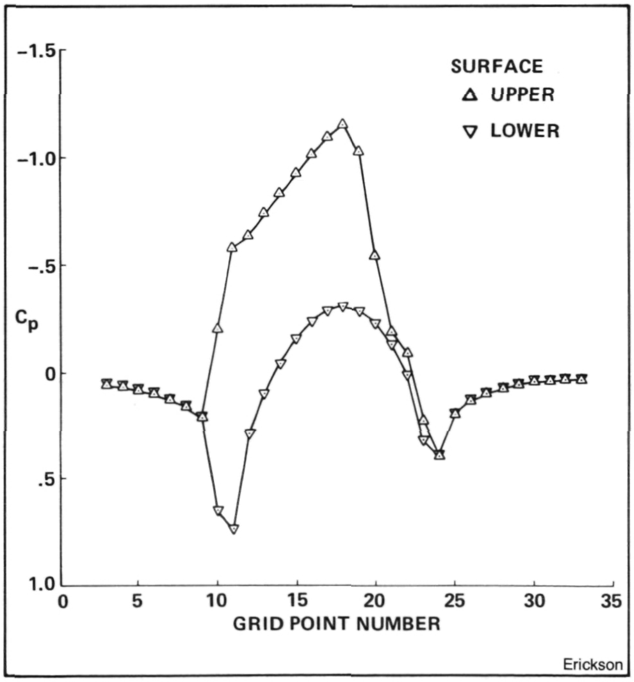

Transonic PAN AIR computed pressure distribution at mid-span of AR = 6 rectangular wing having biconvex airfoil between grid points 10½ and 23½ : M = 0.75, α = 5 deg.

Wind Tunnel Tests Using Two New Rotary-Balance Apparatus

The first test of the new Ames Large-Scale Rotary-Balance Apparatus has recently been completed in the 12-Foot Pressure Wind Tunnel. This unique apparatus was developed to measure the aerodynamics of wind-tunnel models while undergoing a spin motion at high angles of attack and sideslip, and over a wide range of Reynolds numbers. The principal purpose of the test was to verify the performance of the new apparatus in the wind tunnel, and to document the aerodynamics of a 5% scale F-15 model (actually a replica of the NASA Ames/Dryden F-15 Spin Research Vehicle), and a T-tail general aviation model of interest to Langley Research Center. The data from the F-15 model will be used in part to compare with data from free-flight spin tests of the SRV aircraft at Dryden to assess the ability to predict spin motions with wind-tunnel rotary-balance aerodynamic data. Data from the general aviation model will be used by Langley to clarify what are believed to be Reynolds number effects in the discrepancies between spin tunnel and rotary-balance data at low Reynolds numbers and full-scale aircraft spin motions.

The first test of the new Ames Small-Scale Rotary-Balance Apparatus has been carried out successfully in the Ames 6- by 6-Foot Supersonic Wind Tunnel. The aerodynamic characteristics of an F-16-like research model (Standard Dynamics Model) and a fuselage forebody shape were obtained for the vehicles in a steady spin or coning motion. These measurements complement forced-oscillation measurements recently obtained on the SDM at the National Aeronautical Establishment in Ottawa, and provide a means for performing an internal check of the aerodynamic math modeling ideas proposed by researchers at Ames.

Malcolm/Schiff

F-15 Spin Research Vehicle mounted on the Ames Large-Scale Rotary Balance Apparatus in the 12-Foot Pressure Wind Tunnel

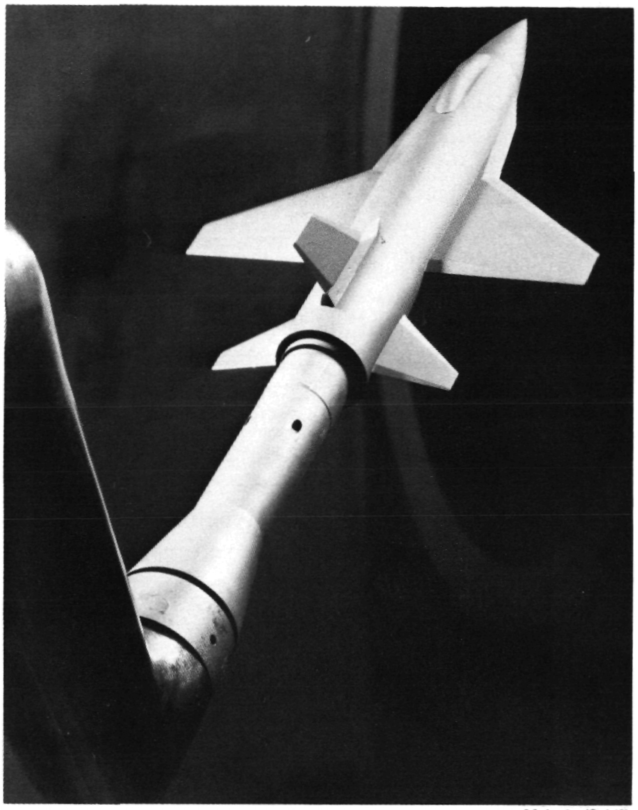

Malcolm/Schiff

Standard Dynamics Model mounted on the Ames Small-Scale Rotary-Balance Apparatus in the 6- by 6-Foot Supersonic Wind Tunnel

(G. Malcolm and L. Schiff, Ext. 5836)

Computer Graphics in Aerodynamic Research

Computer graphics, an important tool for aerodynamic research at Ames, is used daily to display geometry, theoretical predictions, and experimental results. An optical memory disc recorder (OMDR) is currently being used to efficiently store the large number of computer-generated images in video format.

The OMDR uses laser technology to record up to 15,400 frames on a single 200 mm video disc.

Its rapid access (less than 0.5 sec) to any frame on the disc allows the researcher to quickly compare different pictures. The user can control the OMDR manually or with a computer to record, to search for a particular frame, or to display a sequence of frames in forward or reverse at speeds from 30 to 0.33 frames per sec.

A database was developed that contains information about the frames that were recorded on the video disc. This was an important procedure since there could be 15,400 frames each containing different information. Software was developed to allow the user to select a picture or an animation sequence from the database and then instruct the OMDR to display it on a monitor.

The OMDR's ability to record and display animation sequences at far less cost than making a movie with film, makes it a unique research tool. Animation provides the researcher the ability to view spatial or time-dependent phenomena, and to gain some insight to a problem that might not be obvious from studying individual pictures. Some examples where the OMDR was used are: aircraft aerodynamic characteristics that change with different flow-field conditions; aircraft configuration optimization processes; and streamlines, electromagnetic fields, and other flow field phenomena.

(F. Enomoto and M. Madson, Ext. 6133/6010)

Prop-Fan Installation Aerodynamics

Tests to define the installed efficiency potential of wing-mounted, single-rotation, prop-fan powerplants have been completed in the ARC 14-Foot Transonic Wind Tunnel. The present test program focused on a contoured over-the-wing (OTW) nacelle design integrated with supercritical wing and slipstream to minimize the strong viscous interactions encountered with simpler designs in previous tests. Such interactions, which cannot be determined with 3-D computational analysis, can result in unacceptable high drag penalties. Fortunately, the use of flow diagnostic techniques has offered clues leading to configuration improvement.

Powered performance data from the contoured OTW nacelle just tested are presently being analyzed. Preliminary results for the prop-off version indicate that the new nacelle contours derived from incompressible theory are essentially correct.

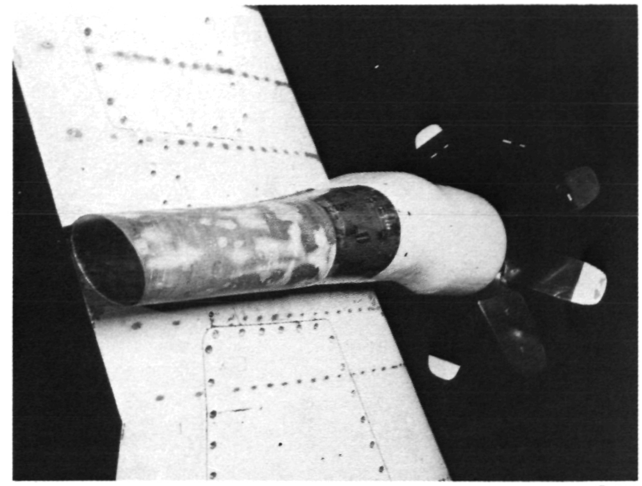

Smith

Turboprop model over the wing nacelle with tailpipe extension

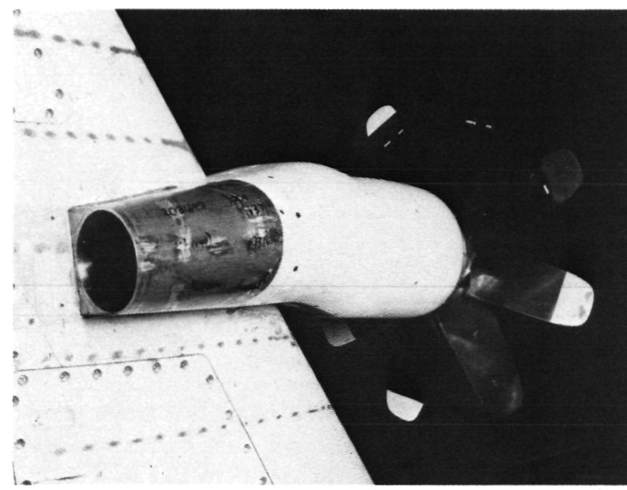

Smith

Turboprop model over the wing nacelle without tailpipe extension

In previous tests, surprisingly low slipstream interference with the wing flow-field was observed when the basic wing/nacelle flow was fully attached. This led to the supposition that the wing acted as a guide vane to convert some of the slipstream swirl momentum to useful thrust. To investigate this possibility, a wake survey apparatus was set up in the slipstream behind the model. Surveys of the propeller slipstream were then made at Mach numbers from 0.6 to 0.8 in regions above and behind the wing. Results of these tests are expected to verify and quantitatively define the swirl conversion process.

(R. Smith, Ext. 6272)

Oblique Wing Research

NASA has studied oblique wing technology since the 1950s and has found that oblique wings have advantages for many aircraft missions, both military and civilian. For missions that require both long subsonic range and/or endurance and a good supersonic dash capability, the oblique wing designs have lower wave drag, lower structural weight, and reduced storage plan area when compared with other variable geometry configurations. The advantages have been confirmed by analytic studies, wind tunnel tests, and lightweight aircraft flight tests. These features have potential for Navy fleet air defense missions where spotting range, endurance, and dash speed are important factors. As yet, no operational vehicle has been developed due to the risk inherent in such a departure from conventional design practice.

During the past year the NASA and the Navy have agreed to conduct a flight test program to develop the technology for oblique wings and verify that such a concept provides a versatile and efficient aircraft. NASA has conducted a feasibility study to modify the NASA Digital Fly-by-Wire F8 research aircraft for an oblique wing. An aircraft model was then tested in the 11- by 11-Foot Wind Tunnel and several computational analyses have shown that the oblique wing concept has potential for performance improvement in several important areas. A phased program to design and test the oblique wing F8 has been proposed as a new initiative for a research airplane that is expected to fly in 1989.

(T. Gregory, Ext. 5881)

Wind Tunnel for Studies of Turbulent Boundary Layer Control

A small-scale research wind tunnel has been constructed and qualified to provide a highly two-dimensional flow with low free-stream turbulence for basic research into boundary layer turbulence structure and control. A dedicated minicomputer data acquisition system with software for experiment control, on-line data reduction, and graphics has also been developed to facilitate the research.

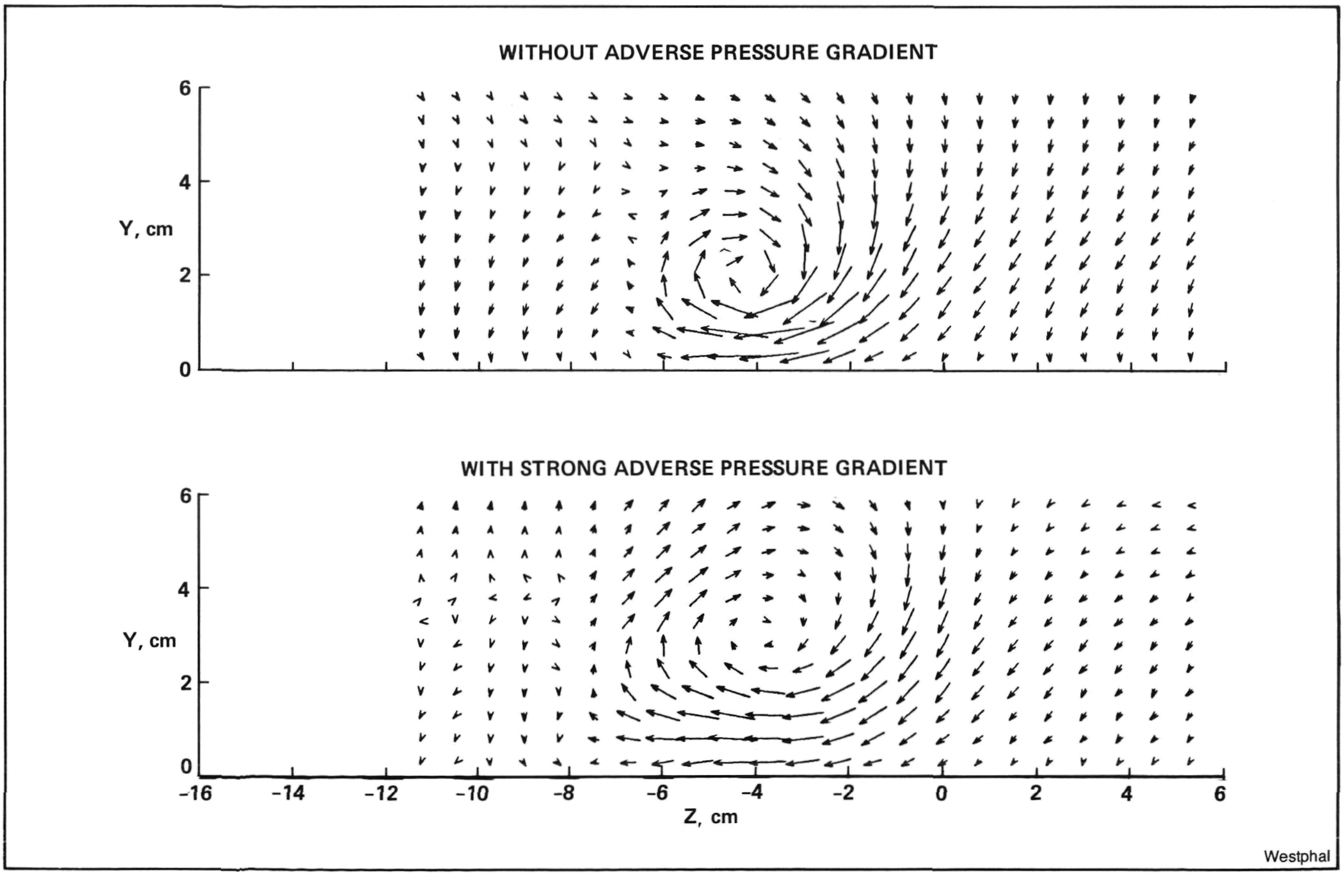

Crossflow plane velocity vector flow patterns

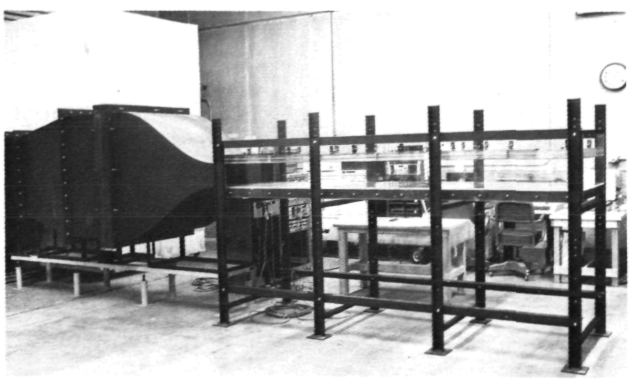

Boundary layer wind tunnel

Longitudinal vortices at moderate angles of attack are often introduced to control boundary layer separation on the suction surface of airfoils. Similar vortex/boundary layer interaction occurs unsteadily over helicopter blades due to strakes or leading edge extensions. In all cases, the interaction involves a vortex and turbulent boundary layer in the presence of adverse pressure gradient.

Initial experiments were performed during 1984 to examine the effect of adverse pressure gradient on a single streamwise vortex imbedded within a turbulent boundary layer. Four-hole pressure data, crossed hot-wire anemometers, and interferometric surface oil flow visualization were used. Crossflow (Y-Z) plane velocity vector flow patterns show that the effect of the imposed adverse pressure gradient is to enlarge vortex core diameter, move the vortex away from the surface, and to attenuate circulation. Other quantities compared include the surface flow angles and skin friction, turbulence Reynolds stresses, and mean vorticity components.

(R. Westphal, Ext. 5856)

Unsteady Boundary Layer Wind Tunnel

An unique unsteady boundary layer wind tunnel has been constructed which will permit detailed analysis of the effects of free-stream unsteadiness on laminar and turbulent boundary layers. This especially designed unsteady flow tunnel will permit investigation of changes in the character of the boundary layer due to unsteadiness, with emphasis on near-wall behavior, and changes in turbulence structure.

The unsteady flow in this tunnel is created by oscillating a tapered wedge within a "choked" nozzle. The exit of this tunnel is connected to a large evacuation compressor which maintains sufficient suction to induce sonic velocity in the nozzle which is located in the oscillator section of the tunnel. When sonic velocity is reached in a convergent-divergent nozzle, no further increase in mass flow can occur; the total mass flow through the system is governed by the area of the nozzle at this minimum area location. This fact is used in the present design to create an oscillating free-stream flow – a wedge is sinusoidally moved in and out of this sonic throat – continuously changing the cross-sectional area and thereby inducing an oscillatory velocity change in the tunnel test section.

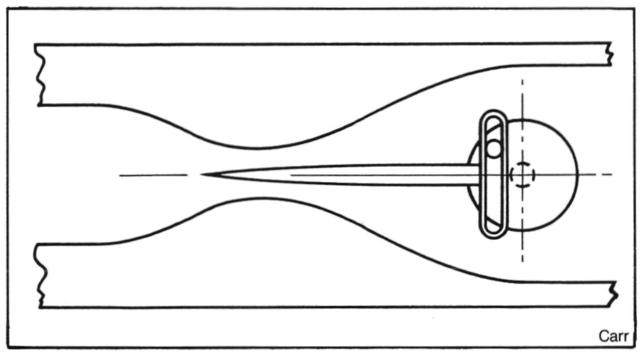

The oscillating flow mechanism

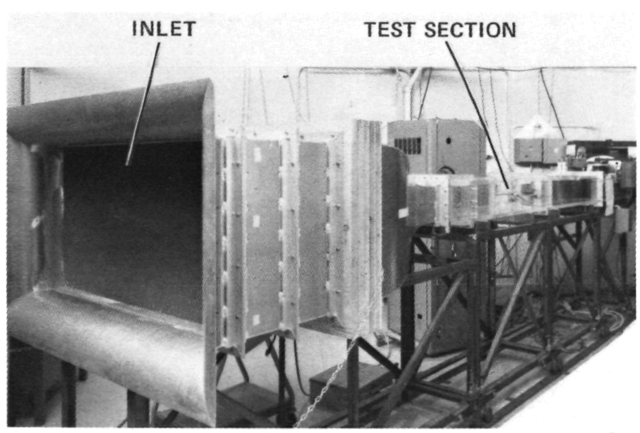

Unsteady boundary layer tunnel

A major benefit of this technique is that there is no up-stream propagation of noise and other disturbances caused by the oscillator mechanism, since no sound can pass through the sonic velocity of the choked nozzle. This results in exceptionally high quality flow in the test section, containing little or no higher harmonic content.

(L. Carr, Ext. 6396)

Advanced Helicopter Airfoils

Airfoils for high-speed helicopters must function well over a wide range of flow regimes for every revolution of the rotor blade. A recently developed program for transonic airfoil design-by-optimization has been successfully applied to the problem of reducing drag under typical advancing-blade conditions, while preserving the high-lift capability required on the retreating blade. Redesign of the Ames-01 airfoil was accomplished with FL06QNM which consisted of a transonic full-potential analysis code coupled with a nonlinear optimization routine. This program permits simultaneous consideration of the computed flow at three distinct design points. The resulting design was refined using a boundary layer code and another new program, PROFILE, which permits constrained manipulation of an airfoil's curvature distribution and thickness.

Both the Ames-01 airfoil and the new Ames-03 airfoil were tested in the Ohio State University transonic airfoil tunnel. The result of the tests indicated that the design goals were largely achieved; the drag divergence Mach number of the new section was increased by about 0.01, with substantial improvement in the drag level at lower Mach numbers as well. The "drag creep" exhibited by the Ames-01 airfoil was eliminated, while the maximum lift coefficient, pitching moment, and section thickness were essentially unchanged.

Aerodynamically, the new Ames-03 airfoil is comparable to the best current designs. While no single measure of merit is conclusive for rotor airfoils, comparison of the maximum lift coefficient at low speed vs the Mach number at which drag begins to rise, indicates that the Ames-03 extends the feasible performance envelope of low pitching moment rotor airfoils. It is also noteworthy that the new airfoil is thicker (t/c = 10%) than its high-speed/high-lift companions. This offers structural advantages since, for a given weight, a thicker blade is better able to resist bending and twisting forces.

(R. Kennelly and R. Hicks, Ext. 5944/5656)

Boeing 767 Wind Tunnel Correlation Program

An extensive series of correlation tests using a model of the Boeing 767 transport have been completed in the 11- by 11-ft transonic wind tunnel leg of the Ames Unitary Plan Wind Tunnel. The correlation program is a joint effort of the Ames and Langley Research Centers and the Commercial Airplane Group of the Boeing Company. The 0.03-scale model of the 767-200 airplane which serves as the basis for the program, was specifically designed and fabricated by Boeing for testing in the National Transonic Facility (NTF) at Langley. The NTF is a new wind tunnel capable of achieving full-scale Reynolds numbers on small-scale aircraft models by testing at cryogenic temperatures while maintaining moderate values of tunnel dynamic pressure. Since the correlation program calls for testing the model in the Boeing Transonic Wind Tunnel (which is an atmospheric test facility) as well as the Ames 11-Foot Wind Tunnel (which is capable of operating at two atmospheres of pressure) and the Langley NTF, the design and fabrication of the model and support-sting had to satisfy a range of loading conditions over a broad range of operating temperatures.

Over the past year, the model has been tested several times in the Boeing wind tunnel where the unit Reynolds number is about 3.5-million/ft. At Ames, the tests were conducted at unit Reynolds numbers of 3.5-million/ft (to match the Boeing data); at 5.5-million/ft (which is the lowest operating condition in the NTF); and 7.5-million/ft (which is the maximum operating condition in the 11-ft tunnel). In addition to the actual investigations of the 767 model aerodynamics characteristics, the Ames tests included a complete Mach number calibration of the 11-ft wind tunnel and a tunnel-empty flow-angle survey of the test section flow field.

A preliminary analysis of the Ames test results indicates good agreement with the Boeing test results and consistent variations of aerodynamic parameters throughout the range of test Mach numbers and Reynolds numbers. The data should be excellent for wind-tunnel-to-wind-tunnel correlation studies as well as for wind-tunnel-to-flight extrapolations and correlations.

(J. Daugherty, Ext. 6045)

Numerical Methods for Vortical Flow Fields

Numerical methods for computing nonplanar vortex wakes represented by finite-core vortices have been developed. The approach solves for the velocity on an Eulerian grid, using standard finite-difference techniques; the vortex wake is tracked by a Lagrangian method. In this method, the spanwise distribution of continuous vorticity in the wake is replaced by a group of discrete vortices. An axially symmetric distribution of vorticity about the center of the discrete vortex is used to represent the finite-core model. Two distributions of vorticity, or core models, were investigated: a finite distribution of vorticity represented by a third-order polynomial, and a continuous distribution of vorticity throughout the wake. The method provides for a vortex-core model which is insensitive to the mesh spacing.

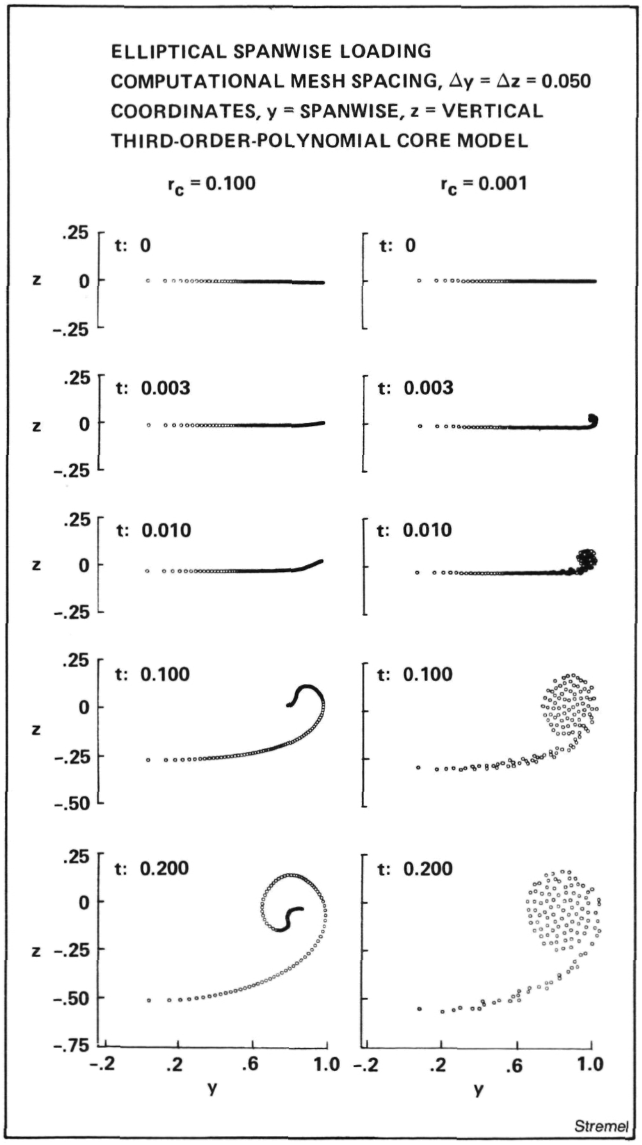

Elliptical spanwise loading

Numerical experiments to test the above technique were conducted. In order to test the method, several computational parameters were varied and solutions calculated. The parameters were varied and include the mesh spacing, the vortex-core radius, the spanwise distribution of the wing vorticity, and the vortex-core model. The roll-up of the vortex wake generated by an elliptical spanwise load distribution for varying vortex-core radii can be seen in the attached figure. In addition, comparisons between the wake velocity predicted numerically and velocities measured experimentally from a twisted semi-span wing were made. Favorable results were obtained with a smaller vortex core radius which exhibited significant improvements in predicting peak wake velocities. However, extensions to the method are needed to model the development of the vortex wake forward of the trailing edge of the wing as was measured in the experimental data.

(P. Stremel, Ext. 6714)

Three-Dimensional Streamline Tracing with a Laser-Doppler Anemometer

Laser-Doppler anemometry (LDA) is a recently developed technique which is used in wind-tunnel investigations to obtain detailed, nonintrusive measurements of the velocity fields around experimental models of aircraft or related components. The velocity measurements are used to compute aerodynamic forces or to be compared with analytical flow predictions. In the conventional mode of operation, the laser beams are focused on successive locations defined by a predetermined survey grid.

The performance of the 3-D LDA of the Low Speed Aircraft Research Branch at Ames has been recently enhanced to allow real-time tracking of complex flow streamlines. This advanced technique, which was developed for the 3D-LDA

system, has the advantage of greatly reduced measurement time for high-resolution traces, and permits direct comparisons at run time with the results of flow visualization studies. This technique was used in a recent wind tunnel investigation of a jet in a crossflow, which is associated with VSTOL aircraft, such as the AV-88 Harrier. A typical sample of streamline traces as seen by an observer looking into the jet is shown in the attached figure.

The technique is based on the fact that the velocity vector at a point in a flow defines the tangent to the streamline passing through that point. The algorithm allows relatively large measurement increments by computing streamline curvature and curvature change rate at each location. The accuracy of the procedure has been demonstrated with the retracing of complex streamlines by reversing the trace direction. Other enhancements to the 3D-LDA, including the addition of high-speed buffers for data acquisition, automated preprocessing of the signals from the photomultiplier tubes, and improved real-time graphical display of velocity and streamline data, will significantly improve the ability to analyze the complex flows associated with modern, high-performance aircraft.

(W. Horne, Ext. 6678)

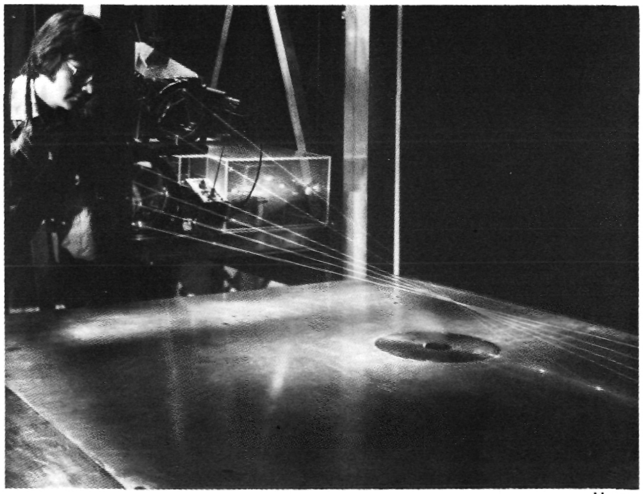

3-D Laser Doppler Anemometer positioned for measurements of a jet in a crossflow in the Ames 7- by 10-Foot Wind Tunnel

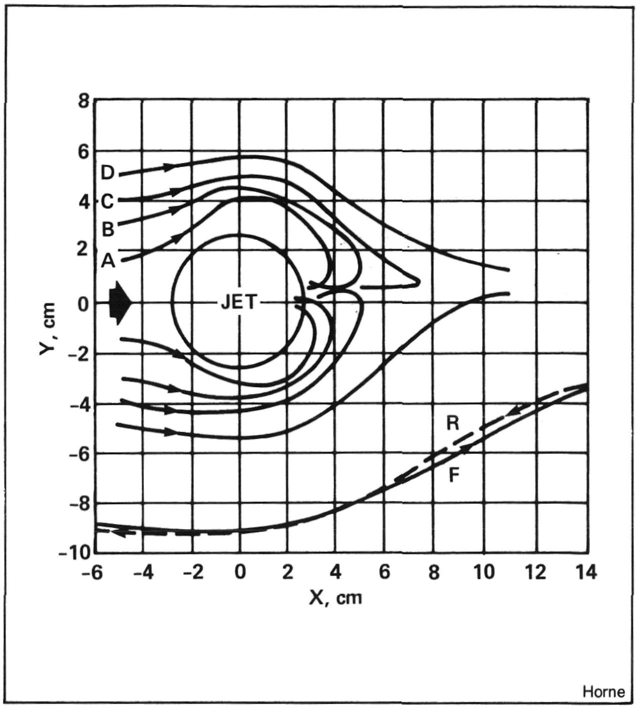

Measured streamlines around jet

Noise Generation from Vortex Motion Near Rigid Surface

A significant source of noise in aircraft and helicopters is unsteady vortex motion near rigid surfaces. In order to improve the understanding of this mechanism, detailed flow and acoustic measurements of jet interactions with walls and other surfaces have been taken. The periodic nature of these tone generating flows permit essentially instantaneous, high-resolution measurements of the velocity field so that acoustic source distributions can be computed directly. The results of these studies will be reported to the NASA/AIAA Aeroacoustics Conference.

(W. Horne, Ext. 6678)

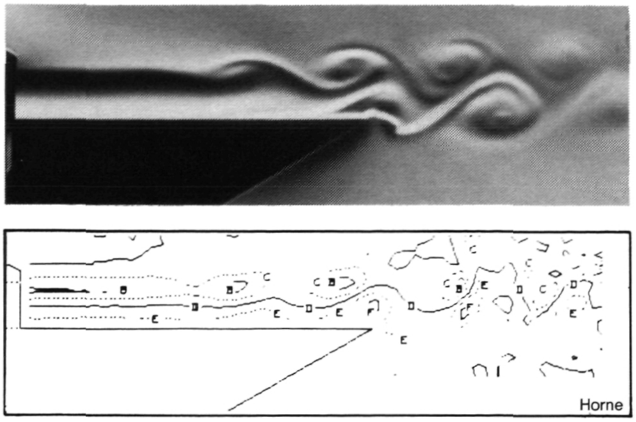

Two dimensional unsteady vortex flow near a wall
Top: Schlieren flow visualization
Bottom: Contours of constant vorticity as measured with a hot-wire anemometer using phase conditional sampling

Pusher Propeller Noise

In recent years, renewed interest in propeller-driven aircraft has led to designs with propellers mounted at a number of locations on the aircraft. Pusher propellers mounted behind the fuselage, for example, have certain aerodynamic advantages and create less cabin noise than a tractor propeller. However, the noise on the ground can be high. This problem was the object of a recent study of a model propeller operating in the wake of an empennage and fuselage in the NASA Ames 7- by 10-Foot Wind Tunnel. The wind tunnel was operated with an open jet, which allows microphone placement outside the test section as shown in the photograph. A number of geometric and propeller parameters were systematically varied such as empennage type (Y-tail, V-tail, I-tail), tail loading, tail-propeller spacing, propeller height, propeller operating condition, and wind speed. Hot-wire measurements of the wake velocity distribution and turbulence were made to identify the inflow disturbance at the propeller.

A large set of acoustic data is being published as a NASA CR-data report prior to detailed aero-acoustic analysis. The data show that the empennage wake/propeller interaction caused the noise of order 5 and more at blade passage harmonics to increase substantially. The type of empennage tested did not matter greatly, but the tail loading affected the noise levels. Moving the propeller aft reduced the noise levels as expected. That effect depended on empennage chord and acoustic frequency. Generally, for a tail/propeller spacing normalized by empennage chord, there was a large noise decrease due to a spacing change from 15% to 30% chord, and a lesser rate of decrease beyond that. Analysis of the aerodynamic and acoustic data is under way.

(P. Soderman, Ext. 6678)

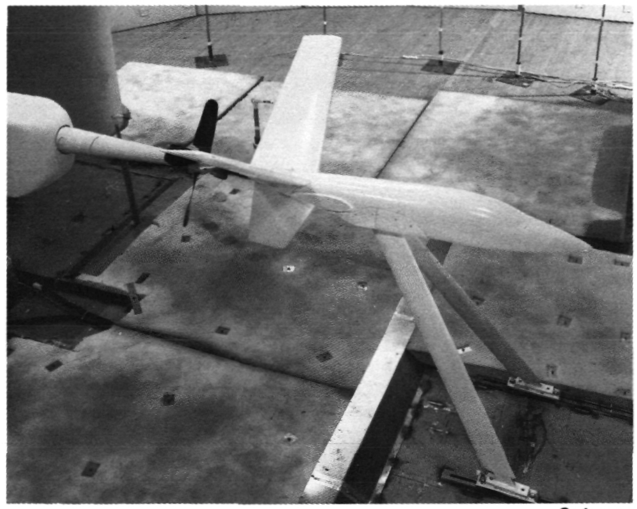

Pusher propeller wind tunnel model

Research Testing with New Model Rotor Test Rig

The Ames small-scale rotor test rig (RTR) was calibrated, checked out, and operated in a recently completed hover test in the 40- by 80-Foot Wind Tunnel test section. The RTR has the capability of measuring complete rotor forces and moments as well as trim operating conditions. The control system includes both a primary control system for setting trim and a dynamic control system for high-frequency blade feathering. The rig may be operated with the rotor thrusting up or down, rotating clockwise or counterclockwise. A fully articulated 0.16 scale S-76 rotor was tested; however, the rig can be adapted to other rotor hub configurations.

A thorough systems calibration of the RTR balance, torque load cell and control system was conducted, as well as a shake test prior to research testing. During the test, hover performance and acoustics data were acquired. Correlation with full-scale whirl tower results and analytical prediction is in progress.

(P. Shinoda and W. Warmbrodt, Ext. 6679/5642)

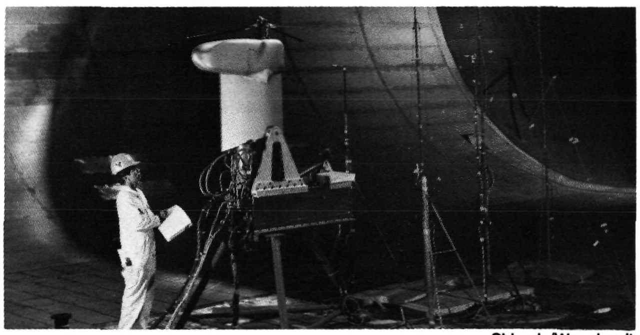

Shinoda/Warmbrodt

Rotor test rig

Modified Slender Body Analysis of Axisymmetric Body Influence on Helicopter Rotors

A computationally efficient body analysis has been coupled with a comprehensive helicopter analysis to calculate the body-induced aerodynamic effects on rotor performance and loads. A modified slender body theory was the basis of the body model. To demonstrate the accuracy, efficiency, and application of the method, the analysis was restricted to axisymmetric bodies at zero angle-of-attack. Comparing the results with those from an exact analysis for simple body shapes, the modified slender body theory proved to be an accurate potential flow solution even for moderately thick bodies. The theory required only a 10%–20% increase in computational effort over that of an isolated rotor analysis. The computational ease of this method provides a means for routine assessment configurations used in the Ames 40- by 80-Foot Wind Tunnel, and in the rotor-body interference tests being conducted at Ames.

The figure shows the change in angle of attack of the rotor blade caused by a test module (used in the small-scale interference tests at Ames) for two longitudinal hub positions. Moving the hub position aft changes the angle-of-attack distribution significantly and increases rotor performance. For the full-scale configuration of this test module, a negligible change in performance was calculated. However, significant increases in the oscillatory edgewise bending moments were predicted.

(G. Yamauchi, Ext. 6719)

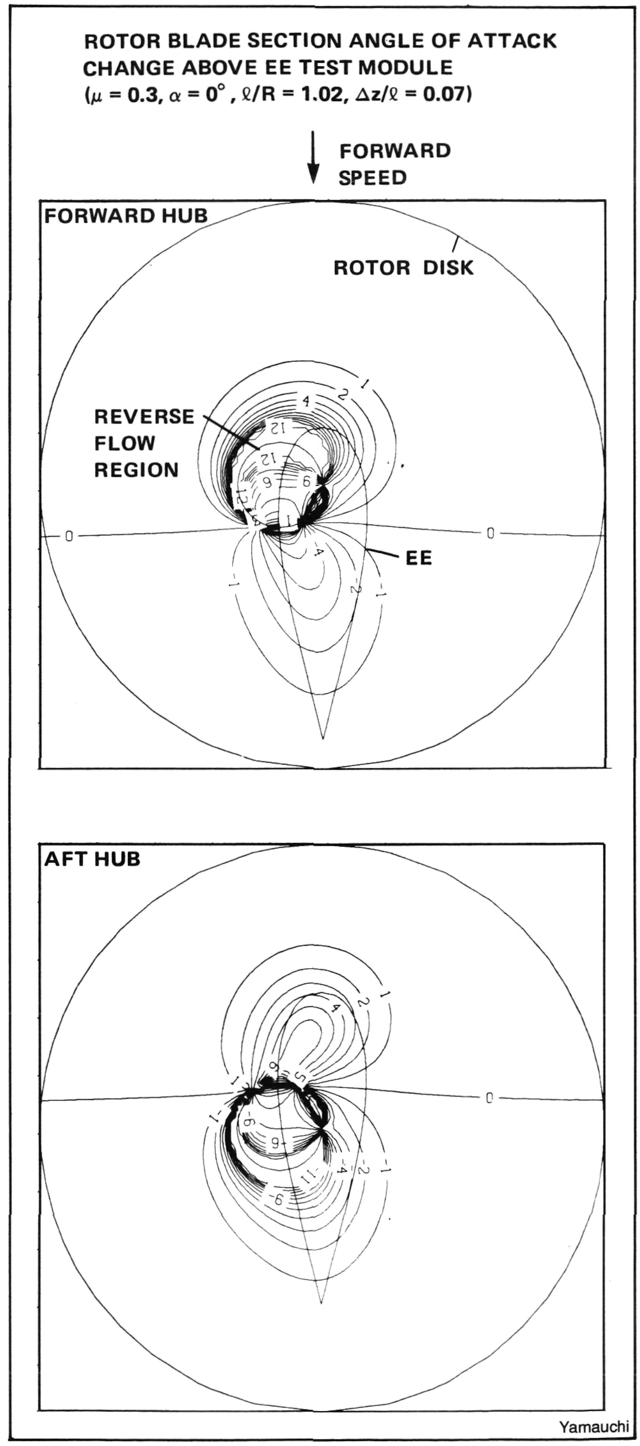

Yamauchi

Rotor blade section angle-of-attack change above EE test module

Dynamics of Advanced Rotor Systems

As part of an on-going program to investigate the aeroelastic characteristics of advanced helicopter configurations, a BO-105 helicopter rotor was tested in hover in the 40- by 80-Foot Wind Tunnel test section. The BO-105 helicopter rotor is a soft inplane hingeless hub configuration. The performance and aeroelastic stability of the rotor was evaluated. Rotor performance and inplane damping data were obtained for rotor operation between 350 and 425 rpm for thrust coefficients ($C_{T/\sigma}$) between 0.0 and 0.12.

With this experimental database an extensive effort was made using the comprehensive helicopter analysis CAMRAD to identify the degree of correlation possible using current predictive technology. Rotor performance and inplane lead-lag damping were calculated. Performance calculations quantified the sensitivity of the far-wake in accurately predicting rotor figure of merit. To model hingeless rotor dynamics, the number of blade modes, amount of structural damping, control system stiffness, and unsteady aerodynamic models were investigated. To obtain the best correlation for rotor stability, blade elastic torsion and a dynamic inflow model should be used.

The data obtained from this hover test were compared with whirl tower and flight test data on the BO-105. Direct comparisons were also made with a soft inplane bearingless rotor test tested on the same test apparatus in the 40- by 80-Foot Wind Tunnel. The bearingless rotor, which has the same basic rotor frequencies, is more stable than the BO-105 rotor system at design tip speed and thrust. However, the bearingless rotor also shows significantly greater sensitivity to rotor speed and thrust.

(R. Peterson, Ext. 5044)

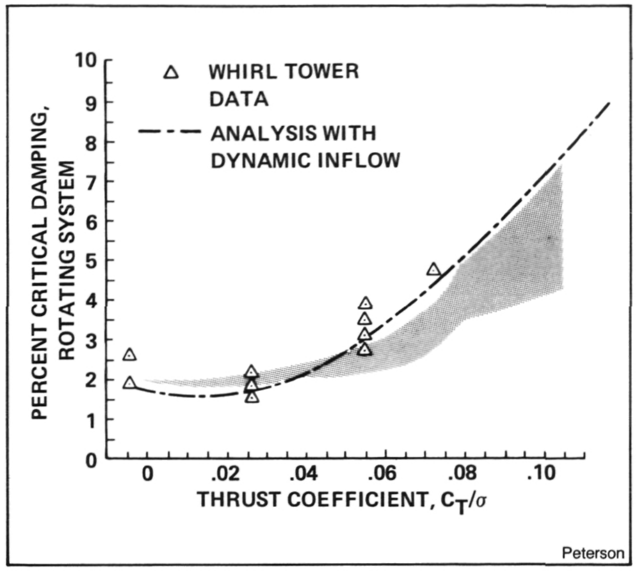

Comparison of hover test results (shaded area) with whirl tower and CAMRAD predictions for BO-105 rotor

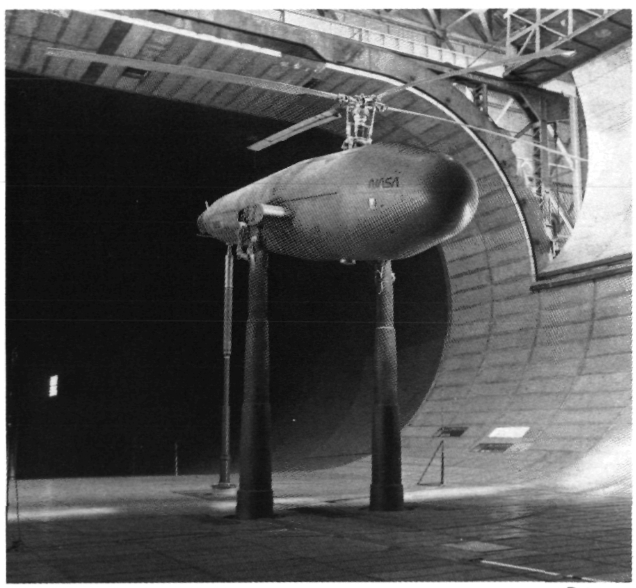

Peterson

BO-105 helicopter mounted in wind tunnel

Powered Lift Applications to Swept Forward Wings

During the past several years, there has been increasing interest in a highly maneuverable, swept-forward wing aircraft. As a result, NASA has initiated a program to evaluate the effects of powered lift on swept-forward wing configurations. The program includes both small and large scale wind-tunnel testing, and theoretical evaluations using several different prediction codes, including PAN AIR.

The first test of a 1/4-scale semispan model in the Ames 7- by 10-Foot Wind Tunnel has been completed. The objectives of the test were to determine the effectiveness of spanwise blowing and BLC flap. Spanwise blowing was investigated at two longitudinal locations and two blowing angles (0° and 40°). Preliminary results indicate that significant increases in C_L and $C_{L_{max}}$ were achieved with both BLC and spanwise blowing. Spanwise blowing was more effective in the forward location; and for both locations tested, the blowing angle of 0° produced better results. A second test has been planned for 1985 to optimize blowing location and angle. In addition, two different canard planforms will be tested to determine the canard/wing interactions with powered lift. Previous tests have shown a favorable interaction between canards and swept forward wings.

As part of this program, a large scale powered STOL fighter model is being modified to a swept forward wing configuration. The model is powered by two General Electric J-97 turbojet engines and will employ the Vectored-Engine-Over (VEO) flap concept in addition to the spanwise blowing and BLC flap. Testing is planned at the Outdoor Aerodynamic Research Facility in 1985 and in the 40- by 80-Foot Wind Tunnel in 1986.

The results from the semispan test will be compared to predictions made using several different codes including PAN AIR, VSAERO, VAPE, McAERO, and a simple vortex lattice method. The ability of each code to predict the aerodynamics of the powered and unpowered wing will be evaluated.

(S. Schmidt, Ext. 6674)

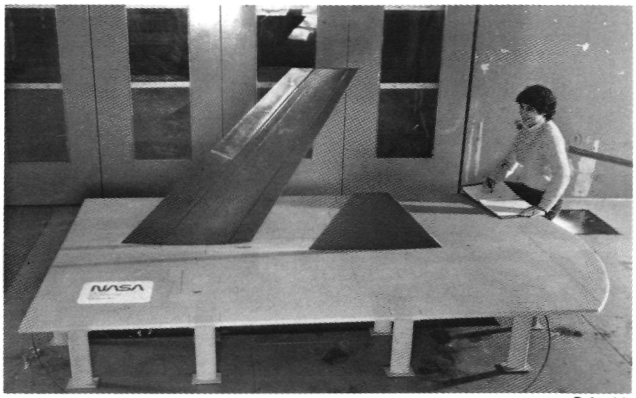

Schmidt

Semispan model of canard, swept forward wing

Rotor Systems Flight Investigations

A major milestone for the Rotor Systems Research Aircraft (RSRA) was achieved during FY84. The aircraft was flown for the first time as a fixed wing aircraft and the operational envelope for this configuration was demonstrated. This operation included several firsts. The RSRA became the first aircraft to operate in three unique configurations: pure helicopter, hybrid fixed wing/helicopter, and fixed wing. It was also the first time a fixed wing has flown with a tail rotor.

During an aeroelastic envelope expansion in the first two flights the speed envelope was expanded to 250 KTAS. None of the damping ratio trends during the aeroelastic expansion was decreasing at the 250 KTAS condition. Control power and dynamic stability data were acquired by step and reversal inputs at 180 and 230 KTAS. Stability data for analysis by system identification methods were obtained by using sine-shape control inputs as illustrated. Hub drag measurements

RSRA fixed wing

Snyder

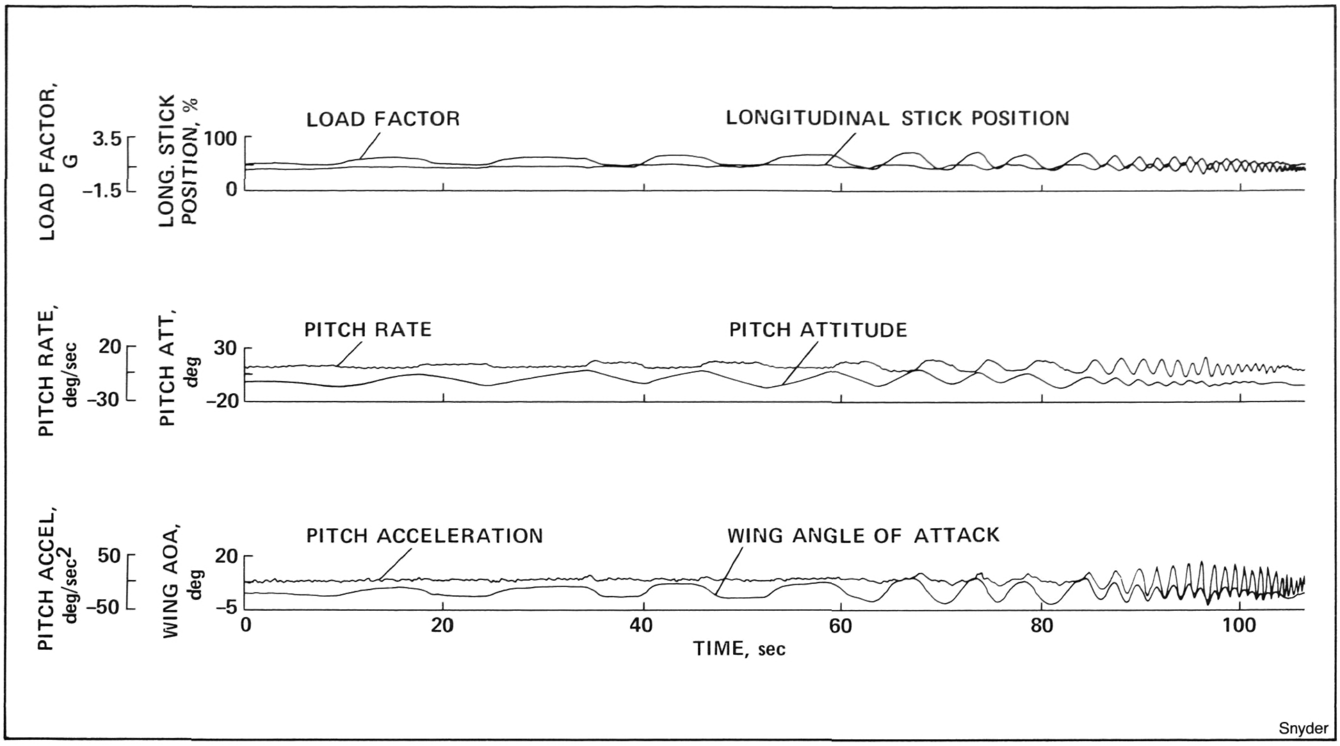

RSRA fixed wing pitch sine input, 200 KCAS

in the hub-on and hub-off configuration were obtained through the use of the unique RSRA rotor force/moment balance system. Baseline acoustic data for the RSRA were acquired in the hub-off configuration.

This program was undertaken primarily to develop a configuration baseline for the RSRA/ X-Wing program, particularly, in the area of control capability. The aircraft appears ready to make substantial contributions as a rotorcraft research tool.

(W. Snyder, Ext. 6570)

Tilt Rotor Advanced Technology Blades

The design and fabrication of Advanced Technology rotor blades for the XV-15 Tilt Rotor Research Aircraft was completed by Boeing Vertol under contract to NASA Ames. These blades incorporate both state-of-the-art composite materials to increase structural capability and service life, and advanced airfoil technology and blade configuration to enhance hover lift capability without penalizing high speed performance. A static performance test of the Advanced Technology Blades (ATB) was performed at the NASA Ames Outside Aerodynamic Research Facility (OARF) in July 1984. The ATB were tested with several alternate configurations, including blade root cuffs on and off, extended trailing edge cuffs, square blade tips, and swept-tapered tips.

Measurements for the isolated rotor were made of the static (hover mode) performance loads, the near and far field acoustic signal, the velocity profile in the near-wake, and the rotor wake tip vortex path. In addition, the baseline XV-15 metal blades and scaled JVX rotor blades were tested on the same rig.

A major accomplishment of this series of tests was the unprecedented accuracy of the rotor thrust and rotor torque measurements. A new rotor balance was designed and built for this test series. The balance was designed for high sensitivity to rotor thrust, with no interactions due to the other forces or moments, and minimal thermal effects. A special rotor shaft was built for accurate measurement of rotor shaft torque. Combined thrust and torque check loadings performed during the rotor performance tests demonstrated that rotor thrust and torque measurements were accurate to within 0.5%.

This test series has produced an extensive hover-mode large-scale rotor data base which will be used by government and industry for valida-

tion of methodology as well as quantitative levels in the areas of performance, wake characteristics, and acoustics. The blades are scheduled to be tested on the XV-15 aircraft in the Spring of 1985.

(M. Maisel and F. Felker, Ext. 5442/6096)

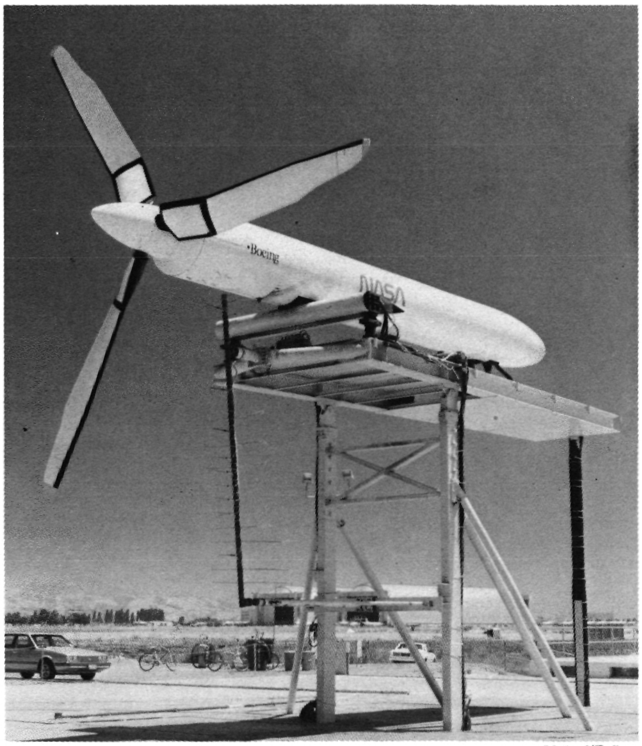

Maisel/Felker

Rotor blades for XV-15 Tilt Rotor Research Aircraft

XV-15 Tilt Rotor Research Aircraft

The XV-15 Tilt Rotor Research Aircraft provides a unique facility for conducting basic V/STOL handling quality tests from hover through conventional airplane flight modes. This is due to its response characteristics to control or disturbances being essentially uncoupled in all flight modes. This permits technically aggressive treatments for augmentation of stability and control characteristics independently for each axis, without contaminating evaluations by other axes responses. These characteristics have permitted implementation of a control law which provides distinct separation of stability criteria from control criteria. This, in turn, permits stabilization of the aircraft to its limit response bandwidth, while providing pilot response within a specified lower bandwidth.

The design analyses for application of this control law, and the limit bandwidth for stabilization in hovering flight is defined by rotor or control lag functions. Application of the control law provides greater than 20 dB attenuation of response to disturbances (uncommanded responses), while preserving the pilot required response bandwidth. Flight test results show attainment of pilot ratings (Cooper-Harper scale) of 3 were obtained by treating the pitch-and-roll modes only.

Under the terms of the contract with Bell Helicopter Textron, Inc. (BHTI) the contractor performed a number of independent research and development (IR&D) test programs. The XV-15 structural aeroelastic stability data base has been expanded by the inclusion of the XV-15 aeroelastic stability characteristics with steel rotor hubs. The original aeroelastic stability tests were conducted with titanium rotor hubs that were later found to have unsatisfactory structural fatigue characteristics. Replacement of the titanium hubs with steel rotor hubs has added 50 pounds per rotor and changed the frequency of some pylon modes. The most significant frequency change has been a shift in the rotor first inplane cyclic frequency. This shift has provided a wider separation between this mode and the rotor one-per-rev frequency. The net result has been a reduced tendency of this mode to be excited by control inputs and pylon motion. This, in turn, has resulted in a significant reduction of rotor blade and rotor hub loads experienced during maneuvering flight and/or during reconversion.

A series of tests were conducted by the contractor to prove the mission suitability of the tilt rotor concept for JVX and LHX missions. The XV-15 has demonstrated that the tilt rotor air-

XV-15 electronic surveillance evaluation

Schroers

craft, using thrust vectoring independent of fuselage attitude, possess a significant advantage over conventional helicopters in the nap-of-the-earth and the air-to-air combat maneuvering environments. It has also been shown that nose-up and nose-down slope landings are easily performed by using rotor tilt to establish desired fuselage altitude prior to touchdown.

Tuft studies have shown that the interaction of the rotor wake on the upper surface of the wing produces an inboard spanwise flow that meets over the fuselage and produces an "upwash fountain." The upwash is a significant portion of the down-load penalty of a rotor/wing design. Flight tests are being conducted to evaluate the effectiveness of wing flow fences that will change the rotor flow from spanwise to chordwise flow. Eight-inch and four-inch flow fences are being evaluated at different wing locations to determine the optimum configuration. Turning the flow from spanwise to chordwise will eliminate the "upwash fountain" and provide a significant improvement in hovering performance.

(L. Schroers, Ext. 5020)

LOADING	
PASSENGER CAPACITY	100
NUMBER OF SEATS ABREAST	5
TAKE-OFF GROSS WEIGHT	90193.2 lb
WING LOADING	110 lb/ft^2
DIMENSIONS AND AREAS	
WING AREA	819.9 ft^2
WING SPAN	85.9 ft.
FUSELAGE DIAMETER	11 ft.
FUSELAGE LENGTH	101.3 ft.
PROPULSION	
THRUST/WEIGHT	0.456
TAKE-OFF POWER	11537.2 HP/ENGINE
PROP-DIAMETER	13 ft.
TIP SPEED	799.6 ft/sec
PERFORMANCE DATA	
DESIGN	
RANGE	1496 nm
MACH NUMBER	0.8
ALTITUDE	30000 ft.
BLOCK FUEL	14053 lb
BLOCK TIME	3.444 hr
D.O.C.	3.6096 c/sm
OFF-DESIGN	
RANGE	200 nm
MACH NUMBER	0.75
ALTITUDE	25000 ft.
BLOCK FUEL	2650 lb
BLOCK TIME	0.694 hr
D.O.C.	5.1155 c/sm
B.F.L./L.F.L.	4590/4374 ft.

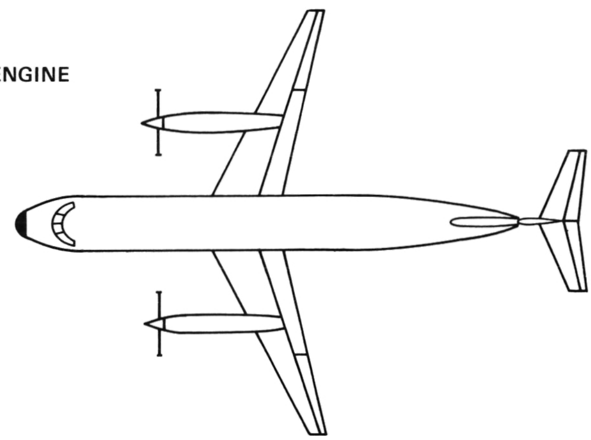

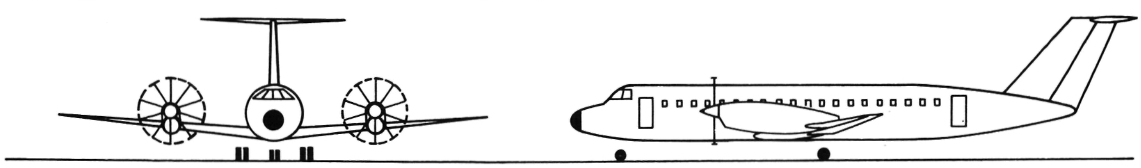

Galloway

Three-view general arrangment layouts of conceptual aircraft designs

Graphic Layout for Conceptual Aircraft Design

During the conceptual design phase of configuration assessment, many parametric evaluations are performed to determine geometry and performance tradeoffs. A limited amount of geometric data are generated during this phase to define the configuration's overall layout. With the increased use of computerized techniques to assist in the design process, a number of arrangements may be explored in a short period of time. With assistance of Informatics General personnel, a software package was developed which interfaces with various Ames aircraft design codes and the widely used DISSPLA graphics software to generate three-view general arrangement layouts of conceptual aircraft designs.

This capability gives the researcher the ability to assess the appearance and feasibility of the concept in a rapid manner and also quickly identify input changes necessary in the vehicle definition process. Only 53 items of geometric data are required as an input file to produce a report quality layout. In addition to the more conventional aircraft layouts, tilt-rotor, joined-wing, canard and pusher propeller arrangements have been displayed.

(T. Galloway, Ext. 6181)

Helicopter Engine-Out Studies

A ground-based simulator experiment was conducted to investigate the influence of rotor and control-system variations on helicopter engine-out control and autorotation landings. This experiment used a mathematical model of a generic, single-main-rotor helicopter and was conducted on a large moving-base simulator with a four-window, computer-generated-image visual display. The nonlinear, total force-and-moment mathe-

matical model featured ten degrees of freedom: six rigid-body, three main rotor-flapping, and the rotor rotational degrees of freedom. The mathematical model of the rotor was expanded to include the aerodynamic effects of operation near the ground, at low speeds, and at steep descent angles. A computer-driven sound system simulated audible cues of rotor speed and ground contact. The simulation experiment reproduced autorotation performance and control effects that are found in actual flight, thus confirming the simulator's usefulness for further autorotation research. The expanded aerodynamic model requires further development for operation in ground effect. The large vertical motion of the simulator provided valuable proprioceptive cues during autorotation landings. The simulation experiment showed that great care must be exercised in selecting visual-scene content and window placement in order to achieve repeatable pilot landing performance.

(W. Decker, Ext. 5362)

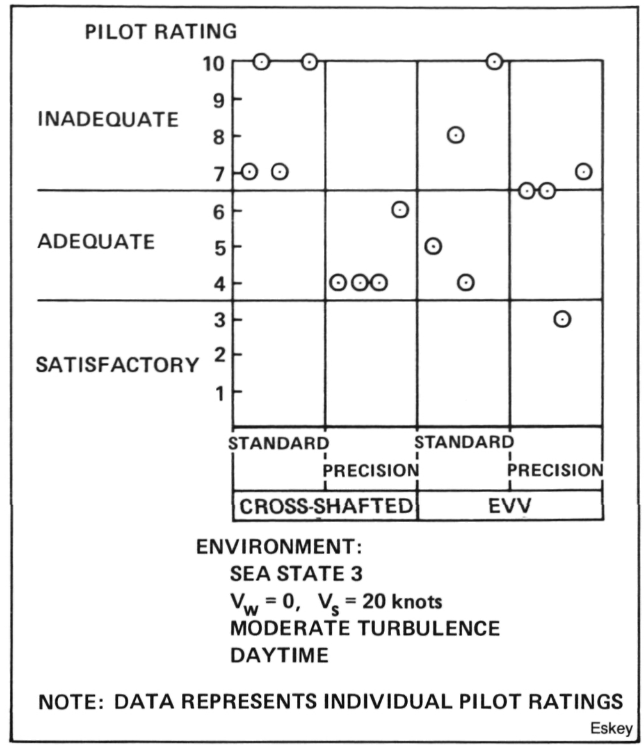

Pilot evaluation of an approach to and landing on an LPH in the vertical motion simulator

Engine Failure Recovery Simulation Investigation of the Tilt-Nacelle V/STOL Concept

Engine-failure characteristics of the Grumman, twin engine tilt-nacelle V/STOL (vertical and short takeoff and landing) concept have been investigated on the Ames Vertical Motion Simulator (VMS).

The flight dynamics of single engine failures and the flight recovery capability of two different propulsion/control configurations were addressed. The first configuration was the same cross-shafted/VIGV (variable inlet guide vanes) configuration examined in previous simulations. The second configuration, the enhanced vertical vane (EVV), included a third vertical vane, used no cross-shafting, and used large vane deflections beyond normal control range to trim the rolling moment caused by failure of one engine. The flying qualities of the EVV configuration were also evaluated. The two flight control systems used were a standard control mode and an improved, precision control mode.

Minimum recovery and ejection envelopes were examined for the EVV and cross-shafted/VIGV configurations. Preliminary results show that recovery is not possible below ~60 knots for the cross-shafted version and below ~117 knots for

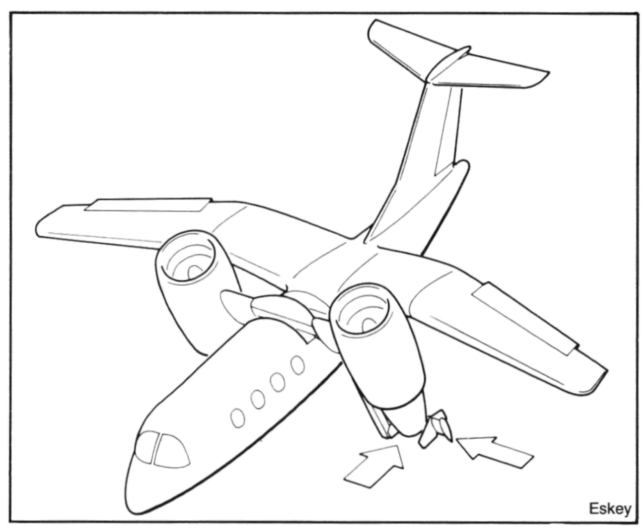

Design 698 Demonstrator aircraft

the noncross-shafted version, suggesting that cross-shafting is required. Pilot ratings were essentially equal for each propulsion configuration, as shown in the figure. There was a significant improvement in ratings, however, when the precision control mode was used in lieu of the standard mode. This investigation was conducted cooperatively with Grumman and NADC.

(M. Eskey, Ext. 5903)

Approximation Modeling Applications for Preliminary Aircraft Design

A key requirement for preliminary aircraft design and analysis is the ability to model accurately and to predict various aircraft systems performance characteristics. Typically, the system performance data are available in lengthy tabular format and must be integrated into the preliminary aircraft design computer code. For example, engine thrust and fuel flow are tabulated as a function of speed and altitude, and table look-up algorithms are used to interpolate function values within the analysis code. This systems modeling approach often results in large program storage requirements to obtain the desired accuracy. The Aeronautical Systems Branch, in a cooperative research effort with San Jose State University, has developed a numerical approximation modeling package for application to preliminary aircraft design which markedly reduces the program storage requirements while maintaining an acceptable degree of accuracy in predicting system performance.

The numerical approximation modeling package consists of a user-friendly interface routine coupled with a least-squares method for multivariable functions in which the user can select the form of the approximating polynomial. Using the model and data base information for the performance of conventional propellers (both fixed and variable pitch), ducted props, and single rotation and counter-rotating propfans, approximation polynomial have been developed to predict accurately power/thrust performance, system weight, and noise characteristics over a wide range of design and off-design operating conditions. Implementation of the approximation models in the

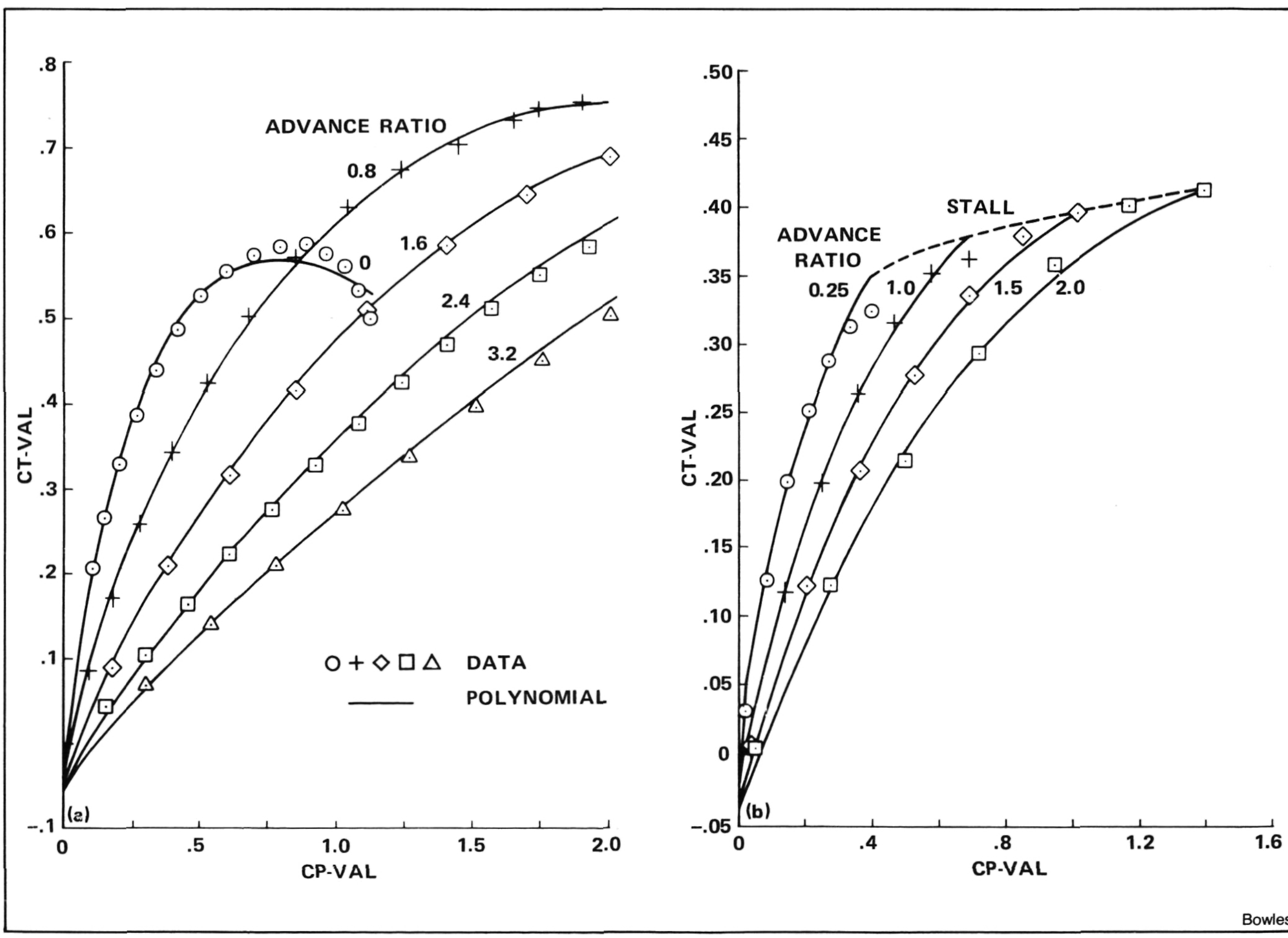

Comparison of approximation model and published data for thrust coefficient as function of power coefficient and advance ratio for (a) Advanced 10-bladed prop fan at low Mach Number, and (b) 4-bladed conventional propeller at 0.2 Mach

preliminary design codes has resulted in significant reduction of program storage requirements for the propulsion modeling subroutines, generally requiring only 3% to 10% of the equivalent table look-up version program size. In addition, dramatic reduction in program execution time has also resulted, with time savings of up to 66% compared to the table look-up method, with predicted results agreeing within 1%. The U.S. Army RTL Advanced Systems Research Office is currently using the propeller prediction model as part of their LHX concept evaluation studies for compound helicopter performance analysis. Implementation of these numerical approximation models will also permit migration of the preliminary design codes to micro-based computer systems with limited program storage capacity.

Another application of the approximation method has been to the modeling of the aerodynamic and propulsion characteristics of the NASA Langley ATOPS Aircraft. The drag coefficient as a function of Mach number and lift coefficient was modeled, producing a smooth monotonic function value well into the drag divergence Mach number range. This math model, again needing relatively modest program storage requirements could be implemented on an on-board micro computer for use in real time flightpath optimization.

(J. Bowles, Ext. 5673)

Joined Wing Weight Evaluation by Structural Optimization

The Navy and NASA have an interest in the joined wing concept. Achieving the potential aerodynamic and structural benefits would yield more flight-efficient vehicles ranging from cruise missiles to transport aircraft. Potential fuel savings of up to 15% have been indicated for 100-passenger transport aircraft.

Automated structural optimization capabilities are being applied to evaluate weight advantages of an unconventional lifting surface configuration called the "Joined Wing." A typical configuration applied to a transport aircraft is shown. The joined wing is expected to have a number of advantages over conventional cantilever configuration. One of the key attributes to be considered is reduced structural weight; however, the internal force distribution in joined wing structures is more complex than in cantilever wing structures and is strongly dependent on the geometrical wing arrangements. Hence, traditional weight estimation methods based on the past statistical data may not be applicable. As a consequence, during the conceptual and preliminary design stage, designers of a joined wing system have to innovate methods to estimate the wing structural weight.

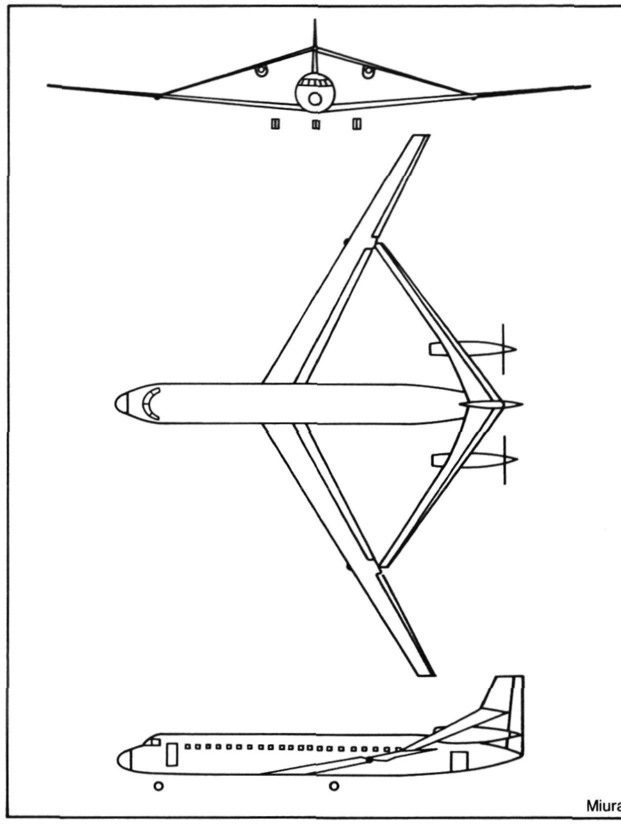

Transport configuration with in-board joint

One innovative approach is to use structural optimization methods which have been developed recently by integrating finite element structural analysis with nonlinear mathematical programming techniques. This provides the capabilities to find an optimal material distribution for a given configuration taking detailed internal force distributions into account. For the subject study a general finite element structural analysis code, EAL, and a general function minimization program, CONMIN, were interfaced. With the help of semiautomated finite element mesh generation and aerodynamic load generation programs, calculation of an optimal weight for a given geometry can be performed within a few man-hours and 10 to 15 minutes of CPU time on a CRAY-XMP computer.

Since the wing geometrical configuration must be determined based on the overall aircraft performances, the weight evaluation capability described above was used as a part of an aircraft preliminary design activity. One of the interesting results found in the present study was that the location of the wing joint was an important parameter. Minimum structural weight was obtained when the rear wing was joined to the forward wing at approximately the 70% span station. The distinct change of the weight trend at about 70% of the joint location was found to be attributed to the shift of the global deformation pattern with monotonic transverse deflection to another pattern with a peak deflection inboard of the joint. This type of phenomenon would be hard to observe without applications of structural optimization capabilities.

(H. Miura, Ext. 5888)

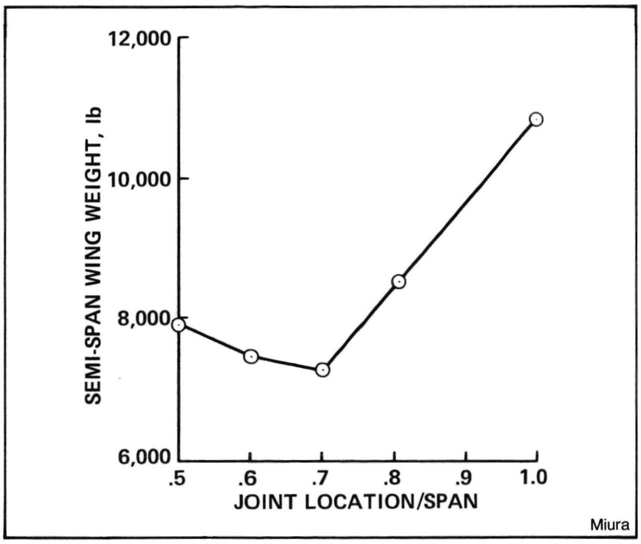

Joint location/span

An Evaluation of Supersonic STOVL Technology

An analysis of the technological status of the short takeoff and vertical landing (STOVL) performance of supersonic aircraft research has been performed in order to determine the readiness of this technology for application. Part of this evaluation involved a survey of concepts, configurations, and ongoing programs. One observation is that the tandem fan concept, which possibly offers significant benefits relative to other concepts, has received little research effort. Although the parallel flow (subsonic) mode has been investigated, the series flow (supersonic) engine mode needs additional attention before meaningful concept evaluations can be performed.

Another aspect of the evaluation is the study of the relative performance merits of STOVL relative to vertical takeoff and landing aircraft having short takeoff capabilities (V/STOL), short takeoff and landing (STOL), and conventional takeoff and landing (CTOL) aircraft designed to the same missions. Three General Dynamics designs, the F-16A, F-16XL, and E-7, were selected as representatives for the CTOL, STOL, and STOVL categories, respectively. The use of these aircraft offers the advantage that they each share F-16A heritage and thus represent modifications required to achieve a given level of performance. Results show that although the STOL aircraft has lower mission fuel consumption, the STOVL design can use its higher thrust to advantage in maneuverability (higher turn rates and sustained load factors, lower acceleration times). The figure presents an alternative comparison approach by using the F-16XL STOL performance as a criteria. Fuel was added or subtracted from the E-7 and F-16A, thereby changing gross takeoff weight, until the distance was met and the mission radius values reflect this fuel load. This and other work is intended to quantify the performance differentials associated with STOVL aircraft.

(G. Kidwell, Ext. 5886)

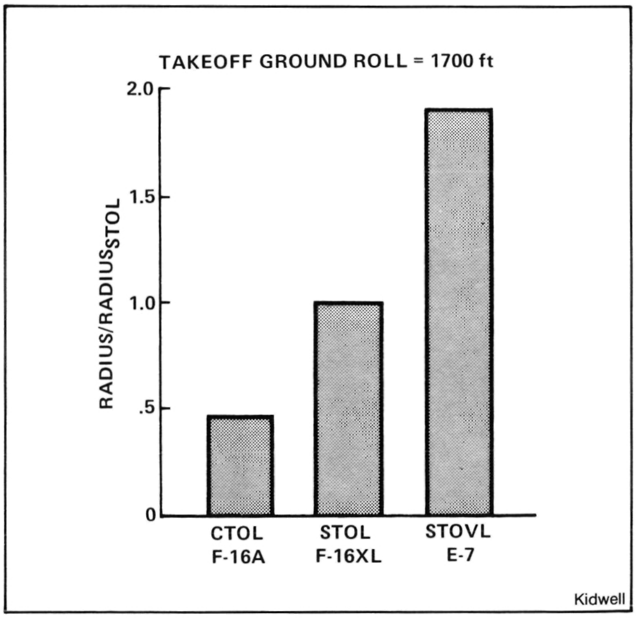

Mission radius comparison for fixed-takeoff ground run

V/STOL Fighter Configuration Aerodynamics

The development of aerodynamic technology for single-engine V/STOL fighter/attack aircraft continued this year in a joint NASA, Navy, and industry program. Prior to FY84, contractors have defined promising V/STOL concepts, conducted preliminary aerodynamic analyses, and identified aerodynamic uncertainties. Wind-tunnel tests are being conducted at Ames to resolve these uncertainties, and results are being published in NASA contractor reports and technical papers.

Two models of approximately one-tenth scale were fabricated for the tests, one by General Dynamics (GD), the other by McDonnell Douglas (McAir). The GD model (designation E7), built in a flow-through configuration, is representative of a design that employs thrust-augmenting ejectors and a deflecting nozzle to provide propulsive lift. The McAir model (designation 279-3) has both a flow-through and a jet-effects version, and on the airplane propulsive lift is obtained through four deflecting nozzles.

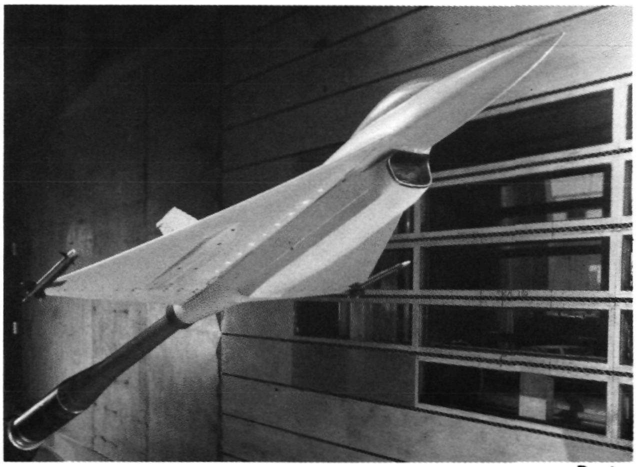

Durston

General Dynamics E7 model installed in 11- by 11-Foot Transonic Wind Tunnel

Tests of both flow-through models were completed in the Ames 11- by 11-Foot Transonic Wind Tunnel during March through May 1984. In both tests, the Mach number varied from 0.4 to 1.4 with Reynolds numbers as high as 7.0×10^6 per foot. Angles of attack ranged from $-4°$ to $27°$, and angles of sideslip from $-10°$ to $10°$. Trimmed aerodynamic characteristics, component buildup effects, wing camber effects, wing-tip variations, and longitudinal and lateral/directional stability and control were investigated in the test of the E7 model. The test of the 279-3 model emphasized trimmed aerodynamic characteristics of the three primary configurations, canard-wing, wing-horizontal tail, and three surface, as well as component buildup effects, and longitudinal and lateral/directional stability and control. A test of the E7 model in the Ames 12-Foot Pressure Wind Tunnel was completed in September 1984. Reynolds number variations at Mach 0.2 were investigated in this test for the cambered and uncambered wing configurations to define better the camber drag increment.

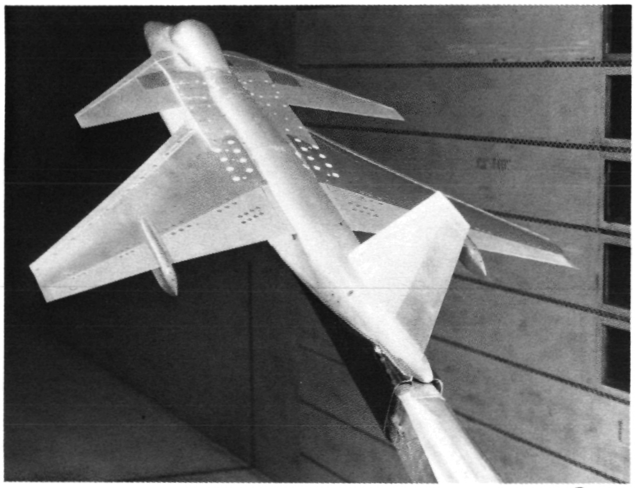

Durston

McDonnel Douglas 279-3 model installed in 11- by 11-Foot Transonic Wind Tunnel

Preparations are well under way for tests of the 279-3 jet-effects model in the Ames Unitary Plan Wind Tunnels to be run in mid-1985.

Investigations of the computer-generated aerodynamics using PAN AIR continued this year for both the GD and McAir configurations. The predictions were made prior to the wind tunnel tests and then were compared to the test data as results became available. This activity allows more extensive analysis of the configurations as well as prediction code development.

(D. Durston, Ext. 5855)

Modern Airship Flight Test and Hybrid Vehicle Computer Program Validation

Since 1973, Ames has been involved in modern lighter-than-air concepts evaluation. Because of the unique problems associated with airship and hybrid-airships, ARC initiated a computer program in 1979 called HYBRDS to analyze the dynamics and control requirements of these vehicles in modern day missions. For example, precise control and hover is required during search and rescue missions, and such precise control allows a major reduction in the number of ground crew required for ground and mooring operations. In 1983, the U.S. Navy and Coast Guard conducted a Patrol Airship Concept Evaluation (PACE) program to evaluate the application of "modern technology" airships to their long-duration patrol and other missions. A modern technology airship manufactured in Britain called the Skyship 500 was used in the program. It incorporates a new lightweight envelope, composite cab, Kevlar cabling, aircraft-type control wheel, and vectored thrust using tilting-ducted propellers.

The Navy requested NASA's expertise in the flight evaluation of the Skyship 500 airship. The airship was instrumented by Ames with a strap-down package containing rate gyros, accelerometers, and recording equipment, plus control surface position sensors and thrust strain gauges on one pylon. Dynamic response characteristics were then measured in flight as part of the test program at the Naval Air Test Center in Maryland. An Ames research pilot actively participated in the test. Frequency sweep techniques were used to excite the vehicles' modes. The dynamic data were then reduced from time histories into frequency plane format. (As an example, the Roll Rate to Rudder response is shown.) The data turned out to be of excellent "almost classic quality" for this type of testing. It is believed that this is the first time frequency response data has been documented for an airship.

The data will be compared to the predicted frequency response using HYBRDS. HYBRDS has been installed on the Cray computer at Ames. This computer program is specifically designed to study the dynamics of vehicles involving combinations of multiple-rotors/props, bouyant lift, and dynamic lift. The program has been used to predict the dynamics and control characteristics of the Piasecki Heli-stat, and to provide instrument scaling information prior to the flight test study of Skyship 500. The program will be used in evaluations of future LTA concepts for DOD missions such as surveillance and patrol.

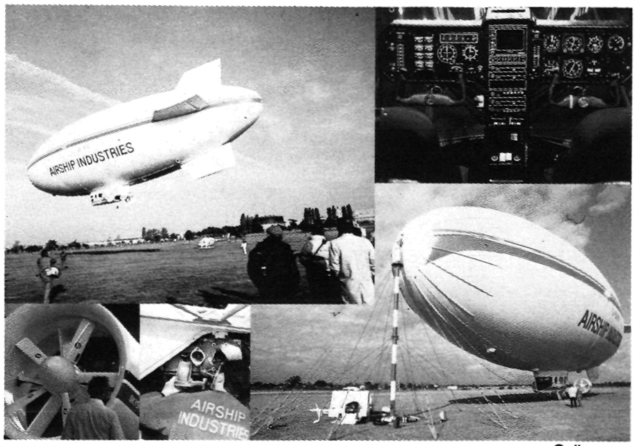

Gelhausen

Modern airship with tilting-ducted propeller

(P. Gelhausen, Ext. 5887)

Quiet Short-Haul Research Aircraft (QSRA)

The bulk of the Quiet Short-Haul Research Aircraft (QSRA) flight activity in 1984 supported the Flight Dynamics Experiments. The current research in powered-lift STOL flight dynamics has two major objectives. These are to define flying qualities design criteria for full envelope flight-path and speed control systems, and for head-up and color head-down displays; and to develop criteria for operational envelope and landing performance margins. This research expands on that previously completed by addressing more advanced fly-by-wire controls and displays, their operating procedures, and the all-weather operational capability which powered-lift STOL aircraft are expected to have.

Flight evaluations of the unaugmented QSRA indicate that the pilot must provide extensive compensation to perform precision instrument approaches using raw-data instrumentation. When attitude stability augmentation is available, the same task requires only moderate pilot compensation. When both stability augmentation and a head-down flightpath oriented display are available, minimum pilot compensation is required to fly a precision approach.

The factors which influence the landing distance of a powered-lift STOL airplane are being assessed by using the QSRA precision guidance system capability to establish intentional offsets at a 30 meter decision height and then requiring the pilot to land the airplane precisely in the marked touchdown zone of a STOL port. The preliminary flight results indicate that the pilot can easily land the airplane on the STOL port centerline from a 30-meter lateral offset at a 30-meter decision height.

Limited aerodynamic performance and stability and control data were acquired to complete the baseline QSRA data matrix. A new technique was introduced to determine more accurately the phugoid and short-period longitudinal characteristics of the QSRA. The pilot inputs a series of sinusoidal elevator commands at varying frequency and, by the use of Fourier transform techniques, the primary response frequencies and amplitudes are derived.

The horizontal tail leading-edge structure was modified to mount six flow direction/flow intensity pressure probes ahead of the tail. Flight tests provided the pressure data matrix which allowed the computation of the downwash flow field at the horizontal T-tail position. Various flap configurations and power settings were investigated to study the downwash sensitivity. An earlier downwash study was conducted on the aft-fuselage in the vicinity of a low-mounted horizontal tail configuration. These downwash data will aid future designers in horizontal tail sizing and in determining the stabilizer/elevator control requirements for powered-lift airplanes.

(D. Riddle and D. Watson, Ext. 6085/5826)

Automatic Flight Control

A methodology is being developed for the design of automatic flight control systems for aircraft having strongly coupled nonlinear dynamics and large operational envelopes. University grants and in-house research produced major accomplishments in the areas of adaptive, robust, and nonlinear control. Necessary and sufficient conditions on the system input for parameter convergence in adaptive control has been obtained. An integrated methodology has been developed for the design of robust regulators in the presence of unknown high-frequency dynamics. Complete conditions for the existence of coordinates in which the dynamics of a controlled process appear linear has been established. A control system based on such linearization and exact model following has been successfully flight tested on a UH-1 helicopter.

(S. Sastry, M. Athans, R. Su, L. Hunt, and G. Meyer, Ext. 5444)

Motion and Visual Cue Requirements in Flight Simulation

The increased use of piloted flight simulation to establish stability and control criteria and to develop aircraft systems has directed the formulation of a research program to identify the levels of motion and visual cue fidelity required to provide confidence in the validity of the results of simulator experiments. The large-amplitude motion capabilities of the Ames Vertical Motion Simulator (VMS) have been utilized in an initial series of experiments to determine the effects of cockpit motion attenuation/distortion on the bandwidth of the pilot's control of precision flight tasks, and on his perception of the handling qualities of the simulated aircraft. Hovering height-control tasks were simulated with cockpit motion cues varying from full motion to highly

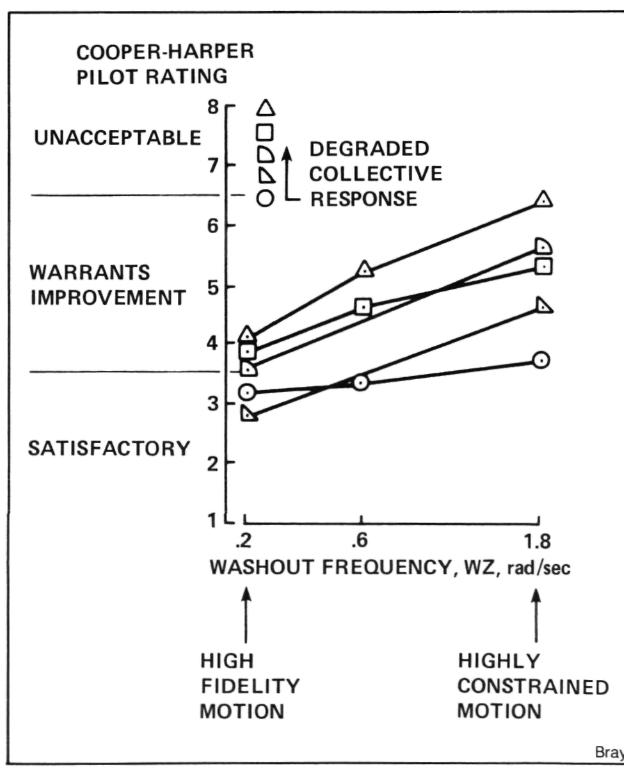

Effects of motion on handling qualities ratings

constrained motion. In stabilization against a pseudo-random vertical disturbance, the pilots exhibited a 30% to 50% decrease in control bandwidth as cockpit motion was constrained. In experiments varying vehicle dynamics and motion cue fidelity, the pilots consistently perceived the cases of reduced motion as representing degraded aircraft handling qualities, specifically, reduced vertical rate damping. The results of additional preliminary tests of motion in lateral and horizontal tasks are being analyzed.

Under a Small Business Innovation Research (SBIR) contract, Systems Technology, Inc. has conducted flight experiments aimed at defining the effects of visual cue constraints inherent in flight simulation. The effects of reduced field-of-view on precision hovering capabilities were seen to be considerably less than the effects of eliminating near-field surface textural detail through the use of semi-fogged glasses in conjunction with an operational site on a dry lake-bed surface.

(R. Bray, Ext. 6002)

Certification Criteria for VTOL Aircraft

A two-part ground-simulation was conducted to investigate the tilt rotor VTOL terminal-area operations. The baseline vehicle selected for the simulations was a generalized version of the XV-15 tilt-rotor mathematical model, which was modified to permit generic variations in forces or moments or both with power or configuration changes. Additionally, changes to wing area and rotor-blade chord were considered as a means of modifying the allowable thrust-angle versus speed relationships (the conversion corridor). These airframe variations were examined in both visual and instrument conditions for varying operation situations represented by three general conversion profiles (150 knot to 60 knot before glideslope; 150 knot to 110 knot before glideslope, 110 knot to 60 knot on glideslope; 150 knot to 60 knot all on the glideslope). The Vertical Motion Simulator at ARC was used in the experiment. Four engineering test pilots conducted over 200 piloted evaluations examining the influence of the experimental variables on their ability to perform terminal-area operations.

The results indicated that, for visual approaches, satisfactory performance was generally achievable within moderate pilot compensation, irrespective of the conversion profile used; crosswinds and a higher level of turbulence had a noticeably degrading effect with the baseline XV-15 SCAS but minimal influence with a higher level of augmentation incorporating pitch and roll attitude augmentation. For instrument approaches, the ratings indicated that desired performance could be achieved with the attitude SCAS and the conversion profile incorporating all conversion prior to the glideslope; but, that performing some or all of the conversion on the glideslope with no additional automation or display enhancement degraded the performance down to adequate (or marginally inadequate) for the other two profiles, respectively. It was found that the marginally inadequate performance for the profile incorporating all the conversion on the glideslope could be improved to the satisfactory level by adding automatic thrust tilt and three-cue flight directors.

(J. Lebacqz, Ext. 5272)

VTOL Controls and Displays for Shipboard Operations

Currently, VTOL aircraft are only permitted to operate from aircraft carriers in good visibility and low-sea states. Flexibility would be vastly improved if the operational capability could be extended to include small ships, low visibility and high seas. This can be achieved with improved controls and displays.

A promising advanced head-up-display format has been tested in a piloted simulation on the Ames Vertical Motion Simulator. An AV-8A Harrier operating off a Spruance-class destroyer was simulated. A variety of control laws were assumed, varying from that of the basic Harrier to full translational command.

The new display format, based on the concept of pursuit tracking, proved to be superior to older type displays using compensatory tracking (flight directors). In zero-zero visibility and sea-state 6, the new display permitted landings using full translational velocity command with satisfactory handling qualities and using attitude command with adequate handling qualities.

(G. Farris and V. Merrick, Ext. 6002/6194)

A Model-Following Control System for Helicopters

A part of a joint research program of the U.S. Army and the Deutsche Forschungs- und Versuchsanstalt fur Luft- und Raumfahrt (DFVLR), under the Helicopter Flight Controls Memorandum of Understanding, an explicit model-following control system has been developed for potential application to a variable-stability helicopter. A model-following control system consists of two dynamic systems known as the "plant" and the "model." The objective of this control technique is to develop control laws that enable the plant to follow the model, whose equations of motion represent the desired or ideal dynamical behavior for the vehicle. The advantage of using a model-following control system on a fly-by-wire aircraft is that the characteristics of the model to be followed can be varied in flight quickly and easily, depending on the desired application.

In order to evaluate the performance and limitations of the designed model-following control system, a U.S. and German piloted simulation experiment was designed and conducted on fly-by-wire helicopters. The NASA/Army variable stability UH-1H V/STOLAND and the DFVLR BO-105 S3, were simulated to test the adaptability of this control system to different planes.

The results of the simulation indicate that the performance of the model-following control system is dependent on the dynamics of the explicit model and on the limitations of the actuating system. Increases in the bandwidth of the explicit model placed higher demands on the control system and resulted in degraded model-following performance. Significant improvements in model-following performance were achieved when a control-law switching feature designed to account for position- or rate-limited actuators was included in the control system. Satisfactory handling qualities were achieved for both augmented helicopters flying the two specified evaluation tasks dolphin and slalom maneuvers. The excellent overall model-following performance obtained and the significant improvements in task performance and handling qualities achieved for

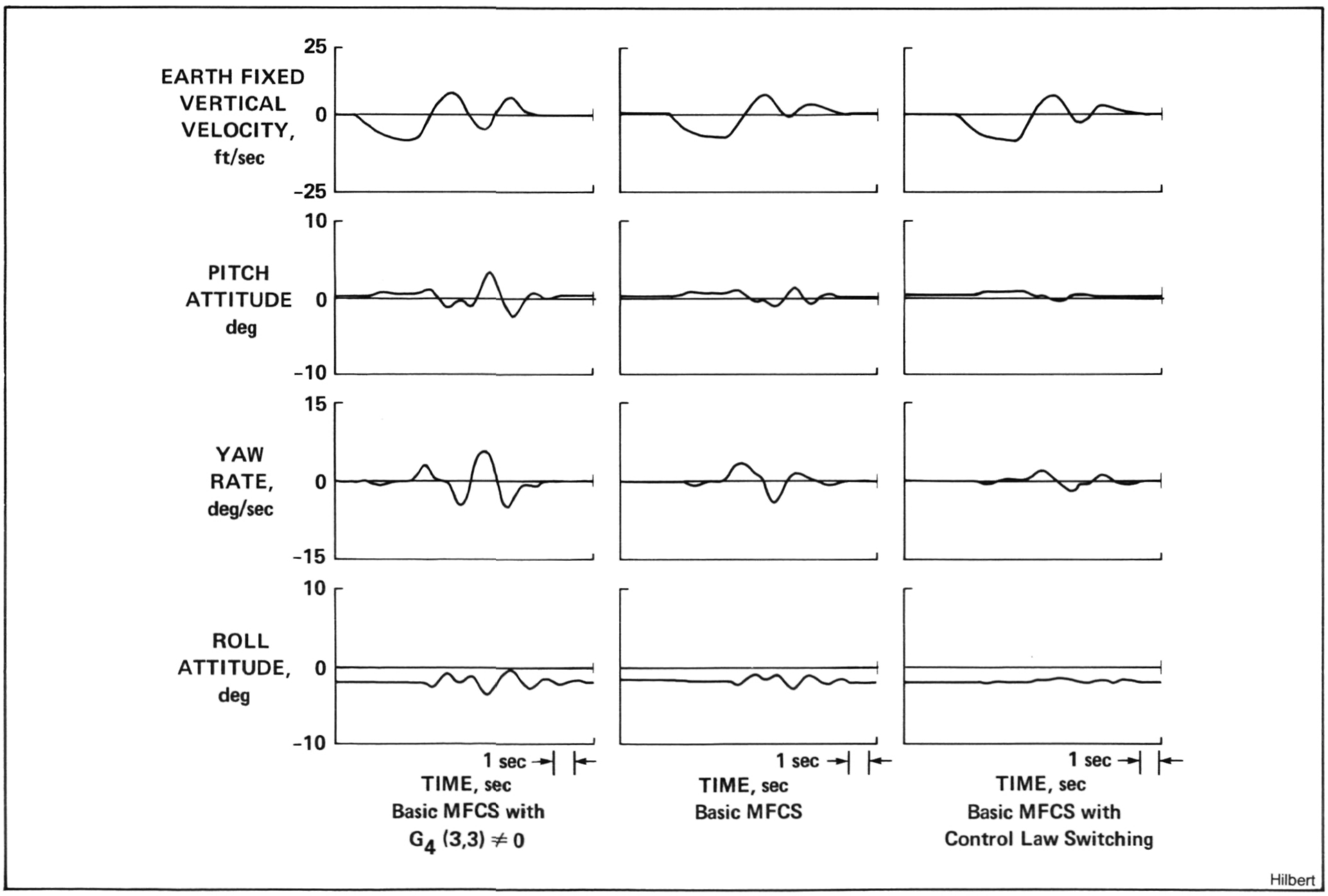

Response of BO-105 to 3-2-1-1 δ_c input at 60 knots

these two radically different helicopters, augmented with the designed model-following control system, indicates the flexibility and versatility of this control technique.

(K. Hilbert, Ext. 5272)

Helicopter Air Combat Simulation

The first piloted simulation of one-on-one helicopter air-to-air combat (HAC) in terrain flight was conducted on the Vertical Motion Simulator in February 1984. Over 200 engagements were flown by a number of pilots in model configurations and initial conditions which examined the effects of SCAS design, rotor hub type, terrain and weapon parameters. Simulation result and pilot comments were extremely favorable as to the engagement realism and the system design.

Many new system capabilities and features for the VMS resulted from the HAC simulation. A second independently maneuverable visual eyepoint was developed to give both red and blue aircraft pilots an out-of-the-cockpit visual scene. A simplified set of kinematic equations of motion for the target ship was implemented which generated smooth and realistic flightpaths from the pilot's joystick controller inputs. An entirely new visual data base was delivered from Singer-Link which allows for smooth occulting between two aircraft when terrain features intervene. A line-of-sight algorithm was also developed to signal when occulting occurred. A system of head-up and head-down displays was designed to give both tactical and flight information to each pilot. Finally, a playback and record feature on the CGI system was modified to allow replays of representative flightpaths.

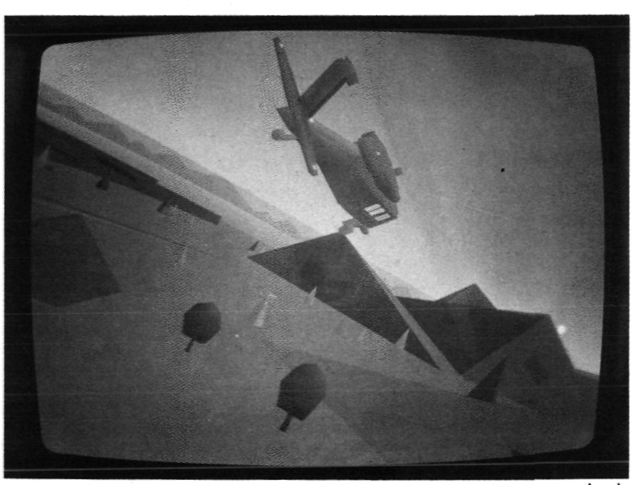

Lewis

Helicopter air combat simulation scene

(M. Lewis, Ext. 6115)

Modern Design Methods for Rotorcraft Flight Control

The CH-47B VTOL System Technology Applications Rotorcraft (VSTAR) has just completed a program to demonstrate the use of modern multivariable control design methods for rotorcraft flight control systems. These new techniques are attractive since they permit the control loops for all axes to be designed at the same time, rather than sequentially as is the case when using classical techniques. Under a grant to Stanford University, a control system design methodology has been developed that initially uses linear quadratic Gaussian methods to obtain a stable compensator giving desired control characteristics. The complexity of this high order regulator/Kalman filter pair is then reduced using balanced realization methods, and the resulting suboptimal form is reoptimized using a finite-time dynamic programming method (also developed at Stanford). A robustness feature is included at this stage of the design to yield the controller giving the best performance for any number of neighboring operating conditions. Finally, the compensator resulting from this design method is converted to a minimal block diagonal form that simplifies its implementation in the flight computer.

With the direct participation of the Stanford researchers, two separate pilot-in-the-loop controller designs using this method have been implemented and flight-tested in the CH-47. The first was a relatively simple longitudinal two-control stability and command augmentation system (SCAS) intended to prove the feasibility of the design method. These tests were successfully carried out in April 1984, providing the confidence to undertake a second more ambitious design consisting of a hover-hold and an associated translational-rate-command system for near-hover maneuvering. Both systems have shown performance in flight comparable to that obtained from simulation runs during the design process.

(W. Hindson, Ext. 5008)

Ultrareliable Fault-Tolerant Control Systems (UFTCS)

A fault-tolerant flight control system concept capable of delivering less than 10^{-13} per hour probability of failure is being examined by researchers at Ames Research Center. The concept is predicated upon configuring the redundant members of the system as independent entities, thereby providing for construction of a fault-tolerant system whose elements have no common features. (Common features limit achievable system reliability and are a major reason for catastrophic loss of fault-tolerant system function.) Multiple versions of the application program are run on dissimilar hardware. Fault tolerance is achieved through the use of static redundancy management. As the redundant elements exist as autonomous members of the system, it is possible and advantageous from the perspective of survivability to disperse the elements throughout the structure under control.

The research program includes a grant with the City University of New York and contract studies with Search Technology, Inc.

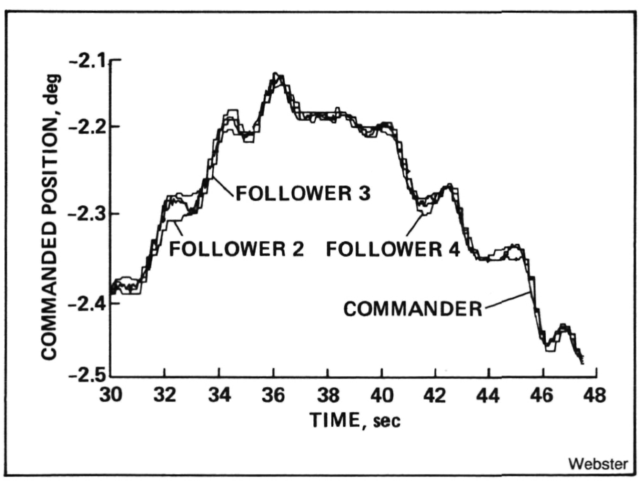

Independently generated UH-1H pedal commands

A working example of a UFTCS has been configured and tested at NASA Ames Research Center. It is a microprocessor-based, quadraplex-redundant, control system configured with independently operated redundant elements. The system is structured to provide real time control of all four axes of a UH-1H helicopter. Laboratory and manned simulation testing of the device have proven highly successful with several hundred simulated "flight" hours having been logged to date. The four channels have demonstrated acceptable votable levels of channel divergence. During simulated flight, the redundantly separated control values for each of the four axes remain within 0.1° (0.7% full scale) of full agreement.

(L. Webster, Ext. 5941)

Development of Computer-Generated Imagery for Flight Simulation

Providing high quality visual displays for handling qualities flight simulation research has provided the impetus for development of unique computer generated imagery (CGI) concepts.

A major drawback to using CGI in flight simulation has been that current technology limits the amount of detail that can be presented in the scenes, resulting in a very simplistic, "cartoonish" picture. This lack of detail translates into a lack of motion cue information necessary for valid handling qualities research.

A major effort has been to evolve concepts of modeling that will provide scenes with adequate motion cues which do not exceed the limitations of the system. Three of these concepts are discussed below.

In many cases it has been found that the classic realism of a scene may be sacrificed to allow presentation of unrealistic, but effective, motion cues. For example, a VTOL landing pad originally consisted of a flat gray surface with appropriate runway and hover pad markings. The flat gray and white surfaces, though realistic in the reproduction of actual landing area markings, provided few motion cues during slow approach and hover. The addition of numerous small features, however, quickly exceeds the scene-detail limitations of the system. The chosen solution was to place a black and white checkerboard over the existing pad and add red and white posts. The addition of larger, more regular features, though unrealistic, provided good motion cues within the limitation of the system. The high contrast of the colors selected enhanced the effectiveness of the cues.

A second concept used has been the addition of "known size" cues to the scenes (e.g., trucks, people, tanks, other aircraft, etc.). These features can be very simplistic, yet will provide the pilot with an easily identifiable object upon which he can base calculations of movement.

A third concept has been to restrict the area of high detail in a data base to the immediate area of interest for a particular simulation experiment. Recent Space Shuttle simulations at Ames required a Kennedy Space Center runway scene. It was found that an accurate and highly detailed representation of the area surrounding the runway could be sacrificed in favor of a high detail area immediately next to the runway and prior to the threshold (see fourth figure). The lower detail area consisted of flat brown squares representing the overall terrain, the Vertical Assembly Building, and the moat surrounding the runway and taxiways. The highly detailed area included multi-colored ground patches, trees, water texture and rocks. By this means, the KSC scene for Shuttle landing simulation was generated within the limitation of the CGI system.

(L. Tweten, Ext. 6171)

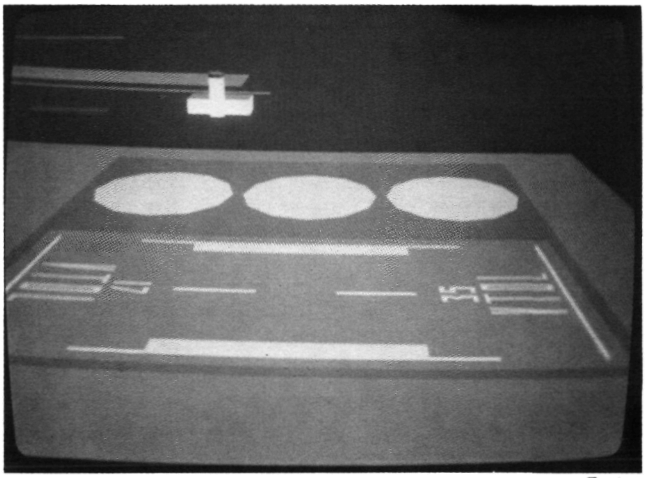

Tweten

VTOL landing area with realistic markings

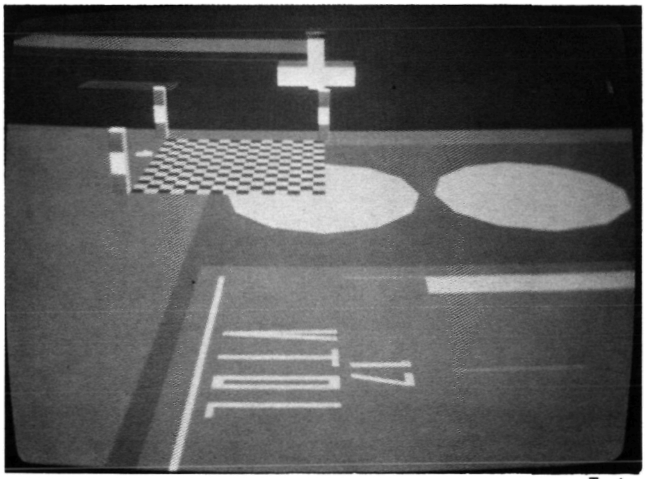

Tweten

VTOL landing area with contrived markings

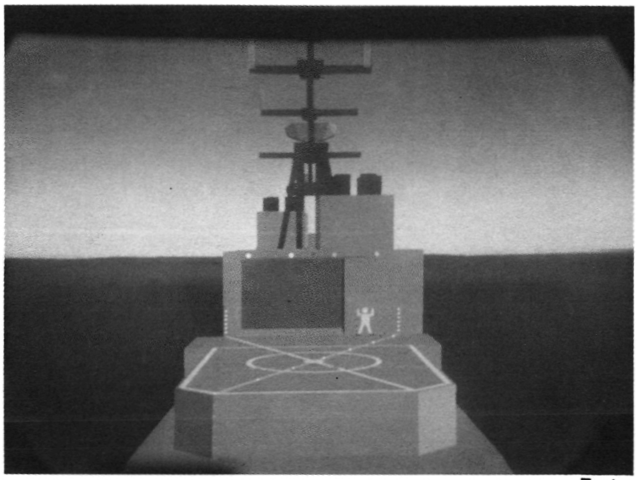

Tweten

DD 963 with landing signal officer

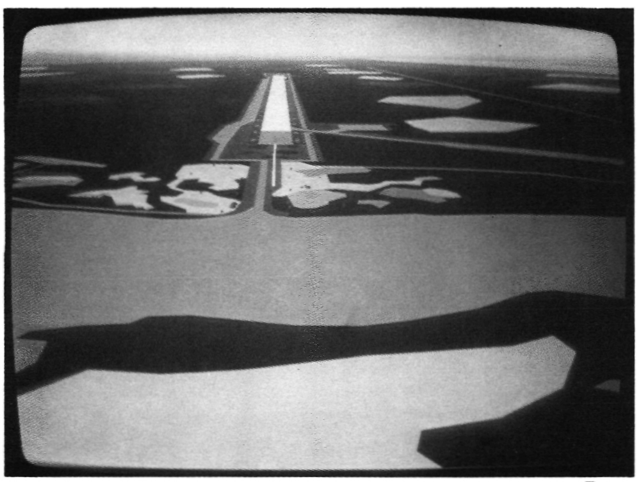

Tweten

Kennedy Space Center runway scene

Air Traffic Flow Management

Concepts for terminal area traffic management using both scheduling and time control (4D) techniques applicable to both 4D-equipped and conventionally equipped aircraft are being studied analytically and in real time air traffic control simulations. This study is conducted jointly with FAA's Technical Center and ARC under a cooperative agreement between NASA and FAA.

A recent simulation evaluated the effectiveness of a new algorithm to predict and control large landing time errors of conventionally equipped aircraft. The problem of how to handle such errors has long been a major obstacle to automation of terminal area flow management. The study was conducted on the ATC Simulation Facility at Ames Research Center with controllers from the FAA's Technical Center participating as

test subjects. The facility includes two air traffic control positions and three pseudopilot positions, and was configured to simulate a portion of arrival traffic at the John F. Kennedy International Airport.

The traffic from two jet routes and a low speed aircraft approach route merged to land on a single runway. Controllers were provided with indicated airspeed advisories — generated by the new algorithm — to help them control touchdown time-errors of conventionally equipped aircraft. It was found that one or two speed advisories issued by the approach controller reduced initial errors of 2 min at 120 n. mi. from touchdown to an acceptable 20 sec at the handoff point for the final controller (25 n. mi. from touchdown). Equipped aircraft, which had negligible time errors, followed their 4D approaches without controller interference. Thus, both 4D equipped and conventionally equipped aircraft were able to maintain their scheduled touchdown times accurately. This increased the orderliness of traffic flow in the terminal area and minimized the incidence of difficult conflicts at merge points to be resolved by the final controller.

Landing rate increased uniformly with increasing percentage of 4D aircraft in the traffic mix even when the percentage of 4D equipped aircraft was fairly low.

Future studies of this concept will introduce piloted simulations of a helicopter and a jet transport aircraft.

(H. Erzberger and L. Tobias, Ext. 5425)

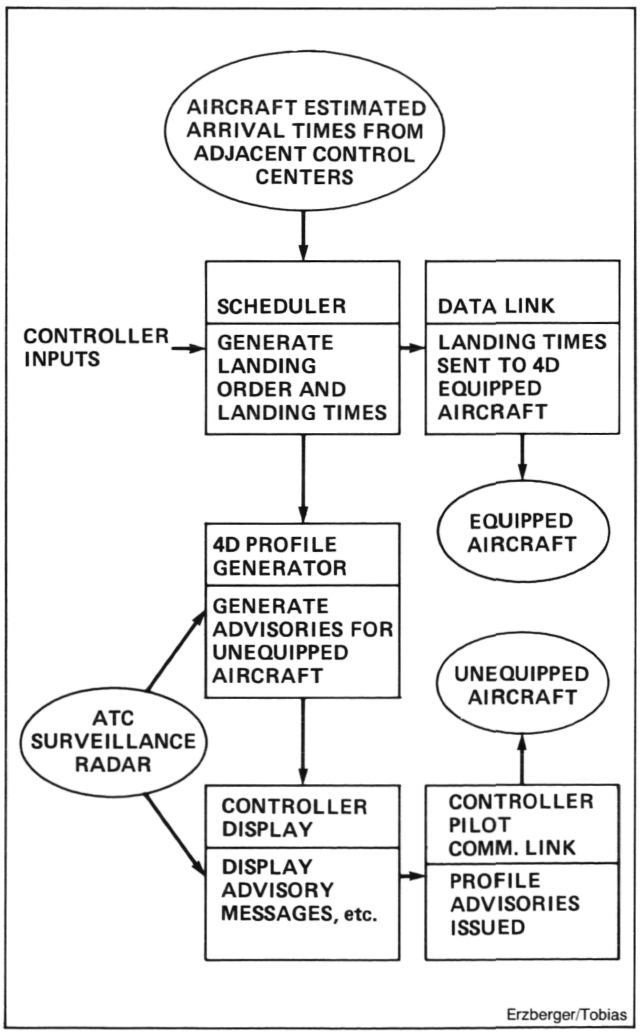

Terminal area traffic management system

Digital Flight Control System Verification Laboratory (DFCSVL)

The DFCSVL, developed under a joint NASA/FAA program, has been utilized to investigate the effectiveness of stress testing and executable assertions to improve the verification process for flight software of digital flight control systems.

Stress testing, developed under a grant with Stanford University, is a technique for dynamically testing DFCS software on a module-by-module basis with a wide ranging input sequence. The outputs of the module under test are compared with outputs generated by an alternate, simplified implementation operating on the same input data. The output differences between the two indicate possible software errors. The current work has focused on the design of a specification language to describe generic flight software functions in order to automatically generate this alternate flight software implementation. (The results

Doane/Saito

Digital Flight Control System Verification Laboratory

of this investigation are being presented at the 6th Digital Avionics Systems Conference in Baltimore.)

The application of executable assertions to test flight software is being studied. Previously, assertions have been utilized in nonreal-time software applications. This study has revealed major differences in using assertions in the flight software environment and has resulted in recommendations for writing assertions for flight software. Experimental investigations were conducted into the effectiveness of assertions in finding various categories of software errors in modules coded in AED and PASCAL languages. (Results of this study are being presented at the 6th Digital Avionics System Conference and the 18th Asilomar Conference on Circuits, Systems, and Computers.)

(D. Doane and J. Saito, Ext. 5048)

Severe Turbulence Encounters

Recently, there have been a series of severe turbulence encounters involving wide-body airliners at altitudes from 37,000 to 39,000 feet. The nature and cause of this high-altitude turbulence is being investigated in conjunction with the National Transportation Safety Board, using the time-history data available from the digital flight-data recorder onboard the aircraft. These flight data, along with air traffic control radar data, are used to reconstruct the turbulent wind environment. The results from the analysis indicate the airplanes encountered vortex arrays which were generated by destabilized wind shear layers associated with strong temperature inversions near the tropopause. The destabilization of the wind-shear layers appear to be caused by lower-level barriers such as a mountain range or line of thunderstorms. The encounters have been found to be in the lee wave at a location about 14 to 30 miles downwind of the lower-level barrier.

Vortex modeling is being used to achieve a better understanding of the periodic, deterministic nature of the severe turbulence. The vortex parameters such as size, strength, and spacing obtained from the airline flight data appear consistent with predicted values based on previous theory and ground-based observations. These vortex models obtained from the wide-body airline flight data provide a way to simulate and investigate the operational problems for the other types of aircraft that unexpectedly encounter this severe turbulence.

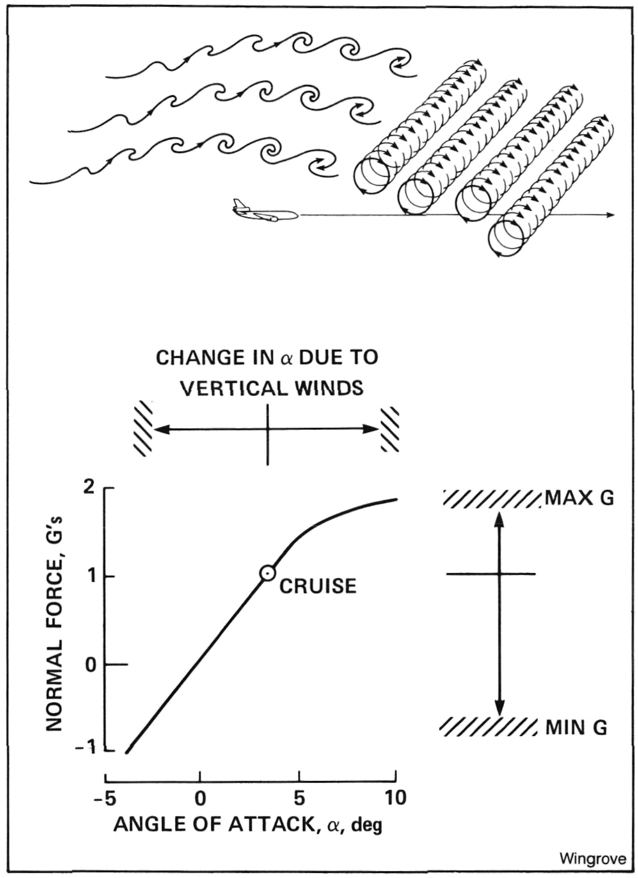

The formation of turbulent vortices at high altitudes

(R. Wingrove, Ext. 5429)

Rotorcraft Cockpit Intelligence Laboratory

A Rotorcraft Cockpit Intelligence Research facility has been developed to investigate the impact of advanced digital avionics systems on rotorcraft single pilot IFR missions. The baseline digital avionics was developed under a contract with Honeywell, Inc., by modifying the demonstration Advanced Avionics System.

The facility consists of a fixed-base rotorcraft simulator having a flexible panel and a baseline digital avionics suite consisting of a moving map display, a multimode autopilot, and a flight management system. The flight management

system includes: 1) a 10 waypoint, 10 navaid RNAV/VNAV system; 2) a performance/flight status system; 3) a configuration monitoring and warning system; 4) a stored check-list system; 5) a computer aided weight and balance system; and 6) a built-in monitoring and maintenance system. The initial experiments will be oriented toward identification of the major difficulties of operating a rotorcraft with the baseline system in the National Airspace System. Future studies will address improvements offered through the use of data link, voice actuation and synthesis, and artificial intelligence.

(G. Callas and B. Nedell, Ext. 5454)

Helicopter Satellite-Based Navigation

The Ames Research Center is continuing a research program to evaluate the use of NAVSTAR Global Positioning System (GPS) to support civil helicopter precision approach and landing. Differential GPS provides significant improvements in performance when compared to conventional GPS systems. This additional performance may prove sufficient to support helicopter precision approach-and-landing operations into areas not currently served by ground-based guidance aids. Offshore explorations, operations into

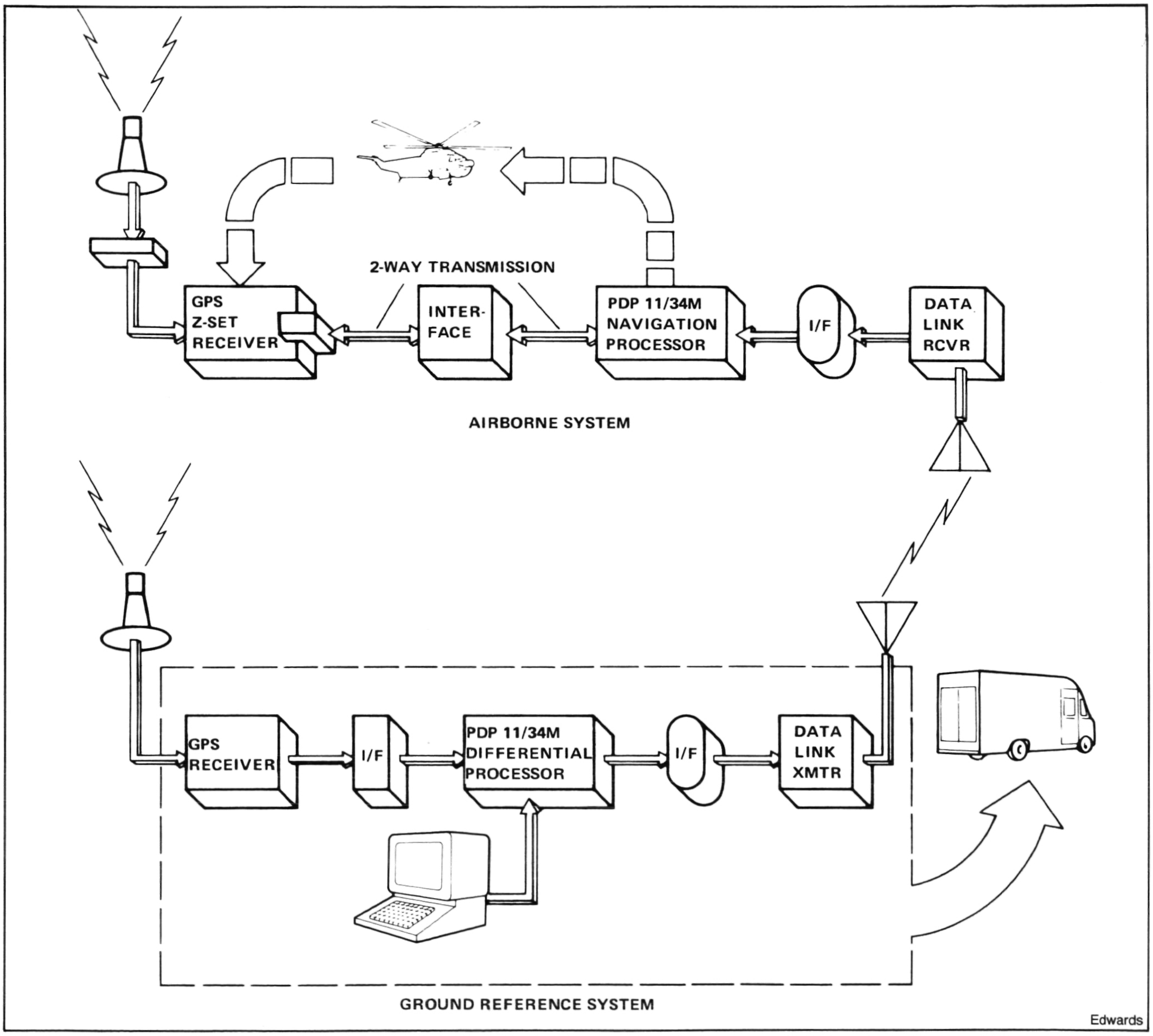

Differential GPS system development

remote and mountainous terrain, and inter/intra city emergency medical rescue are examples of helicopter missions that can be supported by differential GPS.

One of three candidate differential GPS concepts is being evaluated in flight tests at Ames. The concept requires both an airborne and a ground-based GPS system. The airborne research system has been under development inhouse and is being installed in a NASA helicopter vehicle.

Nonreal time differential flight tests were conducted during the late spring 1984 using the partially completed airborne system and an off-the-shelf ground reference receiver. A post-mission merge and analysis of these data resulted in an understanding of the characteristics of the error components of the differential uplink correction information. This understanding will be helpful in establishing the uplink message frequency and data content.

The ground-based component of the differential system is being developed under contract by Ohio University. This system will be installed in a mobile van and delivered to Ames during the fall of 1985. Inflight evaluation of the concept is scheduled for the following winter and spring.

(F. Edwards, Ext. 5437)

NASA/FAA Helicopter Microwave Landing System Curved Path Flight Investigation

Helicopter instrument approaches to airports have long been constrained by the necessity to fly terminal-area approaches that were developed for conventional takeoff-and-landing aircraft. NASA, together with the FAA, has conducted a series of flight tests to address this problem utilizing the Microwave Landing System (MLS). The latest flight test was conducted during the summer and fall of 1983 to develop criteria for operating rotorcraft along curved paths and making steep glideslope approaches utilizing flight director guidance.

Straight-in, U-turn, and S-turn approaches with glideslopes of 6°, 9°, and 12° were evaluated. Eighteen pilots from various elements of the helicopter community flew a total of 221 hooded instrument approaches. The data from these approaches have provided the FAA a data base

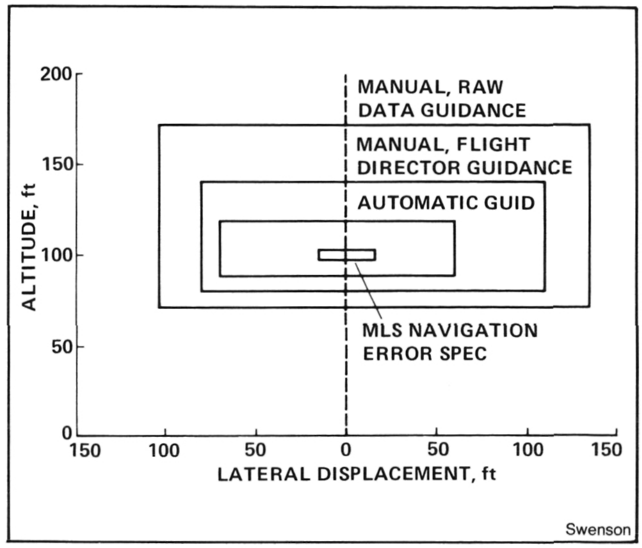

Two-sigma tracking dispersion windows at 100-Foot decision height

for developing Terminal Instrument Procedures (TERPS) criteria for curved path and steep glideslope approaches.

(H. Swenson, Ext. 5469)

Helicopter Airborne Radar Landing Guidance

Airborne radar provides particularly attractive approach and landing guidance concepts for helicopters since it represents a self-contained capability on-board the aircraft, with minimum ground-based navigation facilities. Research programs are in progress at Ames using both high-resolution airborne radar and low-resolution weather/mapping radar to develop improved helicopter approach capability for remote sites.

High resolution radar is a most promising sensor candidate for achieving an all-weather approach and landing guidance capability to remote sites. As an imaging sensor, it can be used for obstacle avoidance and it has the ability to penetrate rain and fog. A research program is under way with the objective of determining the display/control requirements necessary to fly rotary wing aircraft to selected sites in zero visibility conditions using high resolution radar imagery for flight guidance.

Accomplishments on this research program this year include completion of a fixed-base piloted

simulation at Bell Helicopter Textron, and completion of a low-cost, real-time radar simulation developed under a Joint Research Interchange with Harvey Mudd College (HMC). In the Bell study, candidate display symbols to augment the radar imagery were developed. The simulation showed that heading and horizontal situations can be deduced using the radar imagery, but symbols for precise altitude control are required, and horizontal velocity and acceleration symbols are probably required. The next phase of this research program, currently scheduled for the fall of 1985, is to investigate display/control requirements using the NASA/HMC radar simulation mounted in the Ames Vertical Motion Simulator (VMS). This effort will define important criteria for further development of radar derived guidance concepts.

Ames is also nearing completion on another phase of research with an X-band precision approach guidance concept known as the Beacon Landing System (BLS). The BLS combines modern X-band radar technology with digital processing techniques, resulting in ground equipment which is low-cost and portable, and airborne equipment that is easily retrofitted into existing aircraft. Currently, flight tests are being conducted using split-site localizer and glideslope ground stations. A co-located ground station is also being readied for testing. The single, co-located ground station will be approximately 40 in. high, 20 in. wide, and 12 in. deep, and will weigh less than 80 pounds, complete with batteries. The airborne processor is easily installed in the aircraft and provides an ILS compatible output. The airborne equipment was recently installed in a NASA aircraft in less than 5 hours without drilling any holes in the aircraft. Both manual and autopilot-coupled approaches to the split-site ground stations have been conducted. Pilot comments indicate that, from their point of view, the split-site BLS approaches are indistinguishable from ILS approaches.

Clary/Davis

BLS split-site ground stations, localizer and glideslope

(G. Clary and T. Davis, Ext. 5452)

Lull/Swell Guidance for Shipboard Landing Operations

The Landing of a Vertical-Takeoff-and-Landing aircraft aboard a small ship represents a complex and demanding task. The landings must be accomplished at sea onto a moving shipboard landing pad that is approximately 40 ft square. The 15 to 20 sec before aircraft touchdown are especially critical and involve terminal guidance and control problems, not only because the aircraft is disturbed by the airwake turbulence, but because the landing pad is always moving.

To assess the merits of a guidance law that would aid the pilot in determining a landing opportunity, a predictive algorithm was developed and a piloted evaluation performed in a real-time man-in-the-loop simulation on Ames' Vertical Motion Simulator. The algorithm is based upon the alternating lull/swell patterns which are evident in actual ship motions. The algorithm provided a "LAND" or "HOLD" signal which was displayed to the pilot on a head-up display to indicate the initiation and termination of the landing opportunity window.

The results of the study indicated that the pilots were able to determine visually ship lulls and swells prior to landing. However, when using the Lull/Swell guidance system they developed an increased confidence in the existence of a landing opportunity which resulted in significantly shorter hover time prior to landing. The perfor-

mance of the Lull/Swell guidance was conservative in that it forecast the onset of deck lulls and swells later than the pilot could visually perceive them, but it enabled them to land with greater confidence. In no instance did the guidance algorithm falsely predict a ship lull with which the pilot did not agree.

(C. Paulk, Jr., Ext. 5430)

A New Family of Composite Matrix Resins

A new family of composite matrix resins has been developed. These matrix resins are based on copolymers of bisimides with vinyl stilbazoles. This family of polymers is versatile; microstructural variation can produce new and unique properties. When used as a matrix resin for graphite composites this family of polymers resolves three conflicting requirements: 1) retention of properties at high temperature; 2) fire resistance; and 3) processability. Improved impact resistance and toughness are possible with proper selection of monomers.

The development of this class of polymers was reported at the High Temperature Matrix Resin Symposium held at NASA Lewis, the Fortune 500 Review held at NASA Langley, and the SAMPE Meeting, Spring 1984.

The Chemical Research Projects Office has developed a commercial process for this resin so it is available. Numerous requests for licensing and/or for manufacture of these polymers have been received by NASA. Superior secondary composite structures based on this resin have been demonstrated, and composites based on this resin have been shown to have utility for military survivability/vulnerability applications.

(D. Kourtides, Ext. 5226)

Fire Resistant Insulation

Fire resistant interior panels and fire resistant insulation based on aluminized polyether ketone for transport aircraft have been developed at Ames. The fire resistant insulation prevents burn-through while optimizing both the weight and sound insulation qualities. A full-scale fire test of panels and fire-blocked seats has been prepared for this fall.

(R. Altman, Ext. 5986)

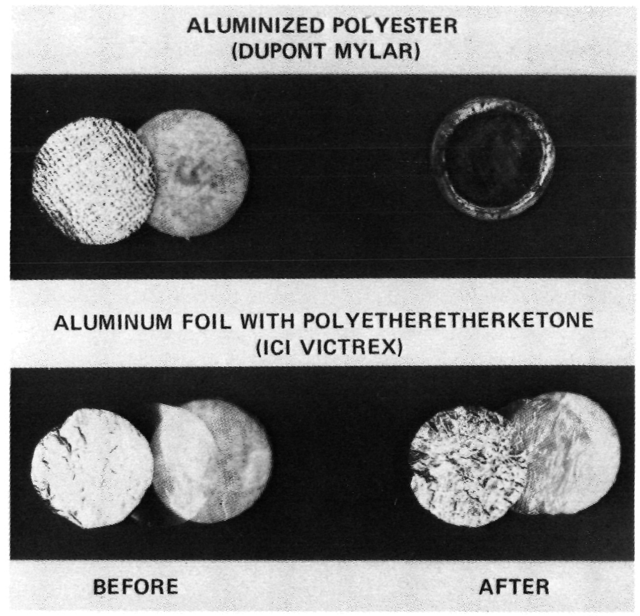

Aircraft sound insulation after five minutes heating at five W/cm²

Computer Code for Processing Control of Filament Wound Case

A processing algorithm to control the quality of the filament-wound case has been developed. This algorithm takes into account kinetically time, temperature, and constitution. It defines the relationships required between these variables needed in the processing of large filament-wound segments for shuttle applications. New processing procedures and instrument control for large filament wound structures have been developed. These include automatic dispensing and metering of the filament winding resin, the use of infrared spectroscopy, dielectric spectrometry, and high pressure liquid chromatography to monitor and control the cure of the resin system.

(D. Cagliostro, Ext. 6190)

Measurements of Fluctuating Temperatures in a Turbulent Flow Using Laser-Induced Fluorescence

A laser-induced fluorescence technique has been developed that provides a practical nonintrusive means of measuring the instantaneous temperatures in low-temperature turbulent flows. Its application to a two-dimensional turbulent boundary layer at Mach 2 is illustrated. The method relies on the fluorescence induced in trace quantities of NO added to a flow of N_2. A temperature is measured with each pulse of a laser system operating at 10 Hz. Measurements are obtained with less than 1% uncertainty in a sample volume having dimensions of less than 1 mm, and with a temporal resolution of 100 ns. An extension of the technique is now being developed to provide simultaneous measurements of temperature, pressure, and density.

(R. McKenzie, Ext. 6158)

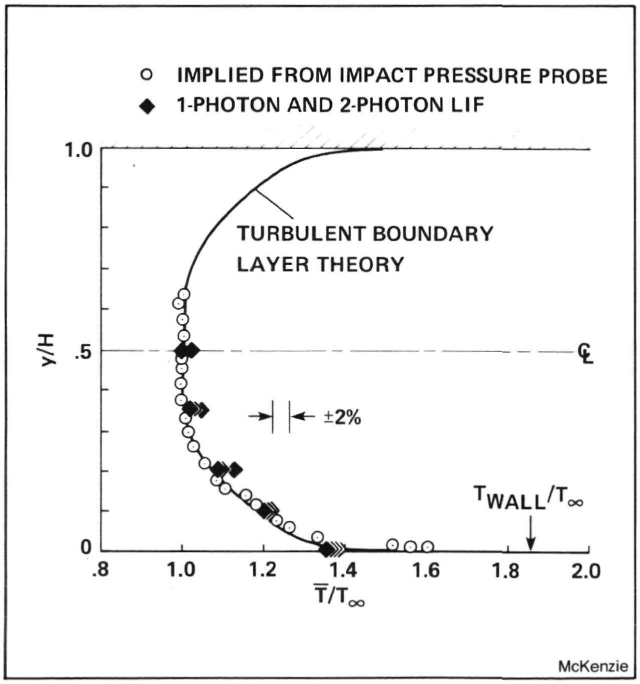

Average temperature distribution through the boundary layer

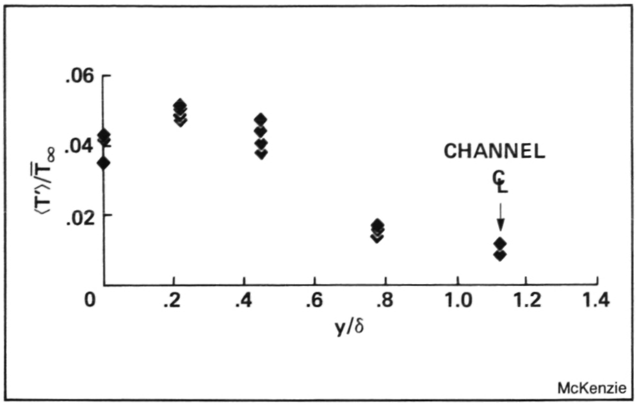

Distribution of rms temperature fluctuations in the boundary layer

Three-Dimensional Turbulent Flows with Massive Separation

The goal of this investigation is to gain an insight into the physics of practical external aerodynamic flow problems — such as the flow around cockpits, fuselage protuberances, control surfaces, etc. — flows which are dominated by massive separation and three-dimensional effects. One such flow was developed over a test body consisting of a right circular cone mounted at an angle of attack on a long cylinder aligned with the flow direction. Flow field and surface measurements are being made in the Ames High Reynolds Number Facility. These measurements will provide a data base for flow model formulation and assessment, which will, in time, lead to accurate predictions of complex flows over realistic shapes.

Preliminary results indicate a massive separation zone (several times the boundary layer height in extent) extending circumferentially around the interaction zone. Computations using a simple two equation eddy viscosity model qualitatively predict surface skin friction lines, mean surface pressures, and the separation shocks. However, the computation significantly underpredicts the extent of the separation zone, indicating the need for a more accurate flow model. Observations of large time-dependent excursions of shock wave position and surface pressures from "mean"

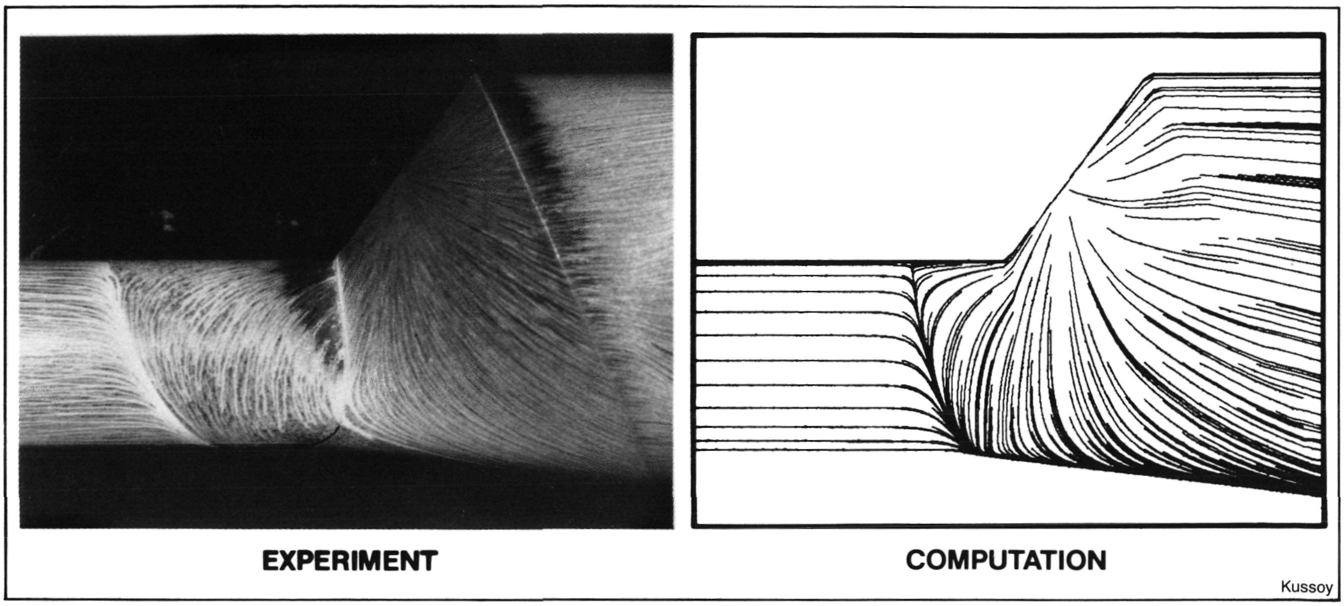

Comparison of experiment and computation for 3D shock wave/turbulent boundary layer interaction flow

valves indicate an important flow mechanism at work which is little understood at present. Observations of these excursions are currently being undertaken using nonintrusive measurement techniques.

(M. Kussoy, Ext. 6452)

Airfoil Measurements in the New Test Leg (HRC-11) of the High Reynolds Number Facility

An experimental study has been conducted of the supercritical flows over the NACA 0012 airfoil at high subsonic speeds in order to acquire aerodynamic data suitable for evaluating numerical-flow codes. The measurements consisted primarily of static and dynamic pressures on the airfoil and test-channel walls and flowfield shadowgraphs. The tests were performed at free-stream Mach numbers from approximately 0.7 to 0.8, at angle of attack sufficient to include the onset of buffet, and at Reynolds numbers (based on airfoil chord) from 1 million to 14 million. A unique test section was employed which was designed specifically for obtaining two-dimensional airfoil data with minimum wall interference effects. Boundary-layer suction panels were used to minimize sidewall interference effects. Flexible upper and lower walls allowed test-channel area-ruling to nullify Mach number changes induced by mass removal, to correct for longitudinal boundary-layer growth, and to provide contouring compatible with the streamlines of the model in free air.

(J. McDevitt, Ext. 5399)

Application of a Three-Dimensional LDV to Turbulent Flow

A three-dimensional laser doppler velocimeter (LDV), developed at Ames, is providing unique new measurements critical to the understanding of turbulence. Using three different color beam-pairs, the LDV simultaneously measures three components of velocity. Components are nonorthogonal (60° angle), and a minicomputer calculates velocities in an orthogonal system. Only velocities measured simultaneously are used to make correlations of the turbulent fluctuations, such as Reynolds stress and triple-products.

One of the first applications of the system was to determine the flow over a cylindrical body with a spinning foresection. The spinning cylinder flow that recovers on the stationary section generates a turbulent boundary layer flow similar to that over a swept wing. Flow in the free stream is aligned with the cylinder, while flow near the spinning cylinder is pulled (by skin-friction) in the direction of rotation. As the swirling flow passes from the spinning cylinder to the station-

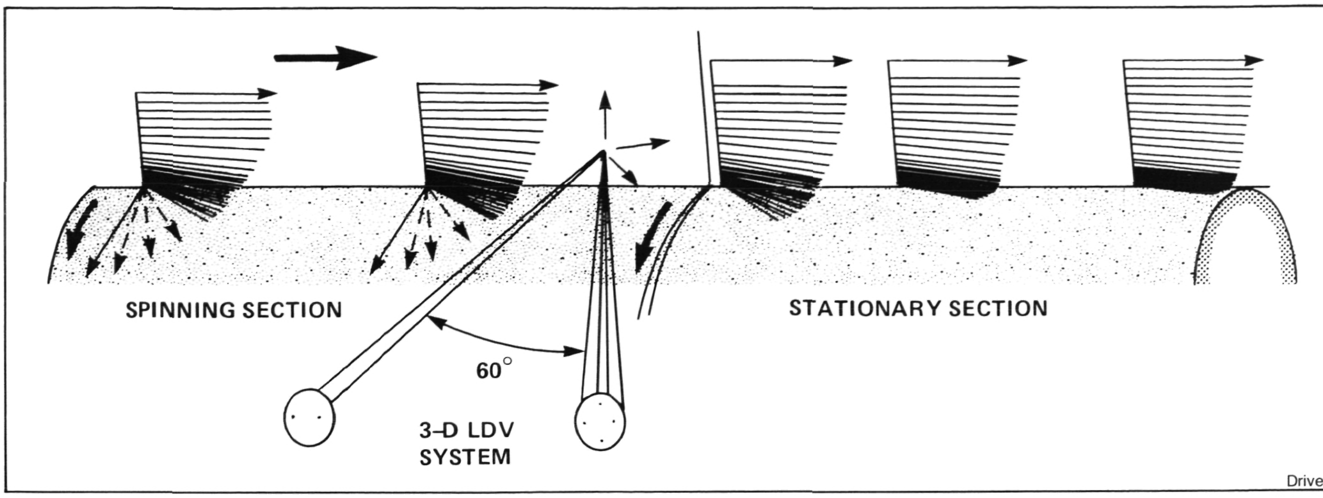

Mean velocity vectors measured with a 3-D LDV

ary section, skin-friction acts to reduce the swirl. These three-dimensional measurements of the velocity and turbulence within the boundary layer are providing turbulence modeling insights never before possible.

(D. Driver, Ext. 6156)

Computer Simulation of Rotating Stall

A rotating stall is an undesirable condition in a staggered cascade where the stall of one blade results in separated flow on the next blade up and attached flow on the next blade down. As a result, a "stall cell" rotates around the cascade and the performance drops drastically. A better understanding of the mechanisms causing rotating stall is required to design compressors and other turbomachinery. It is not possible to use the finite-difference methods to solve the complete unsteady flow field for high Reynolds numbers and complex geometries with currently available computers. Alternate methods must be developed.

A modified vortex method, in which the vorticity field is represented by periodic arrays of vortex filaments, has been used to solve high Reynolds number incompressible flow in two-dimensional cascades. A total of five blades was

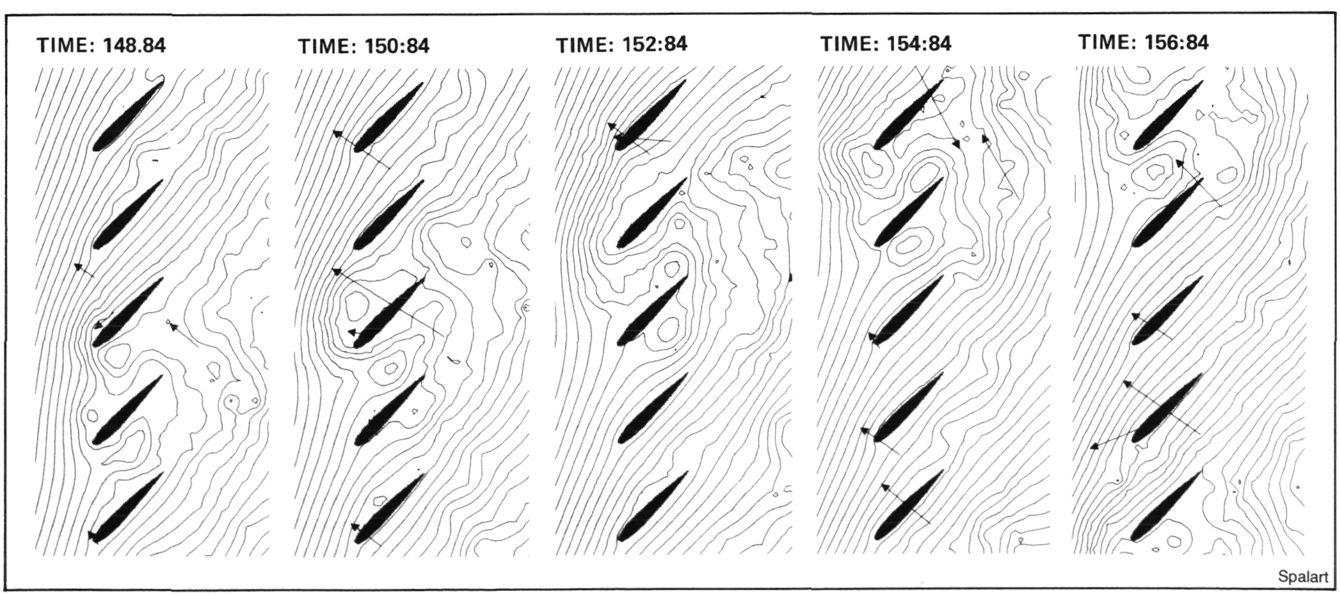

Propagation of a stall cell in a cascade

included in the computational domain with NACA 0012 blade sections spaced with a pitch equal to one chord length. The stagger angle was varied between 45° and 65°, and the angle of attack between 15° and 35°. Rotating stall was observed under certain conditions, and the flow pattern agreed well with experimental results.

(P. Spalart, Ext. 6667)

Adaptive-Grid Method for Fluid-Flow Problems

Adaptive-grid methods are important in computational fluid dynamics because of their potential for improving the efficiency and accuracy of numerical methods. Various adaptive-grid methods have been reported in recent years, but few have been used in practical applications because of their complexity and elliptic character. A practical solution-adaptive-grid method for multidimensional fluid flow problems has been developed using a marching algorithm with the spring analogy. Tension springs connect adjacent grid points and control grid spacing; torsion springs control grid skewness by limiting the inclination of coordinate lines. Multidimensional adaptation is realized by splitting the operation sequence into a series of unidirectional adaptations.

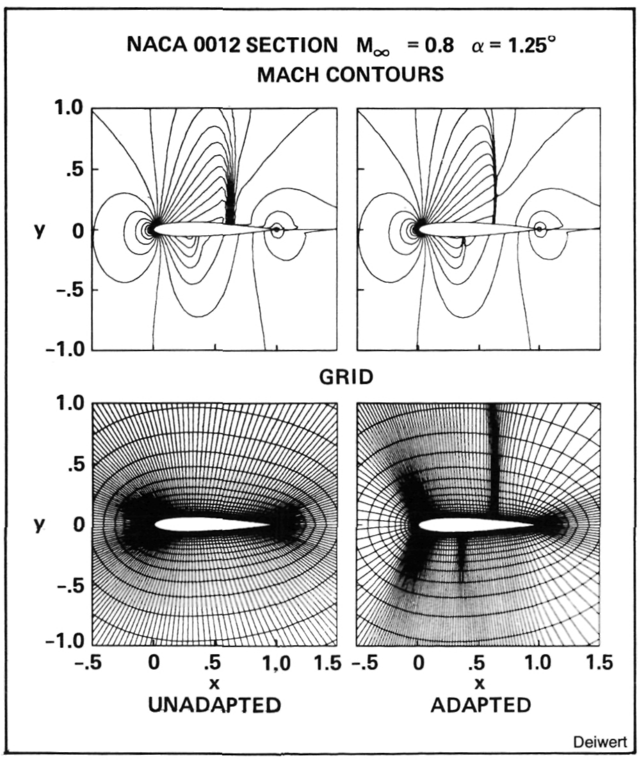

Transonic airfoil flowfield with solution adapted grid

This new adaptive-grid method has been applied to several two-dimensional flow fields, including inviscid flow over an airfoil. The Euler equations were solved for a NACA 0012 airfoil using an initial O-grid. The adapted grid was obtained periodically by clustering points in regions where the solution showed large density gradients. For transonic flow the grid points are clustered near the shock waves that appear on both the upper and lower surfaces. The final solution for the Mach contours shows better resolution of the shock waves.

(G. Deiwert, Ext. 5894)

Design of Diagnostic Probes for Combustion

The results of calculations of spectroscopic properties of diatomic and triatomic molecules are being used to design new nonintrusive diagnostic probes for combustion applications. Theoretical studies are under way to devise methods of monitoring trace species concentrations and gas temperatures encountered during the burning of hydrocarbon fuels. These results are being provided to assist researchers working in experimental aircraft combustion programs at Langley Research Center and Lewis Research Center.

Calculations have been undertaken to simulate multiphoton processes such as Coherent Anti-Stokes Raman Scattering and two-photon absorption in H_2, O_2, and NO. The results of these calculations have been used to provide accurate synthetic spectra, which take into account instrumental effects such as the Stark broadening and shifting of the spectroscopic lines caused by the use of powerful laser fields. New theoretical techniques have been developed to facilitate the calculation of nonlinear spectroscopic transition probabilities. This project is being carried out in collaboration with Dr. W. Huo of the University of Notre Dame.

A diagnostic probe which can be used to measure C_2H concentrations is being designed in collaboration with University of California scientists, Drs. K. Wilson and J. Reimers. For this study, the infrared electronic and vibrational

spectra of C_2H are being synthesized. The low-lying $^2\Pi \leftarrow \Sigma^+$ electronic transition is much stronger than the vibrational transitions and may be used to monitor C_2H concentration in hydrocarbon flames. Believed to be an important transient combustion intermediate and soot precursor, C_2H has not been directly observed in combustion experiments owing to its complete transparency in the visible and UV spectral regions.

(R. Jaffe, Ext. 6458)

Numerical Solution of the Navier-Stokes Equations for Transonic Wing Flow Fields

The numerical solution of Navier-Stokes equations for transonic flow fields about realistic wing geometries has long been a problem of prime importance in the field of computational fluid dynamics. This problem is complicated by the existence of viscous effects which typically arise near performance boundaries or in maneuver conditions. Here the problem is addressed by solving the Navier-Stokes equations about general wing geometries using a block or zonal grid structure. This block-grid structure is utilized for two purposes. First (and most important), it serves to improve the distribution of grid points about complicated geometries. That is, grid blocks far removed from large flow gradients can be relatively coarse while grid blocks near large flow gradients can be fine. In addition, simpler equation sets (e.g., the Euler equations) can be used in regions where all the complexities of the Navier-Stokes equations are not required. Second, since the solution from only one grid block will reside in main memory at a time, the block grid

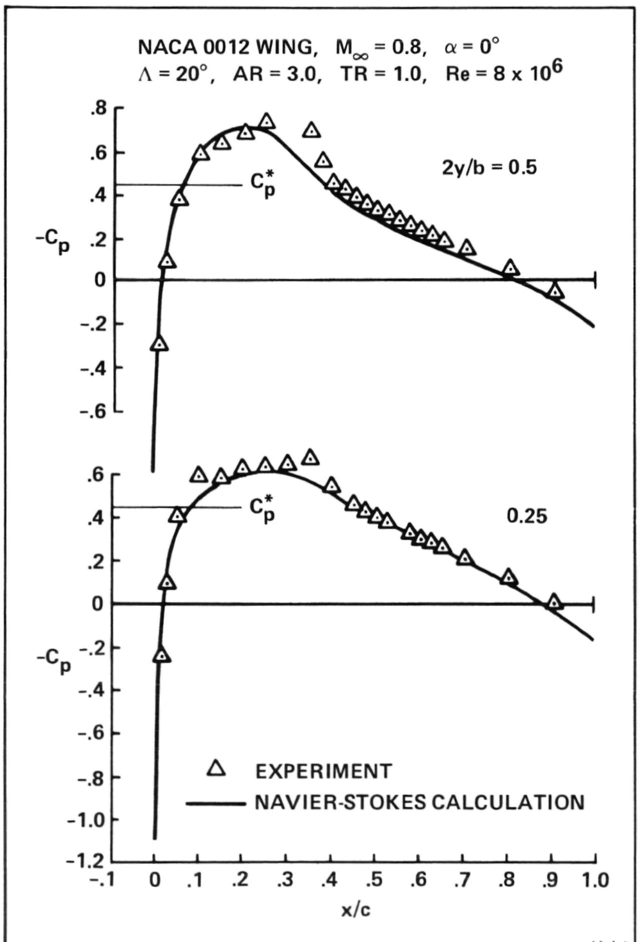

Transonic wing pressure coefficient comparison

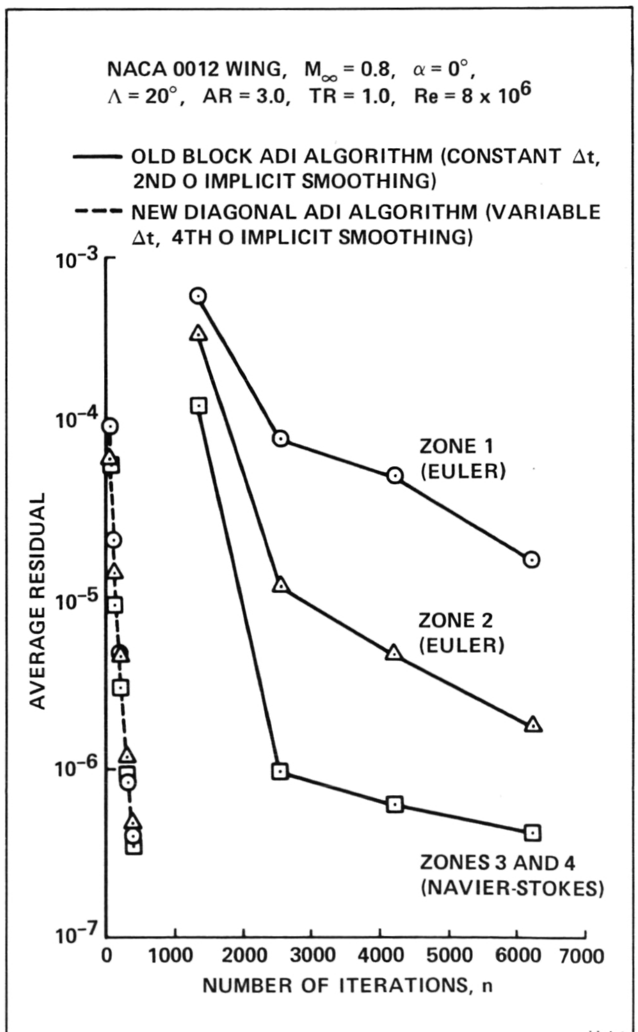

Convergence history comparison

approach provides a convenient mechanism for organizing the data base.

Computed results using this approach are compared with an experiment for a free-stream Mach number of 0.8 at 0° angle of attack. The wing used in this computation has NACA 0012 airfoil cross sections, a sweep of 20°, an aspect ratio of three, and a taper ratio of one. The finite-difference grid for this computation consisted of about 100,000 grid points divided into four zones (two Euler and two Navier-Stokes) and required a total data base of about 4 million words. This computation required about 15 min of CPU time on the CRAY-XMP computer which represents a dramatic improvement in efficiency over older Navier-Stokes flow solvers as shown by the comparison between the new diagonal ADI and old block ADI convergence histories.

(T. Holst, Ext. 6415)

Numerical Minimization of Drag for Wings in the Transonic Speed Regime

The minimization of the drag-to-lift ratio for transonic cruise has long been a central problem with regard to aerodynamic efficiency for a wide variety of aircraft. This problem has been successfully addressed for isolated wing geometries using a numerical optimization technique. The large computational cost usually associated with numerical optimization is eliminated in the present study by using the CRAY-XMP vector computer coupled with the very fast TWING full potential analysis code and the very efficient QNM numerical optimization code. The computer time required by TWING for a typical wing analysis run on the CRAY is about 10–20 sec. Since an entire wing optimization requires on the order of 100 analysis runs, a typical wing design requires about half an hour of computer time.

Unlike all other design techniques, the present approach has several significant advantages. First, this procedure produces an optimal design, and although the ultimate efficiency of the resulting design depends upon how the design space is defined, no other design procedure can make this claim. Second, the final design shape and resulting pressures are obtained as a direct result of the present procedure. In many design procedures the pressures must be specified and the resulting

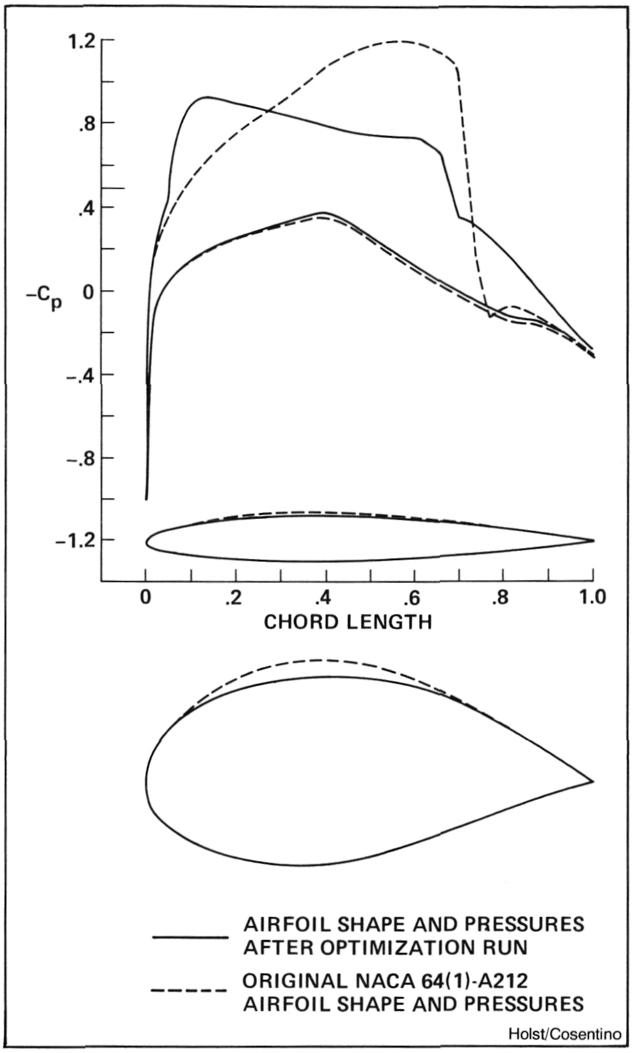

TWING/QNM drag-to-lift ratio minimization result - Gates Learjet Century III wing: 48.5% span station

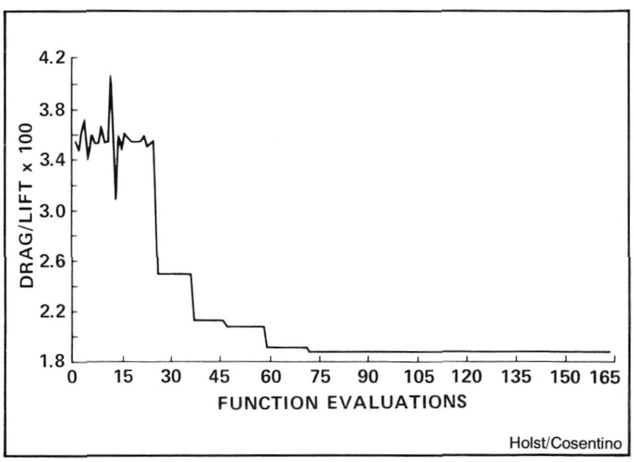

Objective function (C_D/C_L × 100) versus the number of TWING flow solutions: Learjet wing case

shape is then computed. Third, optimal designs which are not shock free may be obtained. Since the most efficient cruise point may actually contain a weak shock, the present approach is superior to one which produces inherently shock-free results. Finally, this approach theoretically allows optimal design around multiple design points. No other design method can make this claim.

An example design by numerical optimization is shown for the Gates Learjet Century III wing. The wing shape and pressure distribution before and after the design are shown at mid-semispan. Note how the strong shock has been replaced by a very weak shock and that the forward loading on the airfoil has been increased largely to maintain the lift. A plot of the drag-to-lift ratio versus the number of function evaluations (wing analysis runs) is also shown. In just 72 function evaluations (drag/lift) × 100 has been reduced by about 50%).

(T. Holst and G. Cosentino, Ext. 6415)

Fast Simulation of Separated Transonic Airfoil Flow

A computer code was developed which is capable of simulating the separated transonic flow about airfoils using a minimum of computer time. The approach used is to simulate the inviscid and viscous regions of the flow field separately using specialized, very efficient flow-solvers. Specifically, the inviscid flow is modeled by a solution of the transonic full-potential equation. Simulation of the viscous regions is achieved by solving the partial-differential boundary-layer equations using a fast algorithm developed for this application. New interaction algorithms were also developed to couple the inviscid and viscous solvers.

Some results of the new code are compared with experimental and Navier-Stokes pressure distributions. Good agreement is obtained. Trailing edge separation is present in both of these cases, while shock-induced separation is also present in the NACA 0012 case. The computer cost of the present method is from one to five percent of that required by the Navier-Stokes algorithms. These new tools are presently being extended to compute unsteady three-dimensional separated flows.

(W. Van Dalsem, Ext. 6741)

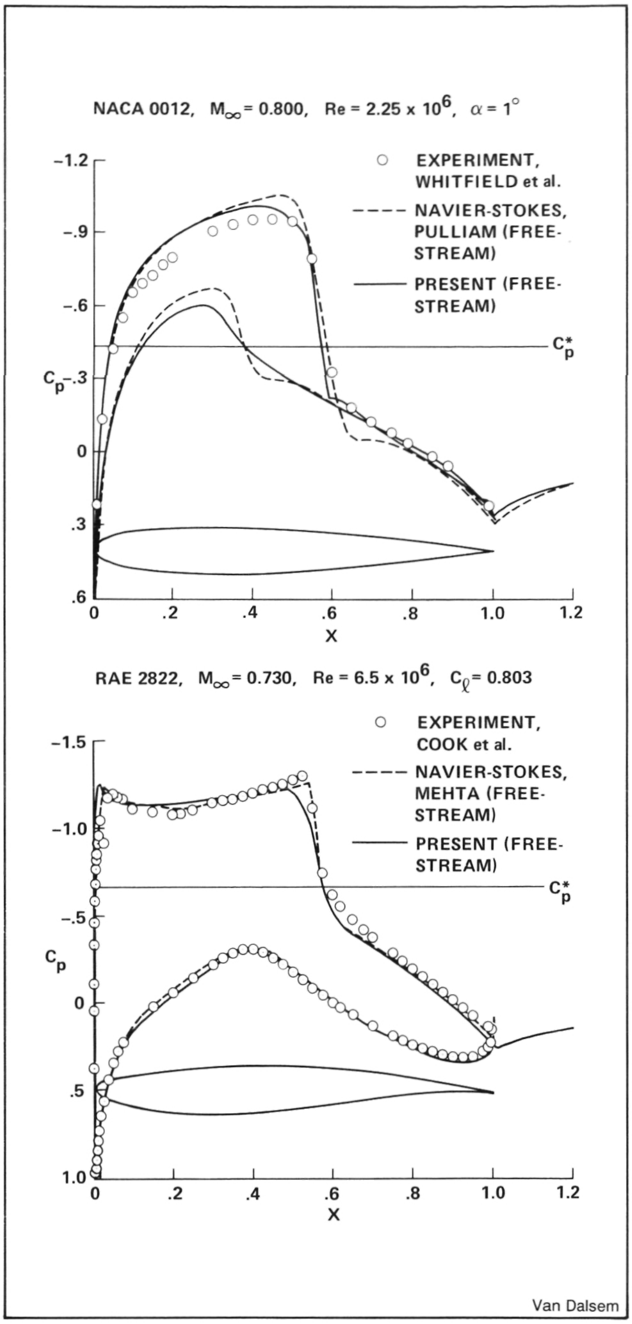

Calculated and experimental C_p distributions

Computational Aerothermodynamics

Recently, a parabolized Navier-Stokes (PNS) code has been used to predict the aerothermodynamics of various aircraft configurations flying at or above the supersonic flight regime. The PNS equations are obtained from the complete Navier-Stokes equations by neglecting the unsteady terms and the streamwise viscous derivative terms. The present code uses the Beam-Warming implicit algorithm to update the interior of the region and characteristic, implicit, spatially second-order-accurate boundary conditions at the outermost shock wave. An elliptic grid generation is used to generate the grid at each marching step.

Numerical results for a turbulent flow past the Space Shuttle Orbiter have been calculated. The flow conditions are: $M_\infty = 7.9$, $\alpha = 25°$, $T_{wall} = 540°$ R, and $Re_L = 60{,}728$/in. The three-dimensional blunt-body code was used to obtain the starting planes for the PNS marching code. This solution was then marched downstream using 61 points in the meridional direction and 45 points in the radial direction. The figure presents the computer-generated particle paths for this case. The particles are injected into the flow field and allowed to convect downstream based on the local flow field properties. Specific features are the vortices on the lee, one set of which are due to the strake-wing. At this angle of attack, the strake-wing vortices will impact on the OMS pod.

(D. Chaussee, Ext. 6742)

Space Shuttle Main Engine Flow Analysis

The overall goal of the current engine redesign effort is to double the Space Shuttle payload by increasing the rated thrust of the main engine by 30%.

A computer code has been developed which permits simulation of the flow field around and inside a variety of practical configurations. This code (INS3D) solves incompressible Navier-Stokes equation in three-dimensional curvilinear coordinate systems. INS3D is being used to analyze the flow field in the current engine power head. The computational fluid dynamic (CFD) analysis provides diagnostic information not readily available from experiments and computed flow features compare favorably with experiments. Both this CFD analysis and experiments show that the center duct of the current three-duct configuration is ineffective. This research version of INS3D is being used for parametric study in the redesign process and will have significant impact on future Space Shuttle engine design and experiments. This is a joint effort by the Applied Computational Aerodynamics branch at Ames and Rocketdyne Division of Rockwell International. Marshall Space Flight Center has also been supporting this activity at Ames.

(D. Kwak, Ext. 6743)

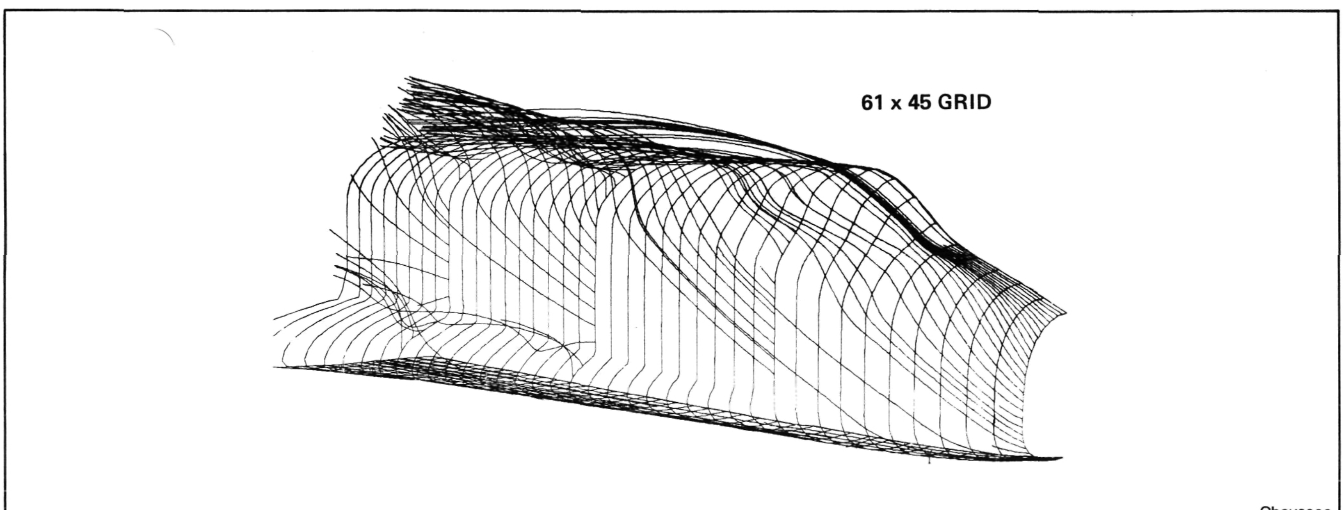

Turbulent flow past the space shuttle

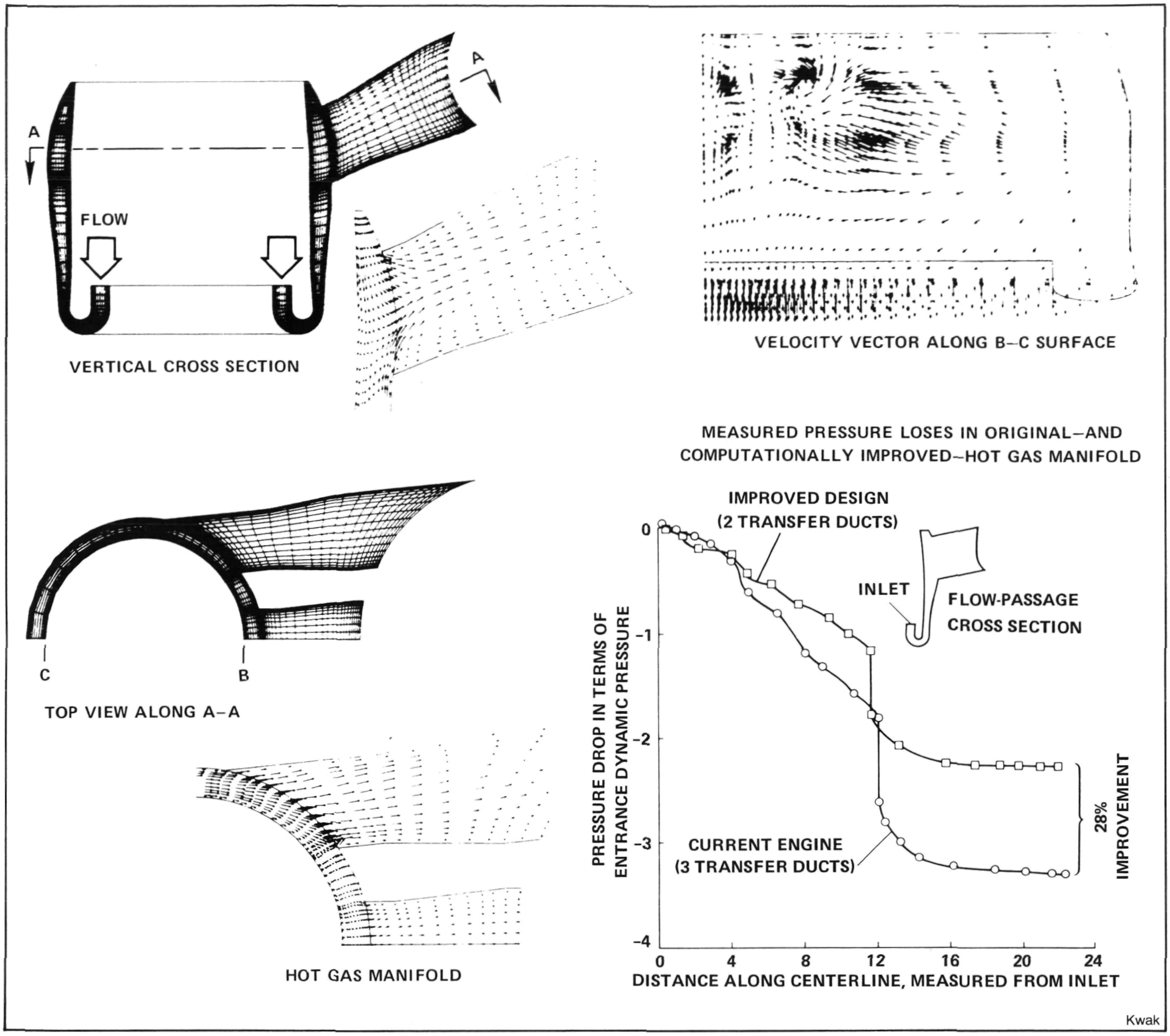

Space Shuttle main engine power head analysis using INS3D

Transonic Aeroelastic Analysis

The study of transonic aeroelastic characteristics of wings is important, especially for the design of modern fighter aircraft. The transonic regime, which is optimum for cruise, may be critical from an aeroelastic point of view. For example, flight tests have indicated that the B-1 wing has aeroelastic oscillation points at M = 0.72 with a low sweep angle, and at M = 0.91 with a high sweep angle. To study the transonic aeroelastic characteristics of such wings, a computer code ATRAN3S has been developed. This code solves the small-disturbance, unsteady, transonic, aerodynamic equations of motion simultaneously with the structured modal equations of motion. Time-accurate, finite-difference schemes are used for solving both the aerodynamic and aeroelastic equations of motion. The code can be used for both coupled and uncoupled aeroelastic analysis. In addition, this code can account for viscous effects (AIAA Paper 84-0870-CP). The code has been successfully applied to typical transport wings (AIAA Paper 83-0922-CP) as well as to a fighter aircraft wing, the F-5 (AIAA Paper 84-0872-CP).

(P. Goorjian and P. Guruswamy, Ext. 5547)

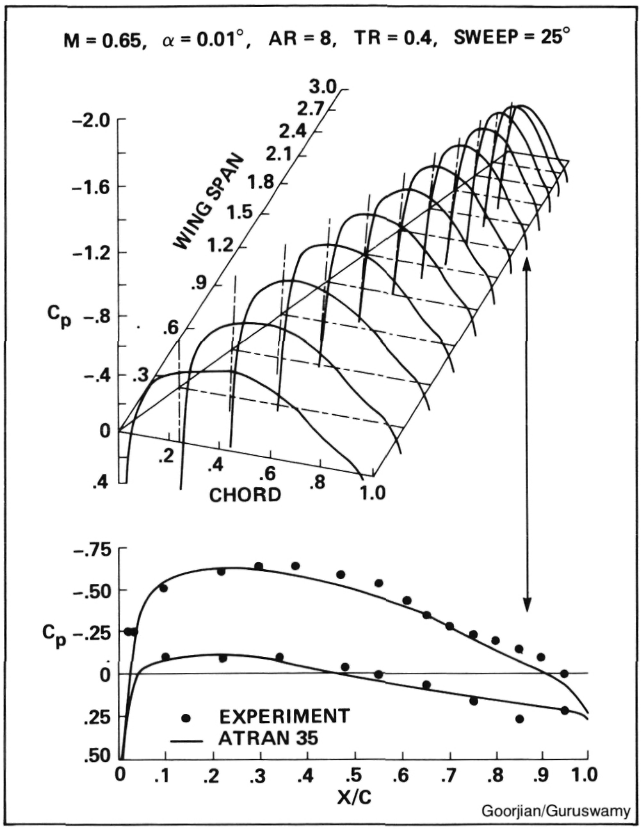

Aeroelastic analysis of the B1 wing

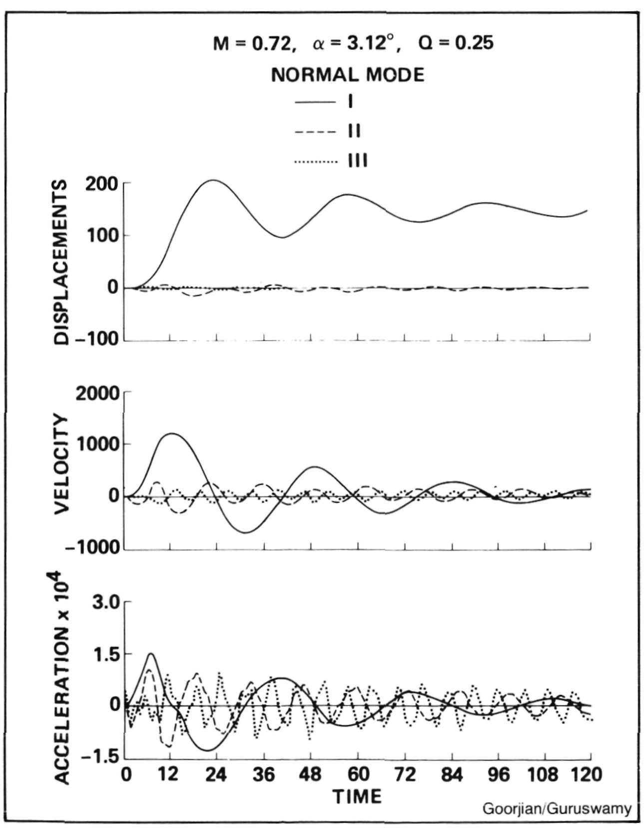

Dynamic aeroelastic response

Atomistic Simulation of Materials

The process of crack propagation has been simulated in the computer (CRAY-XMP) employing a molecular dynamics technique based on the Nordsieck-Gear algorithm. The present software is able to handle systems containing up to 10,000 particles interacting via two-body potentials. Particles in the systems have been treated discretely, and quantities such as energies and stress components are all recorded for many thousands of time steps for statistical averagings. The crack propagation process was modeled imposing a tensile load on a perfect triangular lattice (which is the basal plane of a hexagonal close-pack crystal) containing a small surface crack. Both two- and three-dimensional crystals have been studied. The crack propagation velocity, which was initially close to the sound velocity, was found to be linearly related to the averaged total stress.

The temperature dependence of these crystals has also been investigated. Preliminary results show that the relative temperature dependence of copper crystals agrees with the temperature dependence of the strength of copper whiskers.

These findings indicate that the present simulation method can be used to elucidate complicated mechanisms which are important in the fundamentals of materials strength and failure. This work was conducted in collaboration with Dr. T. Halicioglu of Stanford University.

(D. Cooper, Ext. 6213)

Properties of Molecules and Atomic Clusters

The determination from calculations of the properties of molecules and atomic clusters continues to produce important results for predicting and understanding the properties of matter. Studies have been completed on atoms and diatomic molecules consisting of transition metals (Ni, Cu, Fe, Sc, and Cr) and gaseous species (H and O) which have led to a detailed understanding of metal-metal and metal-gas chemical bonding for simple systems. More approximate, but comprehensive, calculations have been completed for clusters of up to 66 atoms (e.g., Al_{13}, $Ni_{25}O_5$, $Li_{39}Fe_n$, and Fe_nH where $n \leqslant 66$, and $Be_{13}X_2$ where x = H, O, S, Cl, and F. This information has been used to resolve misinterpretations on

nickel-oxygen surface physics experiments and is leading to an understanding of one aspect of how hydrogen dissolved in ferrous materials drastically increases the metal's susceptibility to crack initiation and propagation.

A computational research program has been initiated to study the relationship between the molecular structure and the observed properties of polymeric materials. The first systems to be studied were poly(methyl methacrylate) and poly(ethyl methacrylate) owing to the large amount of experimental data available. The computed conformational energies and torsional barriers are in excellent agreement with the experimental data. However, we disagree with the interpretation of the experimental torsional data. We find that the alkoxy group rotation is highly hindered and that the entire ester side-chain rotation is relatively facile. A more detailed comparison of the computational and theoretical results is in progress.

(D. Cooper and R. Jaffe, Ext. 6213/6458)

Aero-Assisted Orbital Transfer Vehicles

Conceptual studies are being performed using vehicles that would 1) extend the utility of the Space Shuttle, and 2) make effective use of Earth-lunar space. By performing vehicle maneuvers in the upper layers of the Earth's atmosphere, the payload can potentially be increased threefold by reducing fuel requirements.

Two generic vehicle concepts show particular promise. One is primarily useful for transporting large payloads between two low Earth orbits, or from low Earth orbit to distant locations (such as geosynchronous orbit, or a stable libration center at lunar distance). The vehicle maneuvers primarily by drag in the Earth's atmosphere, and achieves orbit-plane inclination change propulsively at its apogee where fuel requirements are minimal.

Concurrent studies of the effective use of Earth-lunar space by such vehicles involve the subtle interaction of many physical phenomena. Results are nonintuitive; for example, a given vehicle can retrieve three times the payload from a distance of five times geosynchronous orbit as it can from simple geosynchronous orbit.

A second generic vehicle concept is a high-lift configuration. This high-lift capability is essential if time-constrained maneuvers are to be made with aeroassist for low Earth orbits. The lift/drag ratio is a measure of the advantage of aerodynamic maneuvers over propulsive maneuvers in the upper atmosphere. The flight trajectory of the high-lift device is a compromise between the benefit of leading-edge heating reduction, and the liability of the lift-drag ratio degradation as altitude is increased. High altitude maneuvers can be achieved by a very shallow entry wherein the lifting surface is rolled such that the lift vector is more than 90° from the vertical. That is, there is a strong "horizontal lift" component and a small "negative lift" (downward) component. This maneuver results in lower leading-edge heating rates but longer heating pulses. Further investigation is being done for an advanced version of this concept that can descend through the atmosphere and land on the Earth.

(J. Howe, Ext. 6113)

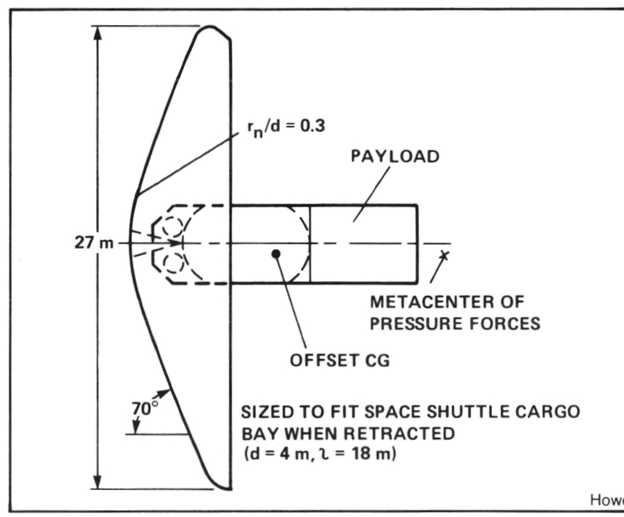

Aeroassisted orbital transfer vehicle

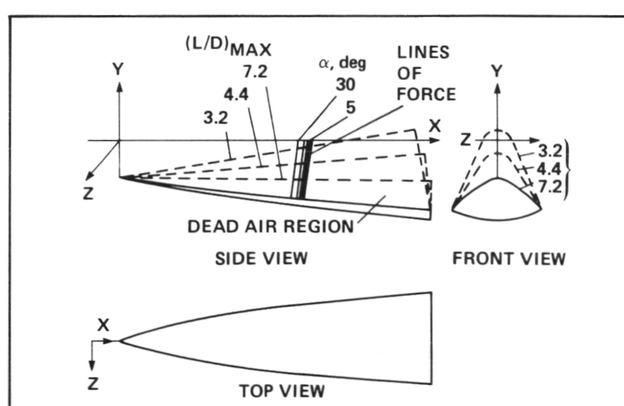

High lift aeromaneuvering vehicle

Space Shuttle Thermal Protection System

The thermal protection system of the Orbiter Discovery, launched in August, included Fibrous Refractory Composite Insulation (FRCI-12) for the first time. The new tile material replaced most of the LI-2200 used on earlier orbiters (about 10% of the shuttle silica tiles), saving 1000 pounds in structural weight. The new aluminoborosilicate material has a lower density and is stronger than earlier heat shield tile materials.

Nearly all of the 8000 white low temperature (LRSI) tiles and some of the coated Nomex felt (FRSI) were also replaced on Discovery with 2300 Advanced Flexible Reusable Surface Insulation (AFRSI) quilts. These new flexible fibrous, silica quilts have been used in limited areas on previous orbiters, but Discovery is the first to have most of the upper surface so covered. The AFRSI, with a new ceramic coating developed by Rockwell International Space Division, offers higher temperature capability than the FRSI, and improved durability, simplicity, and lower weight than the LRSI it is replacing.

(H. Goldstein, Ext. 6103)

Use of Concurrent Computer Architectures to Solve Computational Fluid Dynamics Problems

The CRAY X/MP-22 has been used as a multiple-instruction stream, multiple-data stream (MIMD) computer to solve computational fluid dynamics problems. This required that the spatially split algorithms be partitioned so that half of the grid could be updated by each of the two processors contained in the CRAY X/MP-22. The processors would both have to completely update their half of the sweep prior to beginning the next sweep. Efficiency was found to be greater than 0.9, where efficiency is defined by

$$E = \frac{T_1/T_n}{n}$$

where E is efficiency, T_1 is time to execute on a single processor, T_n is time to execute on a multiprocessor, and n is the number of processors.

A large eddy simulation program was further partitioned to utilize the four processors of a CRAY X/MP-48 located on the CRAY Research Incorporated Software Development Facility. The efficiency, using four processors, remained above 0.9. Additional experiments are planned to determine the efficiency of common memory multiprocessors with up to 64 processors. The work to date indicates that spatially split algorithms such as the full potential, Reynolds-averaged Navier-Stokes, and large eddy simulation algorithms developed at Ames will be able to make efficient use of the increased speed offered by multiprocessors containing a moderate number of processors.

(K. Stevens, Jr., Ext. 5949)

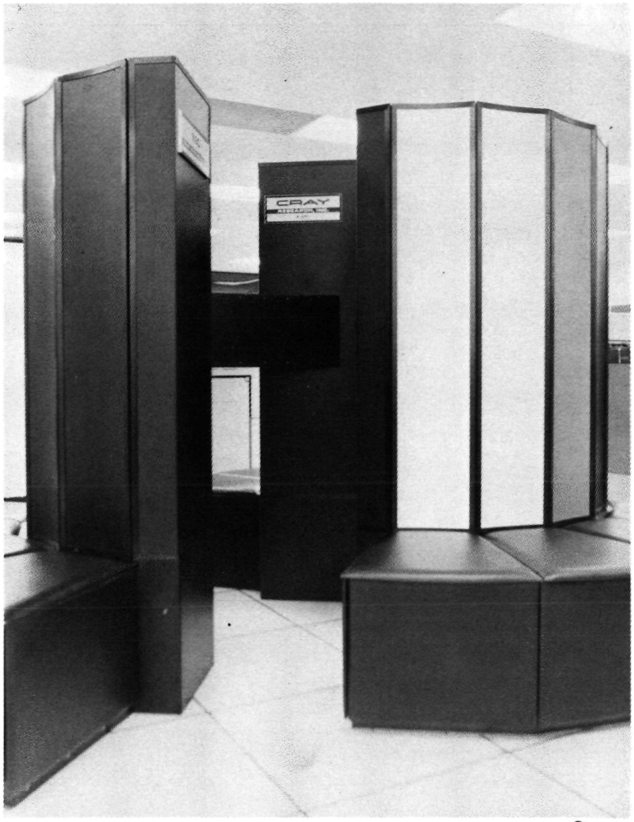

CRAY X/MP-22 computer

Stevens

An Aero De-icing Device Using Electro-Expulsive Forces

There is a need for a means of removing ice from aircraft surfaces such as helicopter rotor blades. A suitable system using electro-expulsive

forces has been developed which has force being generated by pulse currents flowing in opposite directions in parallel conductors.

Calculations of forces needed to remove ice from aero surfaces show that the current required is several thousand amperes. This requirement has previously prevented the use of such a device for removing ice because of the need for large and heavy motor-generators. Many types of de-icing systems have been developed using such techniques as electro-thermal, electro-magnetic, pneumatic boots, hot air, hot oil, and chemical spray. Each has limitations. Patents have been issued in the last fifty years on the electromagnetic repulsive force concept, but none have been issued on a practical expulsive device for aircraft. Aircraft usage requires a system with low power, low weight and small size. Such a system has been developed at Ames.

The system works by discharging a bank of high-voltage capacitors into several low-resistance conductors arranged in a parallel array. The pulsers consist of high-voltage capacitors, relay switches, and electronic timing to provide sequential discharges, which in turn, produces a rippling effect to enhance the de-icing. Various arrangements of the conductors are possible to optimize the removal of ice from the leading edge of an airfoil and other aerodynamic surfaces.

(R. Lee and L. Haslim, Ext. 6496/6575)

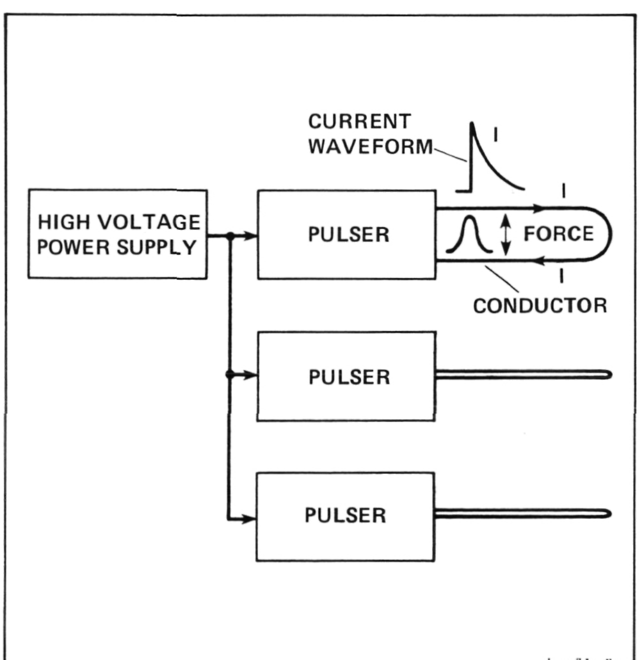

Electro-expulsive de-icer block diagram

Accelerated Characterizing of the Long-Term Mechanical Behavior of Fiber Reinforced Plastics

An accelerated characterizing methodology to predict the long term, time dependent mechanical behavior of fiber reinforced plastics (FRP), polymers, and adhesives is being developed in collaboration with Prof. H. F. Brinson of Virginia Polytechnic Institute and State University. These types of materials exhibit time-dependent viscoelastic properties which can result in a time-dependent change in mechanical properties, such as moduli and strength. Further, this degradation can be accelerated by external parameters such as stress, temperature, and moisture.

The approach taken has involved the application of a nonlinear viscoelastic time-temperature stress superposition principle in combination with a modified time-dependent Tasi-Hill-Zhurkov type failure theory. The procedure has been tried, tested, and is shown to give conservative predictions for times out to 10^4 minutes for both the T300/934 and T300/5208 continuous fiber reinforced composite systems. The procedure involves short-term laboratory testing such as that normally performed for routine quality control. The only additional information required is the production of modulus and strength master curves as a function of stress level and temperature. The determination of these curves can be accomplished in a few days. The extension of this methodology to times on the order of years is a simple and direct task, and can be used now by design engineers to make conservative estimates of service life of laminated FRP structures.

(H. Nelson, Ext. 6137)

Three-Dimensional Adaptive Wall Wind Tunnel

The Ames Mechanical Systems Branch is currently involved in a preliminary design of a 30 cm^2, three-dimensional adaptive wall wind tunnel. The tunnel is designed to operate at a subsonic speed of Mach 0.8 and a flow rate of 50,000 cfm. Its design includes the following sections: entrance, test, model support, variable throat, and diffuser. Additionally, a total of 110 plenum chambers, each equipped with a miniature butterfly valve control system, sur-

round the test section. The control system will monitor the air pressure along the test section and will either blow air in or suck air out of the test section in order to eliminate the effects of the walls on a wind-tunnel model. The final design and fabrication will proceed following the test results obtained from the current two-dimensional adaptive wall wind tunnel program being implemented in the 2- by 2-Foot Wind Tunnel.

(P. Luna, Ext. 5929)

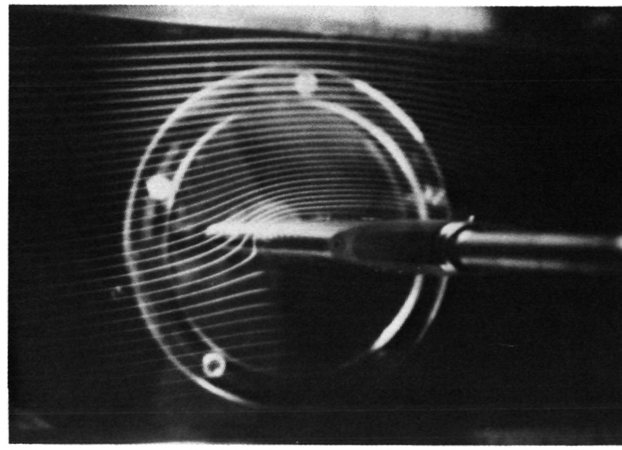

Panontin

Fluid control system

Dynamic Stall on Airfoils Oscillating in Pitch

The Ames Mechanical Systems Branch is developing an In-Draft Wind Tunnel test section for complete local flow visualization around an oscillating model. Flow velocity during dynamic stall will be measured with a laser velocimeter and density variations will be obtained through schlieren photographs. Glass disks supporting and moving sinusoidally with the model will be mounted in bearings in the tunnel wall. The airfoil will oscillate in pitch by a crank, connecting-rod, and flywheel mechanism. The test section will have an adjustable mean angle of attack, oscillation amplitude, driving frequency, and will be designed for a down-stream flow velocity of Mach 0.5.

(C. Sticht, Ext. 6318)

Circulation Control Lift Generation Experiment Hardware

The Mechanical Systems Branch at Ames Research Center has developed a circulation control airfoil (and the accompanying hardware) to allow the investigation of lift generation that is independent of relative-flow velocity and airfoil angle of attack. Designed for use in a water tunnel, the test equipment includes the blown airfoil, the support systems for both flow visualization and airfoil load examination, and the fluid control system, which utilizes hydraulic technology. At present, all components have been fabricated; the investigation will proceed upon qualification of the fluid control system.

(T. Panontin, Ext. 6315)

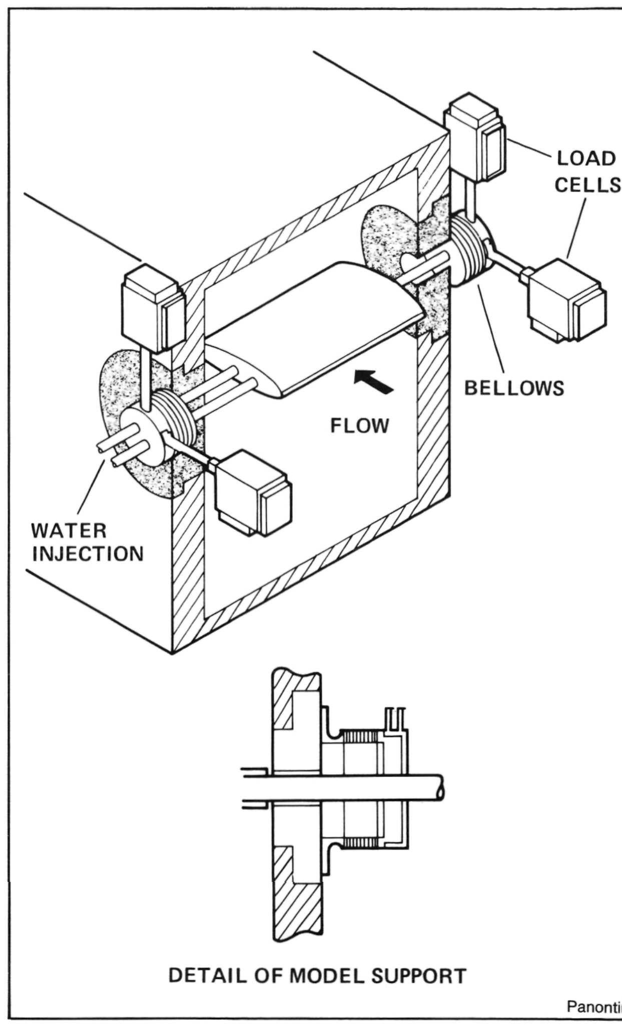

Load measurement support system (Test configuration)

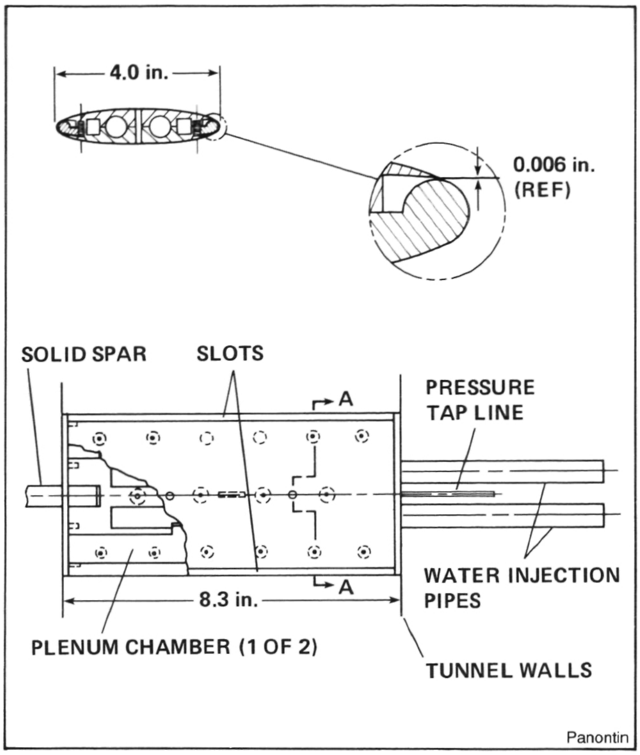

Circulation control airfoil

Surface Reaction Kinetics: Hydrogen on Iron

The isothermal kinetics of gaseous hydrogen adsorption-desorption onto evaporated iron films has been studied in an effort to better understand the role of surface reactions in the hydrogen embrittlement of steels. The work was done in collaboration with Dr. M. R. Shanabarger of the University of California, Santa Barbara. It has been found that hydrogen initially adsorbs as molecular hydrogen, then dissociates and chemisorbs as atomic hydrogen. The rate of adsorption into the molecular state is found to be linearly related to gas phase pressure, whereas the dissociative chemisorption process is independent of pressure and is thermally activated. Therefore, under the correct conditions, the overall surface reaction kinetics can be "rate controlled," either by molecular hydrogen adsorption or by dissociative chemisorption depending upon the gas pressure and substrate temperature. This result is important in interpreting the kinetics (temperature and pressure dependence) of gaseous hydrogen embrittlement of steels. Additionally, the results predict that at temperatures above 250 K, desorption from the chemisorbed state to the gasphase is rate-limited by desorption from the adsorbed molecular state. This result is significant in the interpretation of many of the anomalies observed in the process of hydrogen transport through iron membranes. Modeling of the transport process, using the surface reaction kinetics as boundary conditions for simple Fickian diffusion, has been successful in reproducing all of the phenomena observed in the transport measurements with no adjustable parameters. Finally, for the first time the results have permitted an actual comparison between experimentally determined rate constants and those predicted from fundamental absolute rate theory. Excellent agreement is shown to exist assuming hydrogen is a mobile species on the surface of iron.

(M. Shanabarger and H. Nelson, Ext. 6707/6137)

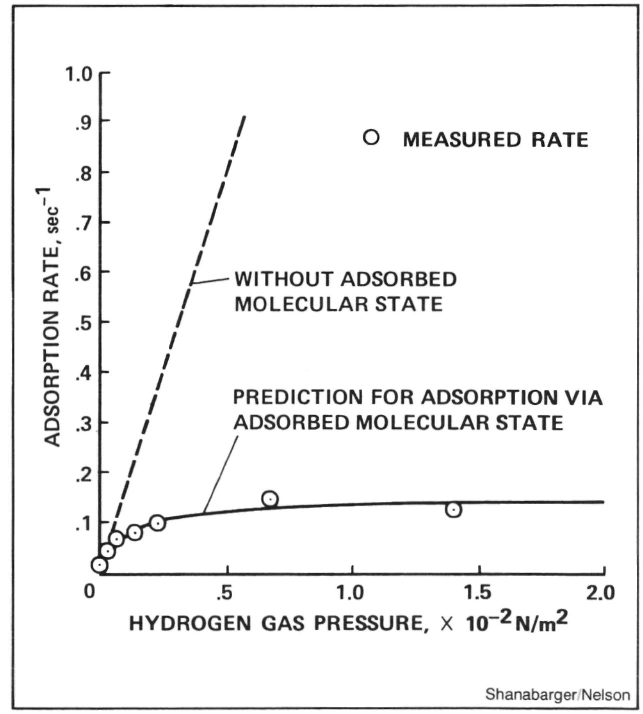

Influence of adsorbed molecular state in limiting rate of hydrogen chemisorption on iron films

Aviation Safety Reporting System

The National Aeronautics and Space Administration (NASA) operates an aviation incident reporting system designed to identify, research, and report on hazards to aviation safety. The Aviation Safety Reporting System (ASRS), provides a means for pilots, air traffic controllers, and others involved in the national aviation system to report on incidents and situations considered detrimental to safety.

Incoming reports (about 500 each month) are screened for critical information and analysed by a staff of experienced pilots and air traffic controllers. Information from each report is entered into a computer and from this computerized database, the ASRS project produces research reports relevant to aviation safety. The ASRS office also publishes a monthly safety bulletin, CALLBACK, which is available upon request to anyone interested in aviation safety data. If information submitted to the ASRS reveals an alleged safety hazard in need of a rapid response, the reporting system produces an Alert Bulletin directed to the FAA or to other organizations in a position to investigate, and if appropiate, remedy the problem. The output of the ASRS database also includes responses to issue-specific requests for data.

The ASRS program, in operation since 1976, is a cooperative venture of the Federal Aviation Administration (FAA) and NASA. The FAA provides program funding; NASA administers the program and acts in the capacity of a neutral third party, thereby protecting the confidentiality of pilots, air traffic controllers, and others desiring to share safety information without fear of incrimination.

The aviation incident reporting system has been used as a model for similar programs in other countries and industries. England has recently inaugurated a voluntary incident reporting program modeled closely on the ASRS; Canada is presently in the process of developing a version of the ASRS system, and other nations have studied the ASRS to gain information on the design and organization of safety data systems. In the U.S., the Coast Guard is scheduled to initiate a similar Marine Safety Reporting System in 1985. The concept of voluntary, confidential, incident reporting in the interest of safety is also under study by the U.S. Nuclear Regulatory Commission, as well as other governmental and industry groups.

(W. Reynard, Ext. 6467)

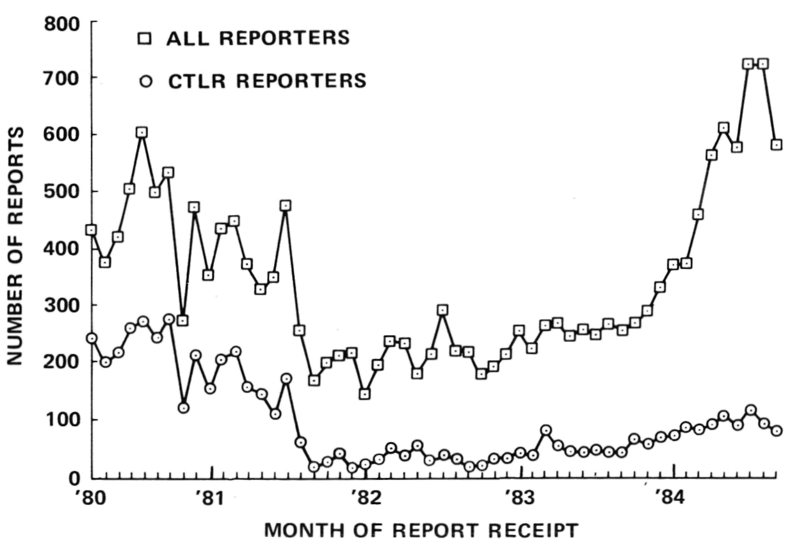

TOTAL REPORTS RECEIVED:	41,533
TOTAL REPORTS IN DATABASE:	35,955
ALERT BULLETINS ISSUED:	797
SPECIAL REQUESTS RESPONSES:	711
TECHNICAL REPORTS PUBLISHED:	24
MONTHLY ISSUES OF CALLBACK:	64

Reynard

ASRS monthly report receipts

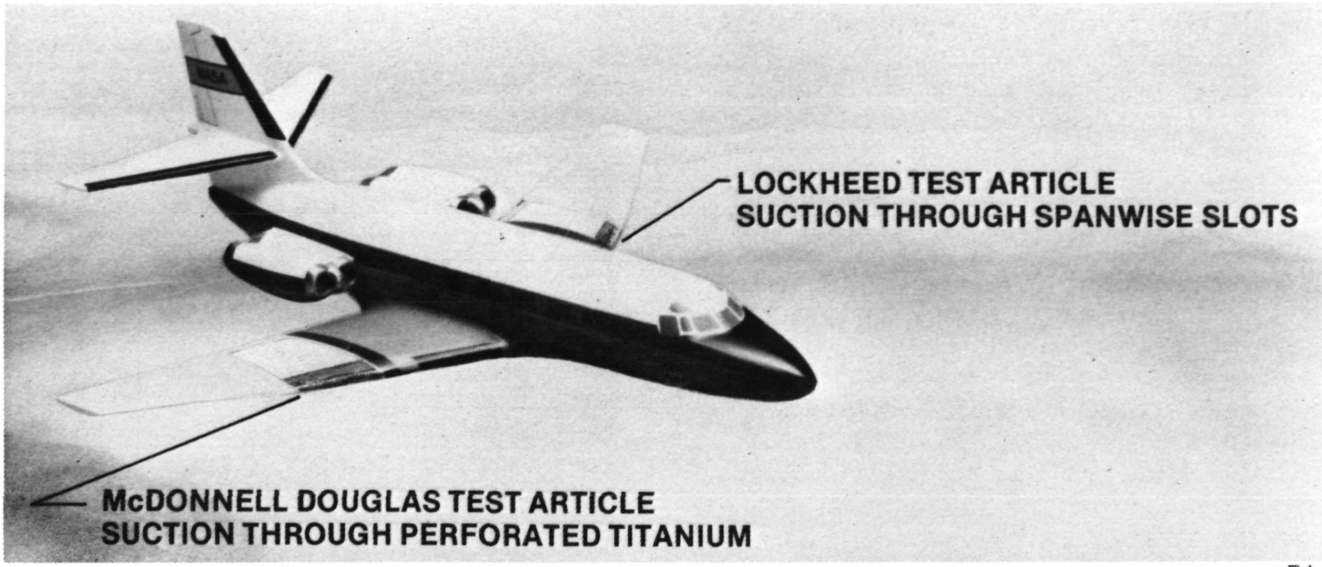

Modified JetStar aircraft with laminar flow control leading edge test articles

Fisher

JetStar Laminar Flow Control-Leading Edge Flight Test

NASA Ames is flight-testing two alternative concepts of a laminar flow control leading edge on a JetStar aircraft. The concepts were developed under contract to the Langley Research Center as part of NASA's viscous drag reduction program. One design by Douglas Aircraft Company uses distributed suction through a porous skin. The other design by Lockheed-Georgia Company uses incremental suction through spanwise slots. The purpose of this work is to demonstrate the effectiveness of LFC leading edge systems under representative conditions in flight up to Mach 0.8 and 40,000 feet.

The leading edge systems include insect protections, anti-ice, purge, and suction. The flight acceptance tests of these systems are being conducted. A series of research flights will follow which will determine the effect of Mach number, altitude, angle of attack, Reynolds number, and suction distribution on the extent of laminar flow.

Simulated airline flights at various NASA centers throughout the country will provide operational and maintenance experience for a laminar flow control airplane.

(D. Fisher, Dryden Ext. 3705)

Axisymmetric Base Drag Reduction Study

Low speed, incompressible, turbulent flow wind-tunnel experiments conducted during the mid-1960s on a body of revolution with a blunt base showed that the base drag could be substantially reduced by mounting a disk of smaller diameter than the body behind the body. The effectiveness of this trailing disk (or trapped vortex concept) in reducing the base drag was dependent on the separation distance between the base of the body of revolution and trailing disk, and on the diameter of the disk relative to the diameter of the body.

The body of revolution shape at the top of the F-111 vertical fin provided an opportunity to study the trapped vortex concept on a larger body, and for higher speeds and Reynolds numbers than the previous studies. Pressure distribution data on the base surfaces were obtained for the hemispherical base (the standard base for this aircraft), blunt base, and trailing disk configuration. Subsequent to the flight study, a full-scale model of the body of revolution was built and tested in the NASA Langley High-Speed 7- by 10-Foot Wind Tunnel. Both force balance and surface pressure measurements were obtained for the blunt base and trailing disk configuration. The flight and wind-tunnel studies provided data for Mach numbers from 0.30 to 0.93 and for Reynolds numbers from 1.6×10^7 to 4.1×10^7. Typical results are shown.

(S. Powers, Dryden Ext. 3703)

Powers

Aft region of F-111, body of revolution is seen at top of vertical fin

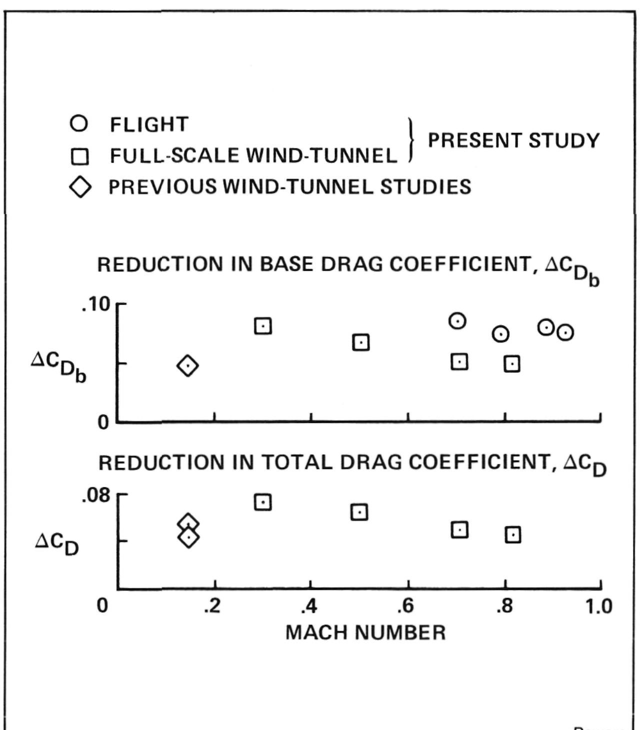

Reduction in drag from blunt base configuration

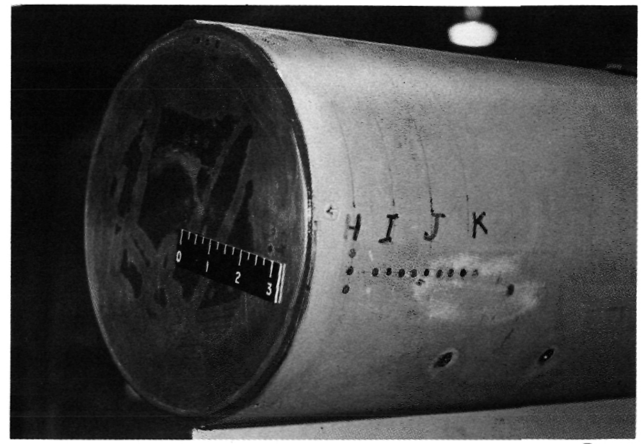

Powers

Side view of blunt base

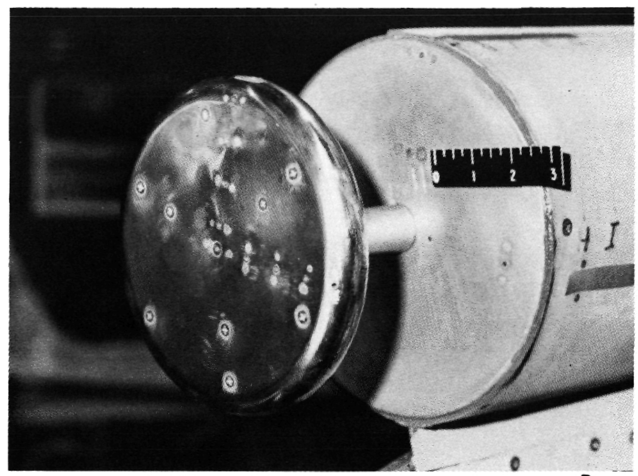

Powers

Side view of trailing disk

Airdata Enhancement via State Reconstruction Techniques

Because of limited in-flight calibration data, the acquisition of accurate airdata estimates during the early Space Shuttle flights and the Highly Maneuverable Aircraft Technology program necessitated the development of an advanced airdata calibration technique. The technique utilized pneumatic, inertial, meteorological, and ground-based tracking data which were combined via a linearized Kalman filter (LKF). A single set of enhanced trajectory estimates resulted. These trajectory estimates are believed to be quite accurate and are used as a known source by which position errors in the pneumatic source may be identified.

Even though it is still in the preliminary stages of development, there are several advantages to using the state reconstruction technique as

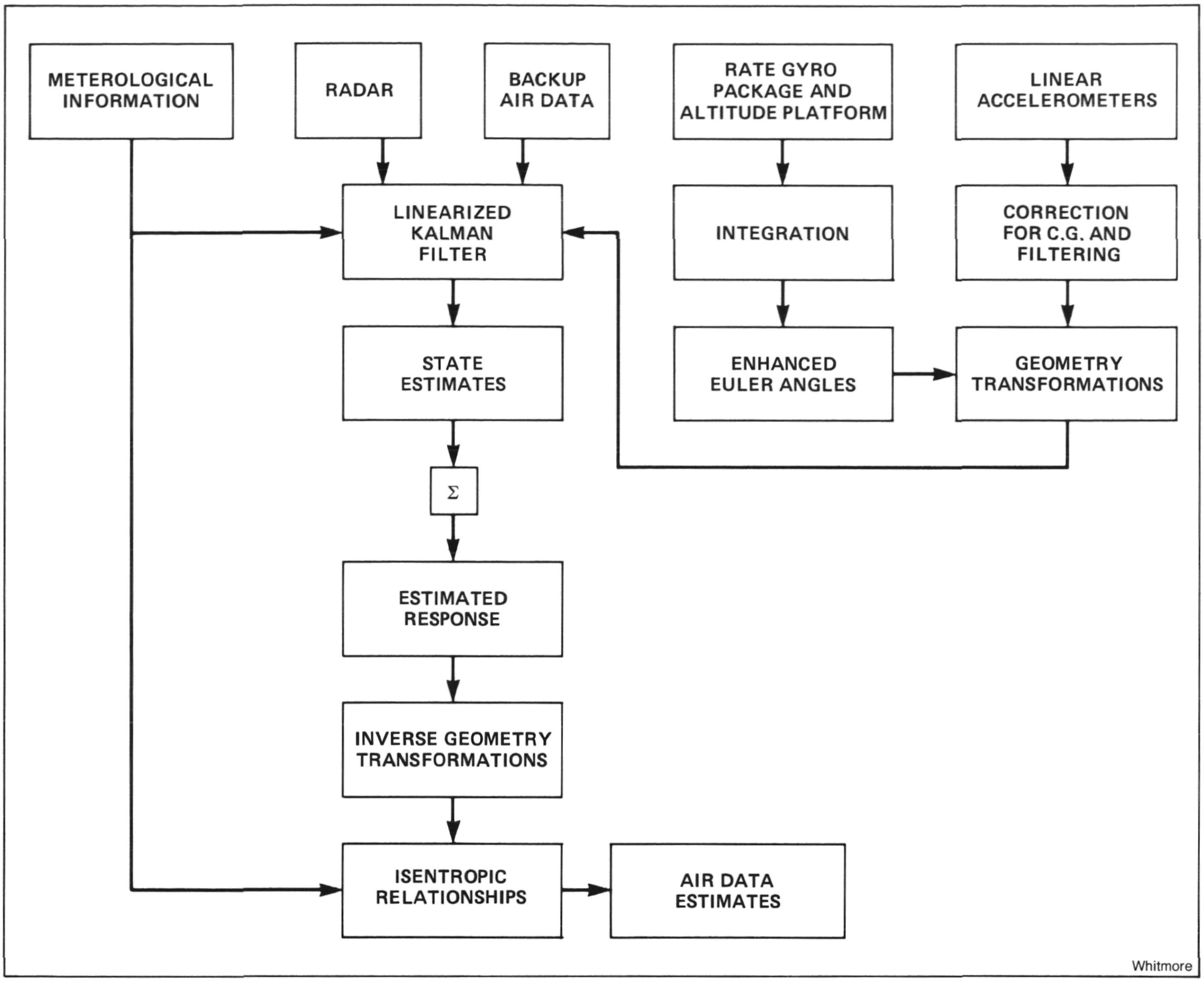

Flow chart of LKF computational scheme

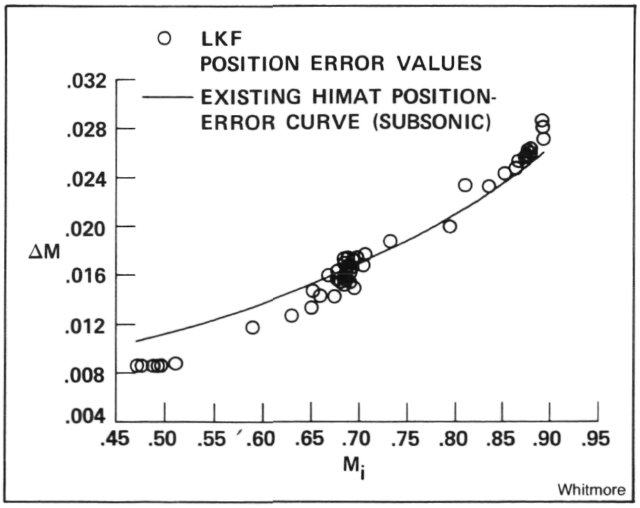

Comparison of LKF position error to existing HiMAT curve

opposed to more traditional techniques. These are: 1) there is no need to fly a pacer aircraft. The LKF reconstruction adequately fulfills this task. 2) The LKF trajectory provides a complete time history from which position errors may be statistically identified. Traditional techniques use only a limited number of selected data points. Traditional results may confuse random errors with systematic, physically caused errors. 3) The use of four independent data sources allows the identification of biases in the data sources. This is not always feasible by conventional means. The LKF technique is shown schematically.

A comparison of the position error curve for the HiMAT aircraft as derived by the LKF method and traditional means is presented.

(S. Whitmore, Dryden Ext. 3699)

F-14 Variable Sweep Transition Flight Experiment (VSTFE) Basic Wing Pressure Distributions

Recent investigations have shown the viability of obtaining significant amounts of laminar flow on small, jet-transport category aircraft. However, one concern is early or premature transition of laminar boundary layer due to leading-edge sweep. Consequently, NASA Ames and Langley have initiated a Variable Sweep Transition Flight Experiment (VSTFE) on an F-14A aircraft. The flight research program will consist of testing several different airfoil shapes having varying "favorable" pressure gradients. These shapes will be "gloved" onto the F-14A wing panels.

The variable sweep capabilities, wing planform, and Mach/Reynolds number envelope of the F-14A were determined desirable for the VSTFE. However, wing-section pressure distributions, span loads, and the verification of the use of side-slip to attain leading edge sweeps of less than 19° (the minimum available on the F-14A) were also needed in assessing the acceptability of the F-14A aircraft as a carrier vehicle for the VSTFE. Only a limited amount of wind-tunnel pressure distribution data were available on the F-14A; therefore, NASA conducted an in-flight wing-pressure distribution study on the aircraft. The pressure distribution data were obtained using chordwise rows of externally mounted tubing at four different span stations.

As part of the preliminary VSTFE evaluation, a wing-pressure analytical analysis of the basic F-14 wing was performed by Grumman under contract to the Langley Research Center and was compared to the flight results. Typical results of the analysis are shown and show a good correlation with the flight data.

(B. Meyer, Dryden Ext. 3707)

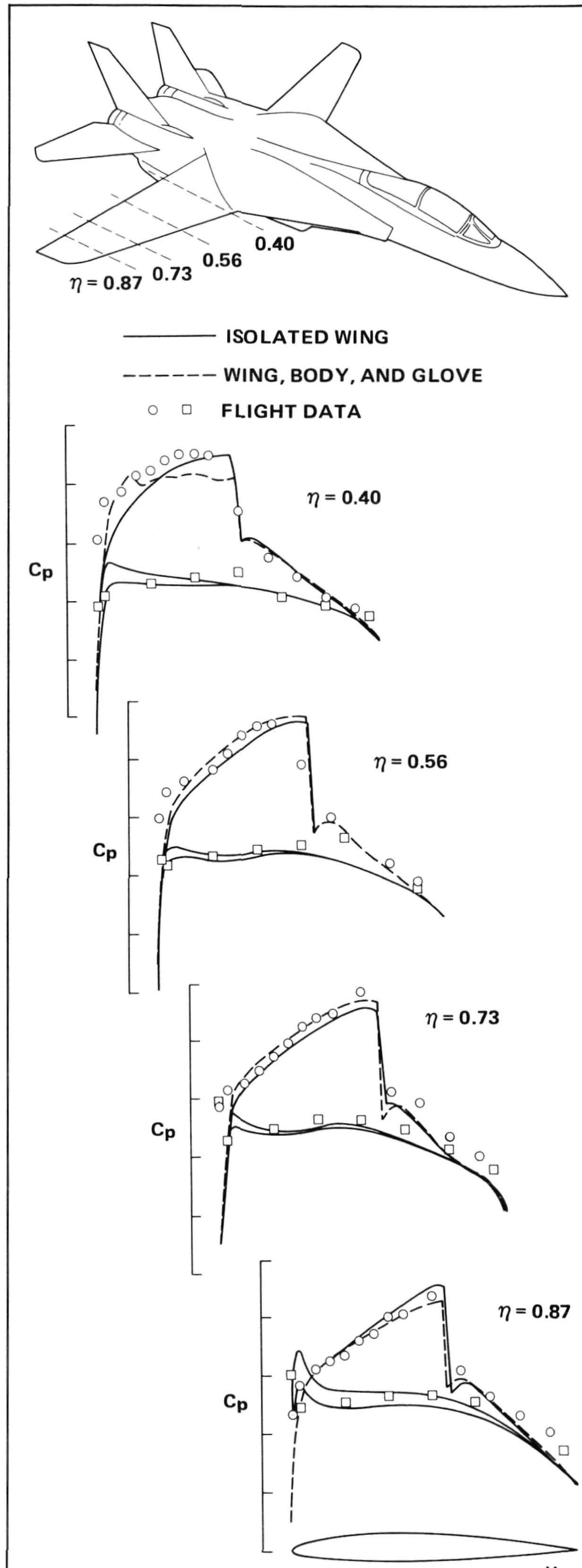

F-14A wing pressure distribution correlation
$\Lambda = 20°, M_\infty = 0.80, \alpha = 1.4°$

Laser-Enhanced, Water-Tunnel Flow Visualization

In its usual mode, the water tunnel can be used to observe three-dimensional flow phenomena by injecting colored vegetable dye into the flow. As a variation of this technique, a two-dimensional cross-section of the flow can be observed by using a laser to produce a thin sheet of intense light. This sheet of light can be easily scanned in the vertical or horizontal directions to survey the structure of the flow. In many instances cross-sectional views are much easier to interpret than the normal operational mode. Documentation can include 35 mm photographs and videotape.

Special dyes which fluoresce when exposed to the laser light are used for this technique. Various laser power settings, exposure times, dyes, and film were tested to optimize the procedure for future use.

Examples of the technique, applied to a space shuttle model, are shown below. The spanwise vortex can be easily located in both views, while the burst point can be identified in the longitudinal view. Photographs such as these have been interpreted and compared favorably to other water-tunnel results.

(C. Beckner and R. Curry, Dryden Ext. 3715)

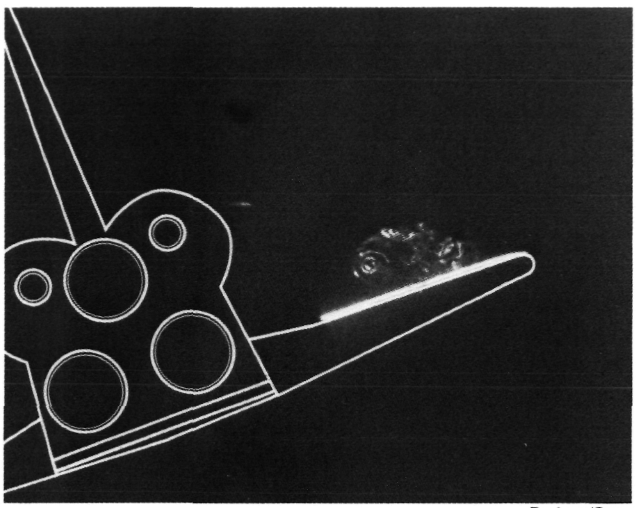

Beckner/Curry

Tail view of shuttle at 20 degrees angle of attack showing the vortex over the wing

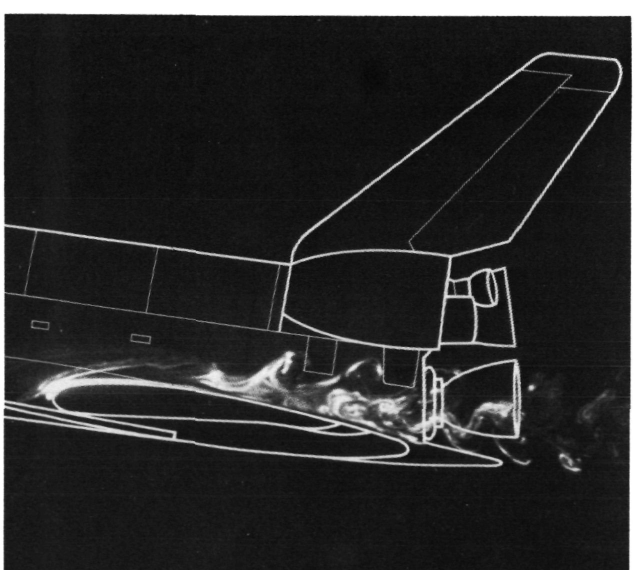

Beckner/Curry

Side view of shuttle at 8 degrees angle of attack showing the flow over and past the wing trailing edge

Airplane Performance Modeling

The objective of this program was to develop, evaluate, and verify a generalized aircraft performance-modeling technique based on a limited amount of quasi steady-state flight test data. Specific subjects studied included the effects of engine power setting on lift and drag characteristics, prediction of stabilized cruise-performance characteristics based on acceleration and deceleration data, development of performance models for engine power settings less than maximum thrust, and development of a simplified in-flight thrust airflow- and fuel-flow calculation method that does not require extensive engine instrumentation.

Redin

Gates Learjet Model 35 aircraft

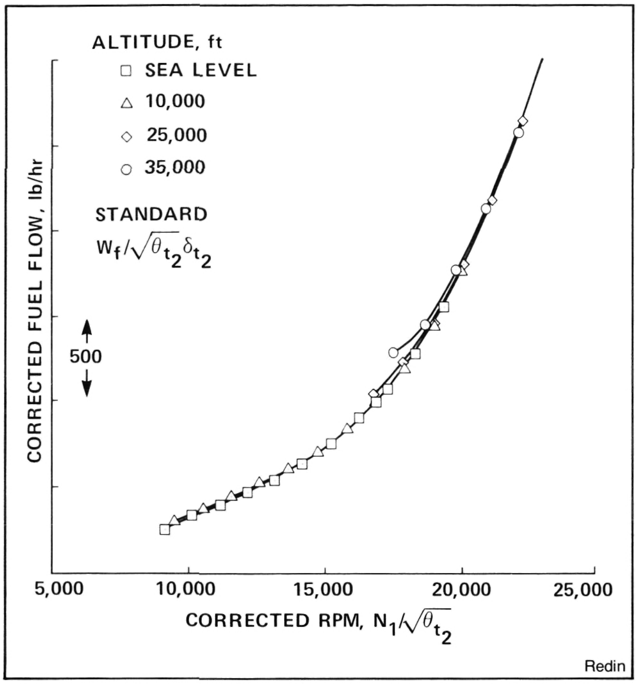

Engine deck corrected fuel flow characteristics, M = 0.45 (before)

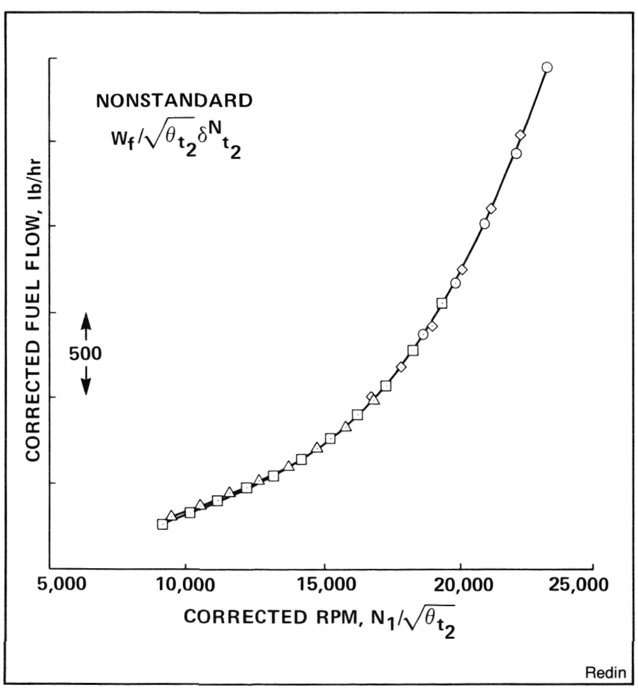

Engine deck nonstandard corrected fuel flow characteristics, (after) M = 0.45, N = 0.96

The program was planned, conducted, and reported (CR 170414) by the University of Kansas under NASA Grant NSG-4028. The airplane used in the flight-test portion of the program was a Gates Learjet Model 35 business jet with two Garrett Air Research TFE 731-2 turbofan engines.

A significant and unique contribution of this program was the development of an engine-airflow and fuel-flow prediction technique that allowed the altitude-dependent variations in these parameters to be collapsed onto one curve as a function of corrected RPM and Mach number. This technique involved adjusting nonstandard corrected fuel flow by an empirically derived exponential factor. The figure shows data before and after being adjusted.

Overall test results showed that stabilized airplane performance could usually be predicted by the developed performance model to within 5% of the traditional speed-power test maneuver results for both full- and part-power engine operation. Significant savings in flight-test time should be realized by employing the performance modeling rationale developed in this study.

(P. Redin, Dryden Ext. 3683)

Adaptive Engine Control System Research

Jet engines are currently operated with a fan-stall margin large enough to accommodate the worst-case combination of inlet distortion, throttle transient, and engine-to-engine variation. Operation with this large stall margin requires the engine thrust to be reduced over what could be required if a smaller stall margin could be used. With the advent of digital engine-control systems, digital flight-control systems, and data buses, it appears to be practical to integrate the engine- and flight-control systems, and to implement an adaptive engine-control system (ADECS), in which the engine-control margins are continuously adjusted to match the needs of the airplane. An ADECS system block diagram is shown. Information from the airplane, from the flight-control system, and from the pilot can be used to estimate the inlet distortion, and to provide a signal to increase the engine-pressure ratio (EPR) when the full-stall margin is not needed. The digital electronic engine control (DEEC) can then move the required engine variables and thrust can be increased.

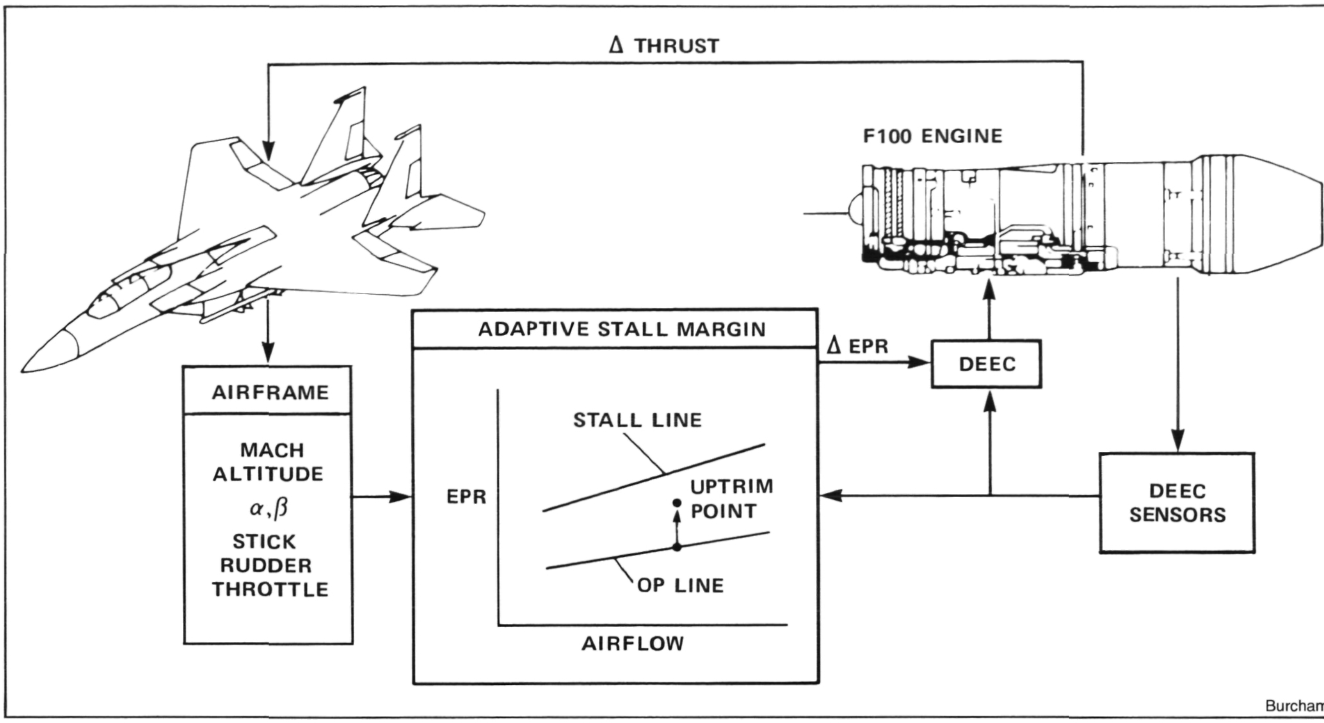

Block diagram of the Adaptive Engine Control System mode

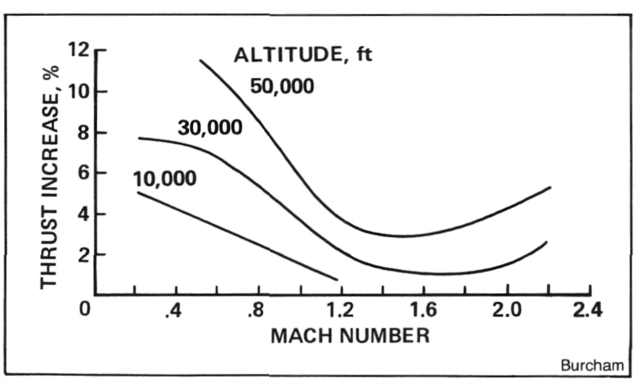

Thrust increase for ADECS mode, maximum power

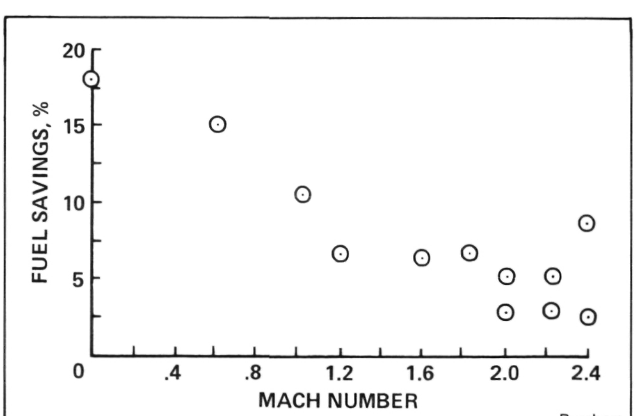

Fuel flow reduction with ADECS to achieve standard engine maximum thrust

Studies of such a system for the F100 engine in an F-15 have been conducted. The percentage increase in thrust varies from 2% to 12%. If additional thrust is not needed, the ADECS mode can also be used to reduce fuel consumption. The decrease in fuel flow is shown to achieve the same thrust that an engine without ADECS would produce at maximum power. These performance increases, while not large, are extremely cost-effective, since, in a production application, the ADECS mode could be implemented in an existing flight computer.

To verify these predicted performance improvements, the ADECS mode will be tested as part of the Highly Integrated Digital Electronic Control (HIDEC) system now being installed on the NASA Ames F-15 airplane.

(F. Burcham, Dryden Ext. 3126)

Flight Investigation of Digital Engine Control Fault Detection and Accommodation

An evaluation of the Fault Detection and Accommodation (FDA) capability of a digital electronic engine-control (DEEC) system has recently been completed at NASA Ames-Dryden. The DEEC is installed on an F100 engine in an F-15 research airplane. The DEEC is a full-authority, single channel, digital control with selected redundancy to maintain digital engine control for any single input-output failure. It also incorporates a simple hydromechanical backup control. The function of the fault protection for the DEEC is to provide additional engine safety and operation in the event of an engine control-system failure. It can detect and identify 160 faults within the control system.

The FDA logic provides three basic levels of engine operation in the event of an engine control system anomaly. The first level maintains normal engine operation with notification that a failure of a redundant parameter has occurred. The second level of fault detection is accommodated and also maintains normal operation of the gas generator, but inhibits afterburner operation. The third level of accommodation is to automatically transfer control of the engine to the backup control. Although the logic is relatively unsophisticated, it comprises 40% of the DEEC control logic.

During three years of flight evaluation only a few of the 160 faults had occurred, and none of these had required operation in the accommodation modes in which the failed parameter is synthesized; therefore, a system was installed on the F-15 to permit faults to be intentionally introduced into the DEEC. This was accomplished by installing valves and switches in the DEEC sensors to permit false signals to be supplied to the DEEC. Those sensors selected were the pressure and temperature sensors that would be synthesized by the DEEC in case of failure. The objective of the DEEC FDA flight test program was to evaluate the FDA logic and to compare the flight results with the predictions.

The test points flown were selected to cover the area of the flight envelope where the engine most frequently operates. Simulation and test facility data were available for comparison. Failures were introduced at steady-state conditions and during throttle transients as shown. Both single and dual failures were accomplished. During ground tests on the DEEC equipped engine, several unexpected events occurred, but during the flight evaluation, all failures were

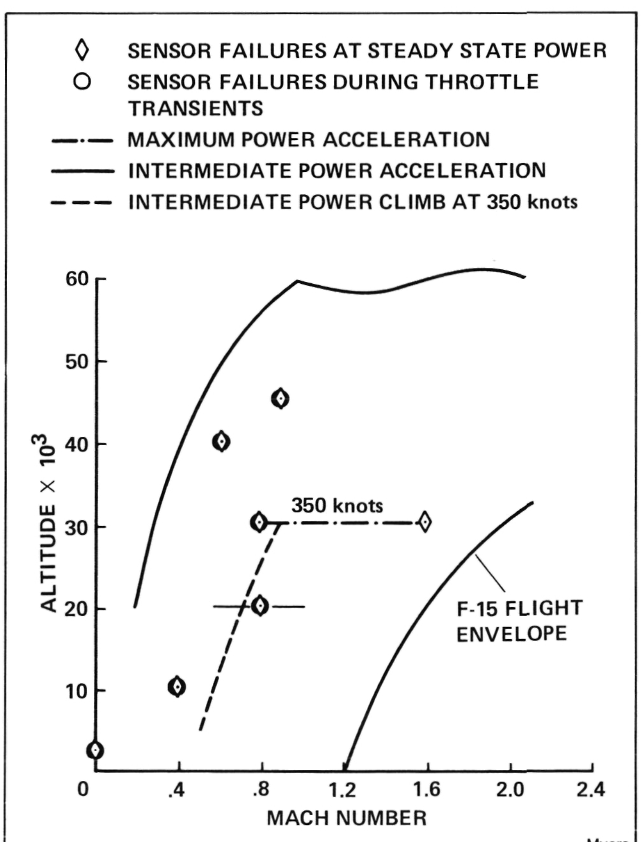

Flight envelopes

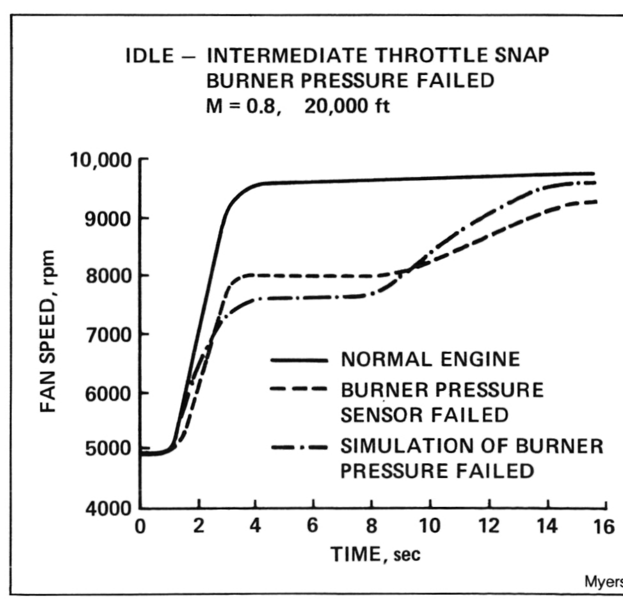

Time history of fan speed

detected and accommodated. A time history of fan speed for an idle-to-intermediate power throttle transiwnt is shown, first with a normal engine, and then with a failed burner pressure signal, at a Mach number of 0.8 and an altitude of 20,000 ft. The simulation with a failed burner pressure is also shown. The predicted engine response matches the actual engine response fairly closely.

Operation with the DEEC synthesized parameter modes was accomplished over much of the F-15 flight envelope, thus greatly increasing the confidence in the DEEC FDA concept.

(L. Myers, Dryden Ext. 3698)

Integrated Sensor System

The Integrated Sensor System (ISS) Project is designed to provide a comprehensive, integrated package that will provide improved accuracy data useful for acquiring aircraft performance data stability derivatives as well as enhancing such measurements as angle of attack, aircraft attitudes, and velocity. Rather than utilizing a single instrument for each measurement as has traditionally been done (such as angle of attack and sideslip from the NASA air data head vanes, linear accelerometers for body axis accelerations, and rate gyros for aircraft body axis angular rates), the approach is being taken to encompass all sensors and real-time processing in a single package. This single-package approach simplifies the initial installation time as well as provides for a more uniform data acquisition process.

The single-integrated-package concept utilizes state of the art concepts for the inertial measurements (ax, ay, az, roll, pitch, and yaw) by incorporating strap-down ring-laser gyro technology. Along with the inertial measurements, the ISS provides the means for acquiring, calibrating, and processing conventional air-data measurements. As an offshoot of this, the ISS will perform the functions of an air-data computer for the inertial measuring unit (inertial measuring units typically need true airspeed and altitude input to them in order to stabilize the vertical loop).

The inertial data acquired by the inertial reference unit is then melded with the air-data measurements in an optimal digital filter. The filter used in the ISS is an extended Kalman filter with time varying gains implemented in real time with the airborne microcomputer system. The results of the optimal digital filtering are enhanced values for the aircraft's position, velocity, and attitude. These enhanced values are then processed in real time for display (in the aircraft as well as on the ground) as well as for telemetering to the ground station via an RF link.

The software for the complex algorithms involved in the navigational formulas is written in Fortran, compiled on a VAX 11/780, and then

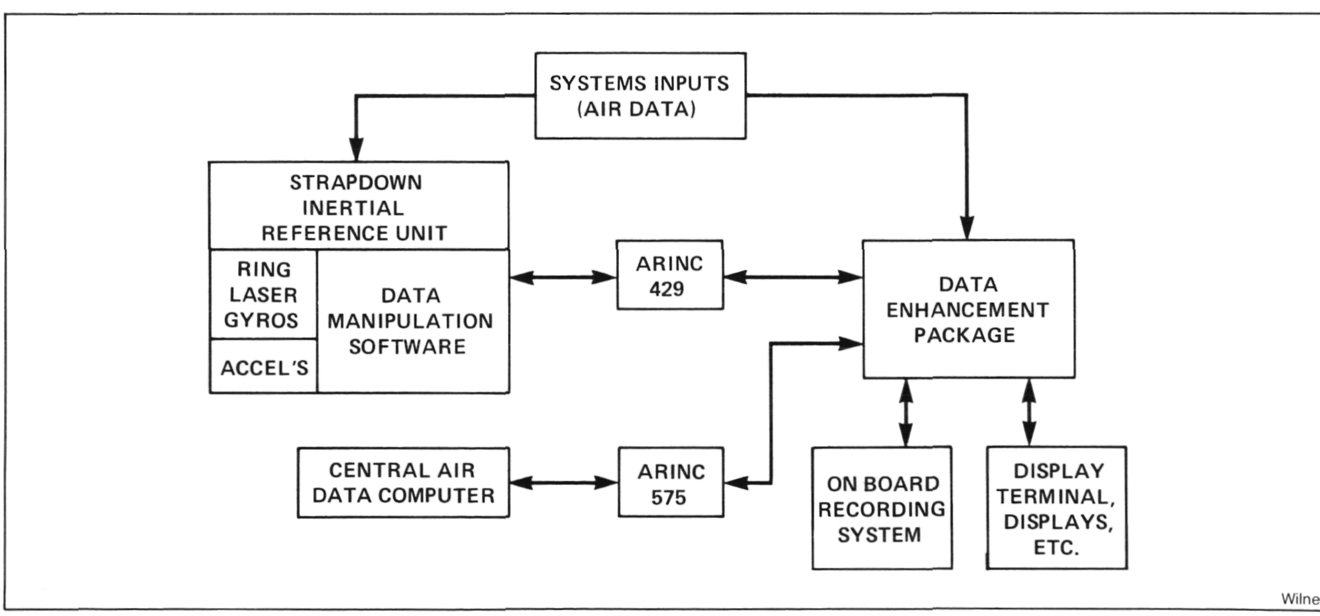

Integrated sensor system

downloaded into a development microcomputer system. The system software, as well as real time input/output calculations, is written either in C or assembly language. The host computer for the development of the C and the assembly language code is an IBM PC-XT system operating under a UNIX type operating system.

The ISS project is currently undergoing extensive laboratory testing and evaluation at Ames-Dryden. Simulated flight test data will be input to the ISS along with actual data from the inertial reference unit to verify the operation and the quality of the data acquisition, the real-time processing, and the extended Kalman filter. After laboratory verification, the ISS is scheduled to be flight tested on the YAV-8B aircraft during 1985.

(D. Wilner, Dryden Ext. 3739)

HiMAT Composite Structural Analysis

A NASTRAN finite element structural model of the HiMAT aircraft was modified based on updated material properties for the wing and canard graphite-epoxy composite skin elements.

The original model wing and canard skin elements used anisotropic material property sets that were based on a lamina shear modulus of 0.35×10^6 lb/in.^{2}. NASA conducted graphite-epoxy composite coupon tests with the intent of better understanding the value of the shear modulus. The analysis of the results of these tests, combined with a survey of the industry, indicated that a lamina shear modulus of 0.68×10^6 lb/in.^{2} would be a more realistic value.

Measured wing streamwise twist distribution data obtained from a static ground test of the aircraft were compared to NASTRAN predicted twist distributions using both the original model and the updated model for the same loading condition. The effect of updating the material properties was a significant improvement in correlation of the predicted and measured results.

(W. Lokos, Dryden Ext. 3924)

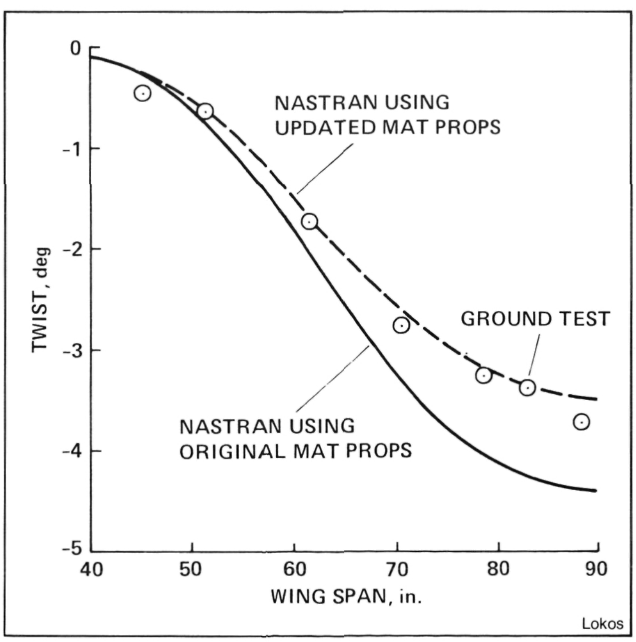

HiMAT outer wing panel streamwise twist versus span (for 8g distributed load)

Hot Structures Research

The stresses induced in the structures of hypersonic vehicles and spacecraft during actual flights or in the simulated laboratory tests are of two types: 1) mechanical stresses due to aerodynamic loadings, and 2) thermal stresses due to aerodynamic heatings. In order to evaluate the structural performance of those vehicles, the mechanical stresses must be separated from the strain-gage-measured stresses. Experimentally, this stress separation cannot be done, but it can be done

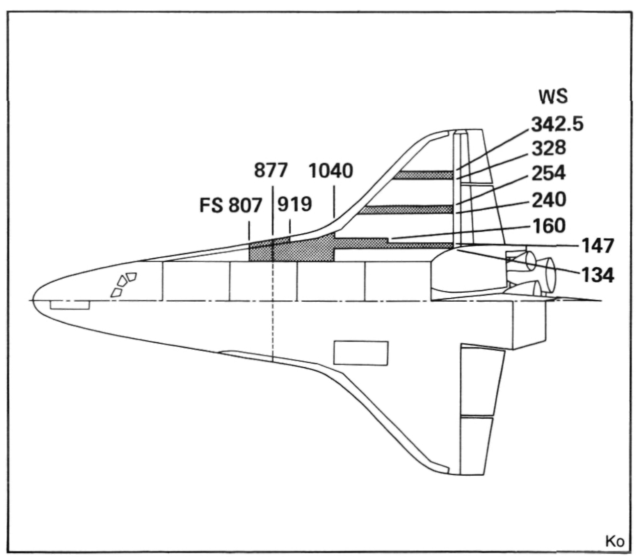

Locations of space shuttle wing segments and midfuelage cross sections analyzed

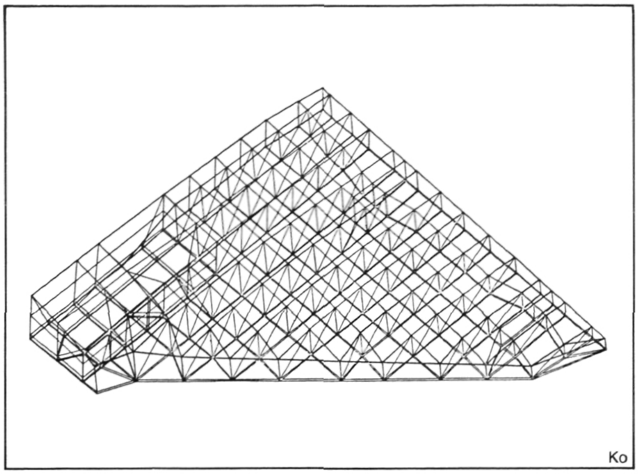

Space shuttle wing spar thermal model

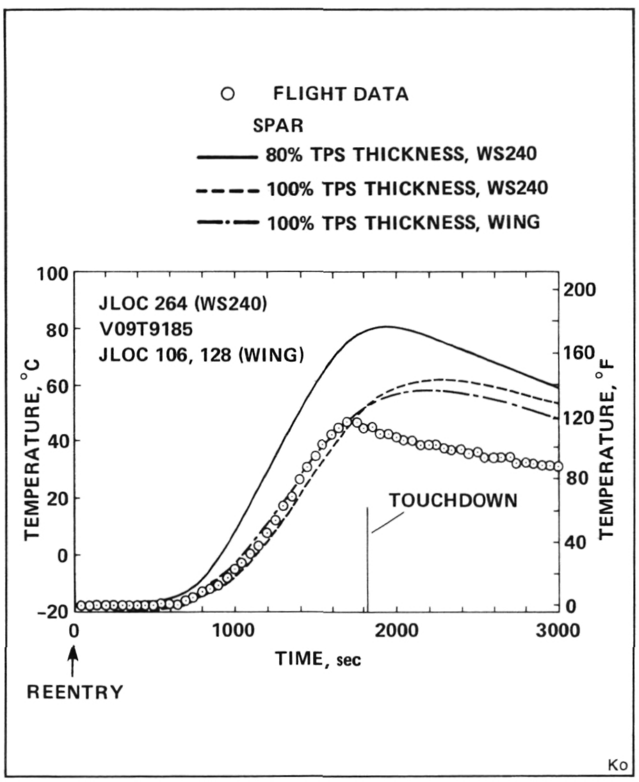

Time history of lower wing skin temperature

analytically. Namely, by performing finite element heat transfer analysis and stress analysis, the thermal stresses can be calculated and removed from the strain gages measured stresses to give the true mechanical stresses.

In order to calculate the thermal stresses, heat transfer analysis must be conducted first. The structural temperature distribution obtained from the heat transfer analysis can then be used as input to the structural finite element model for the calculations of thermal stresses. Several SPAR (Structural Performance and Resizing) finite element thermal models were set up for the Space Shuttle orbiter wing and fuselage for the calculations of the structural temperature distributions. The results showed that the predicted and the measured structural temperatures agreed nicely during the reentry flight up to touchdown. The discrepancy between the calculated and the measured temperatures of the lower skins of the wing and fuselage after touchdown is considered to be due to the effect of natural convection (which was neglected in the analysis) and due to the entering of cool air into the Shuttle interior.

(W. L. Ko, Dryden Ext. 3581)

Numerical Methods Development in Structures and Dynamics Analysis

Development of novel numerical procedures and associated analysis tools enable efficient design solutions to complex practical problems. A research effort toward better discrete modeling of a continuum has resulted in the development of finite dynamic elements. Convergence characteristics of various elements pertaining to the dynamic element method (DEM) employing the dynamic elements are compared with those obtained by the usual finite element method (FEM) for the evaluation of natural frequencies and modes. Such results are depicted in the illustration; it is evident that the newly developed dynamic elements effect significant savings in solution time compared to the usual finite elements.

A recently developed general-purpose finite and dynamic element computer program, Structural Analysis Routine (STARS), incorporating the latest advances in numerical procedures described earlier, has proved to be an effective tool for the static, free vibration, dynamic response and stability analysis of practical structures. In conjunction with an existing aerodynamics program, the STARS routine is also capable of performing divergence and flutter analysis of

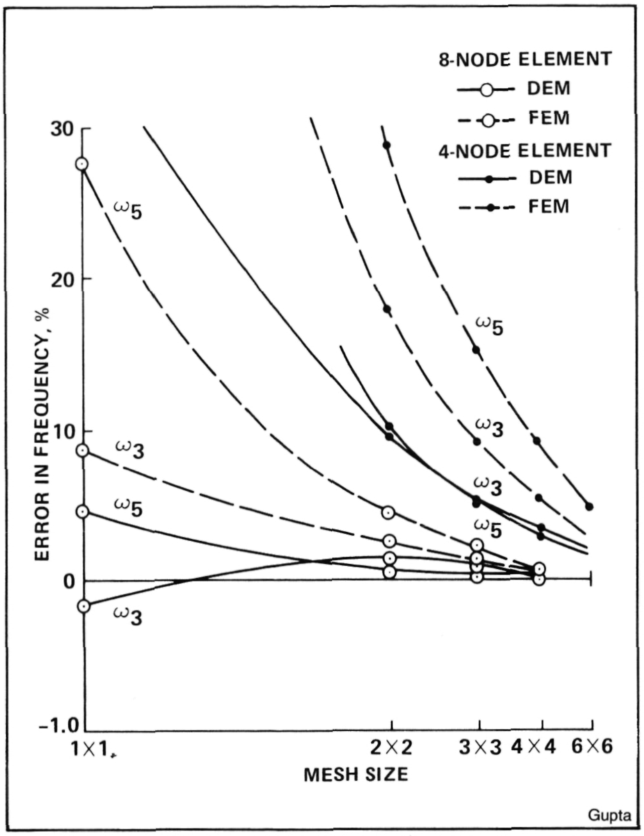

Root convergence comparisons: eight-node and four-node plane rectangular dynamic and finite elements

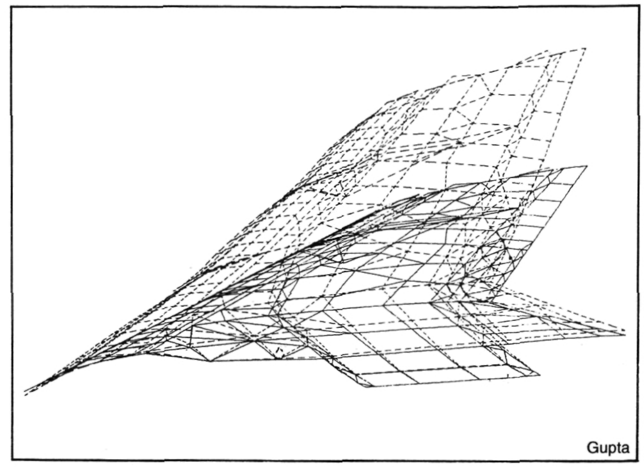

FSW aircraft wing model and first mode shape

structures. The accompanying figure displays a finite element model of the X-29A aircraft wing structure analyzed by the STARS program. The first mode shape is superimposed on the wing model.

(K. Gupta, Dryden Ext. 3710)

Life Science

Preliminary Experiment Results from US/USSR Biosatellite

Four joint US/USSR life science experiments were flown on a Soviet Biosatellite (COSMOS 1514) which remained in Earth orbit for 5 days after a December 14, 1983 launch. This mission was unique since it was the first time that the Soviets had used monkeys and pregnant rats as flight subjects. Because of this, the flight duration was short and emphasized the engineering evaluation of bioinstrumentation and life support systems developed for subjects. Overall, the U.S. bioinstrumentation functioned according to specification during the flight and many valuable science results were obtained. The preliminary results are briefly described below for each experiment.

1. Cardiovascular Measurements During Spaceflight

A miniaturized, plastic cuff with a flow-and-pressure sensor built into the wall was developed by ARC investigators and was surgically implanted by the Soviets around the carotid artery in the neck of one monkey. This cuff, plus associated instrumentation, allowed continuous monitoring of systemic blood pressure and blood flow going to the head.

Data samples were recorded on tape for 5 minutes each 2 hour period from both flight-and-ground control subjects. The data were transferred to the ARC Cardiovascular Research Laboratory for computer analysis. The parameters analyzed by U.S. investigators included systolic, diastolic and mean blood pressure, mean blood flow and heart rate.

The results demonstrate that the U.S. bioinstrumentation functioned well, that blood flow and pressure can be monitored in-flight with a chronically instrumented monkey, and that the parameters measured are within normal values and show typical daily rhythms. A proposed modification of the experiment protocol would allow brain blood flow to be measured directly in space for the first time.

2. Activity and Temperature Rhythms in Space

Flight experiment monkeys as well as ground control experiment monkeys were fitted with U.S. activity and skin temperature sensors plus a Soviet axillary (armpit) temperature telemetry device. All parameters were recorded on a U.S. solid-state flight recorder to allow evaluation of the external (environmental effects) and internal (physiological effects) synchronization of the daily temperature and activity rhythms in space.

The results indicate that the daily rhythms of activity and axillary temperature persisted during spaceflight with subjects on a fixed light/dark cycle. Axillary temperature appears to be 0.5° to 1.0° C lower than values obtained before and after flight. Skin temperature on the ankle was lower, which probably reflects a decrease in peripheral blood flow. Cooler than anticipated spacecraft temperatures may have influenced these changes and a repeat flight at a warmer ambient temperature is warranted to answer this question.

3. Mechanism of Early Bone Loss in Space

The initiation of calcium loss from bone during spaceflight was investigated with the two monkey subjects to determine if it is due to an increase in bone resorption as a primary result of decreased mechanical loading or if it is the result of increased kidney calcium excretion. These effects were studied by placing subjects on a special flight diet which had one natural calcium isotope removed. From continuous tracer analysis of calcium loss in the excreta compared to calcium dietary intake, calcium balance was measured to differentiate dietary and skeletal calcium.

Serial excreta samples were collected preflight and postflight and a bulk sample obtained from the flight excreta collector. The results suggest that the methodology was successful and that there was an increase in calcium loss from bone during the flight due to an increase in bone resorption. Serum samples are required to support the interpretation of the calcium tracer results. Preflight x-rays taken to assess skeletal age of monkey subjects may be useful during future experiments of this type to select flight and control subject candidates who are similar in age, and to monitor pre- and postflight changes.

4. Mammalian Development During Spaceflight

Pregnant rats at gestation day 12 were launched and exposed to a microgravity environment for the 5 days of flight. Following flight,

the structure and function of the neonates as well as the maternal behavior were determined.

The preliminary results, the first of this type ever obtained from space, indicate that the spaceflight environment did not interrupt an established mammalian pregnancy, nor grossly alter basic developmental processes during or after a brief exposure to space. No gross effects were seen in the development of olfactory, optic, vestibular and central nervous system tissues of the neonatal rats from a preliminary evaluation. Some subtle changes in the optic structures were observed but their significance awaits further analysis.

(E. Gomersall, Ext. 5730)

Vestibular Research Facility

The vestibular system plays a major role in the control of eye movements, posture, and locomotion; in the perception of self motion and orientation; and in the generation of motion and space sickness. Because of the importance of this system to man's ability to function effectively in abnormal and normal gravitational environments, a detailed understanding of the structure and function of the vestibular system must be developed. To provide the vestibular research community with unique state-of-the-art capabilities for conducting sophisticated investigations of vestibular function, Ames has established the Vestibular Research Facility (VRF) program to develop techniques and equipment for stimulation and measurement of vestibular nerve activity.

The facility, a versatile modular system which offers researchers a wide range of precision-controlled acceleration and visual stimuli, is currently involved in a series of pilot science investigations for single neuron electrophysiological responses. The most recently completed experiments verified that remote control of the microelectrode during testing is practical, and significantly increases the yield of single neuron recordings; that the acceleration stimuli is essentially free of extraneous vibrations (<5 milli-g); and that the data recordings have minimal noise artifacts. Scientists from the university of Texas Medical Branch, University of Michigan, and University of Pittsburgh are working closely with the Ames engineering team and Johnson Engineering Co. (support services contractor) to evaluate the performance of the hardware. Engineering support is also provided by TRW and Lockheed Missiles & Space Co. for the construction of the equipment.

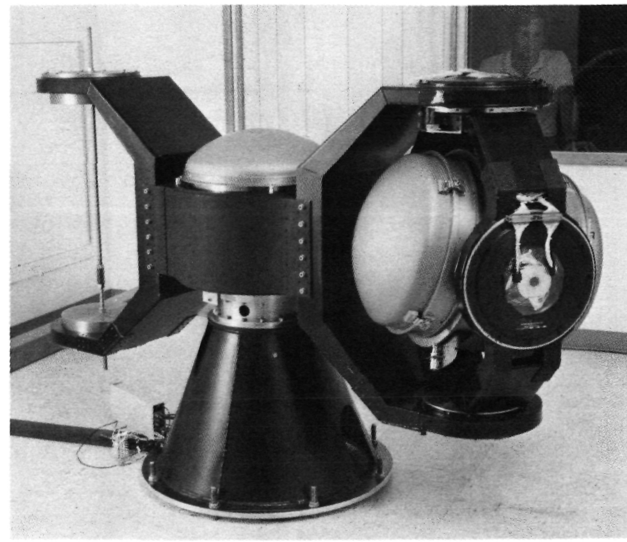

Mah

Vestibular Research Facility

This facility will enable Ames and visiting scientists to do experiments which require combinations of precise rotational and linear accelerations in a variety of test subjects. In essence, the means will be available to investigate the response of physiological systems to vestibular stimulation in a systematic manner.

(R. Mah, Ext. 6538)

Stereotaxic Microelectrode Drive

In the Vestibular Research Facility (VRF), recordings are collected from single neurons in test specimens while those specimens receive motion stimuli. The specimen is held securely and comfortably by a restraint system in an instrumented capsule gimbaled on the arm of the VRF centrifuge. The system features stereotaxic instruments, remote microelectrode controls, a video camera, data collection capability, and life support.

The system is designed for experiments exploring a single neuron electrophysiology. Stereotaxic instruments are used to hold the specimen's head

in a precise location, and to provide a means for accurate and repeatable placement of microelectrodes. With a target as small as a neuron unit, precise positioning is critical. Specialized glass micropipettes, with tips between 1 and 2 microns in diameter, have been developed by scientists from the University of Texas Medical Branch. They are inserted into a vestibular neuron using a modified David Kopf miniature hydraulic drive which was converted from a gear drive to direct drive. This modification increased the control of the micropipette linear travel to within one micron. The driving action is remotely controlled from outside the centrifuge area, and a digital display is provided to read the amount of travel.

During an experiment, EKG, EEG, and body temperature are monitored while the electrical signals from the neurons are recorded; a video camera is used for observation. There are 10 channels available for data which can be stored on disk, or tape, or analyzed in real time.

(J. Kishiyama, Ext. 5572)

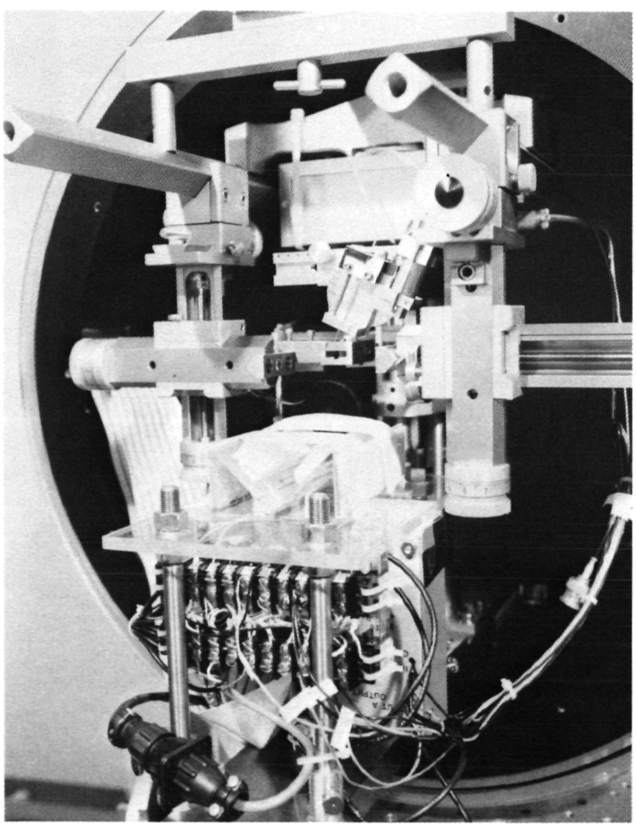

Kishiyama

Stereotaxic microelectrode manipulator system

Spacelab 3

The Life Sciences Flight Experiments Project Office (LSFEP) at Ames is preparing to fly a payload aboard Spacelab 3, scheduled for launch in April, 1985. The payload consists of two Research Animal Holding Facilities (RAHF) and associated equipment, including the Dynamic Environment Monitoring System (DEMS); and the Biotelemetry System (BTS), which will permit the flight of 24 rats and 4 squirrel monkeys in an Earth-like laboratory environment. The equipment, which is the first of its kind, has been developed at Ames in conjunction with three contractors; the Lockheed Missiles and Space Company, Management and Technical Services Company/GE, and Konigsberg Instruments, Inc. Development and ground-based testing has been in progress since 1978 and culminated this year when the equipment was delivered to Kennedy Space Center for integration.

The Spacelab 3 Life Sciences Payload will serve two major purposes: to flight test the new hardware, and to collect baseline data on animals which will be experimental subjects on subsequent Spacelab missions. Future experiments will help to identify physiological responses to the flight environment and to resolve identified biomedical problems experienced by the astronauts. The Ames payload on Spacelab 3 is thus the first step toward NASA's goal of establishing an Earth-like laboratory in space in which to live and study life away from Earth.

(C. Schatte, Ext. 6748)

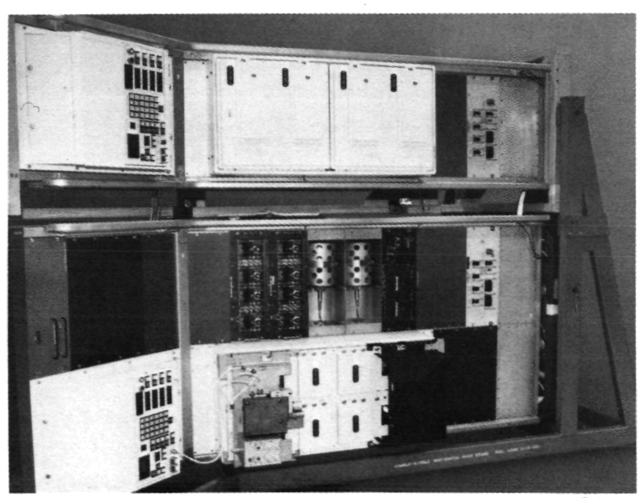

Schatte

Spacelab 3 Life Sciences Payload

Man-Vehicle Systems Research Facility

The Man-Vehicle Systems Research Facility (MVSRF) is a unique national research tool, used primarily to study basic human-factors issues related to human errors in the national aviation system. The MVSRF includes two full-mission flight simulators: one a Boeing 727-200 simulator, and the other an Advanced Concepts Flight Simulator intended to be representative of cockpits of the 1990s time frame. Both simulators are capable of operating alone or interactively with each other in the same airspace, and with a simulated Air Traffic Control (ATC) system. The facility allows the creation of realistic multiaircraft, air-to-ground, and full-mission scenarios. This provides NASA with the capability to study carefully and analyze man-to-man and man-to-machine interactions with the eventual goal of decreasing the incidence of human errors in the operation of the national aviation system.

The interconnection of the major system components is shown. While only the B-727 simulator presently includes a full six-degree motion system, both the advanced and conventional simulators are capable of all aspects of full-mission operation. Each has a dedicated experimentor's lab, for controlling, monitoring, and recording all elements of each simulation. A visual scene-generation system is provided for out-the-window cues in the cockpits. The ATC system simulator provides realistic communication with the cockpits and allows research that examines air-ground communications systems as they impact crew performance.

Styles

Man-Vehicle Systems Research Facility

Styles

Boeing 727-200 simulator

Styles

Advanced Concepts Flight Simulator

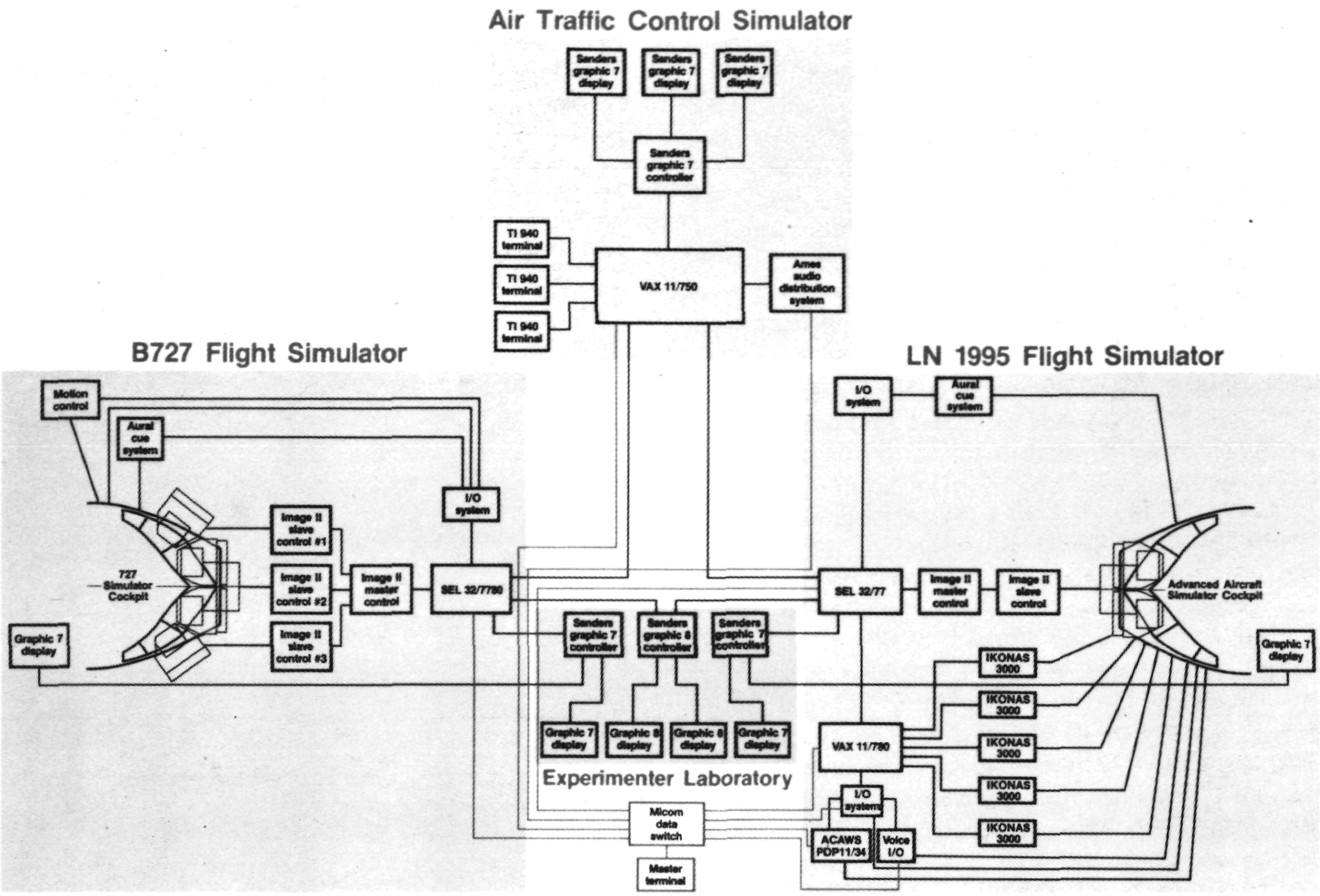

Styles

MVSRF integration

The MVSRF is utilized to perform a broad range of human-factors research with both conventional and advanced aviation systems. The objectives are to develop an understanding of the basis for, and limit the incidence of, human error in aviation operations. The facility is used to conduct human-factors research on:

1. Development of fundamental analytical expressions of the functional performance characteristics of aircraft crews.
2. Formulation of design criteria and principles for environments of the future.
3. Integration of new subsystems into contemporary flight and air traffic control scenarios.
4. Creation of new training technologies that will be required by the continued technical evolution of flight systems and the operational environment.

(F. Styles, Ext. 5728)

Styles

Simulated ATC system

Human Motion Sensor

The goal of artificial intelligence is to automate human function; the goal of display/control design is to optimize the exchange of information between human and machine. Both of these goals require an understanding of natural human functions. The Perception and Cognition Group is seeking this understanding, in part through the construction of computational models of human vision.

A model of motion sensing has been developed that simulates the major features of human motion perception. It accepts as input a sequence of digitized images and produces as output a series of vector fields. Each vector within a field estimates the velocity of an image component of one scale (spatial frequency) at one location. The different vector fields correspond to different scales. This allows the model to be scale-invariant: motion can be sensed equally well regardless of the size of the moving object.

The model has two stages. The first is composed of scalar motion sensors that resemble the direction-selective simple-type neurons in the primate visual cortex. Each scalar sensor measures the component of the image velocity vector in the sensor direction. The second stage resolves these components into a single estimate of image velocity at each location and scale. Model simulations agree qualitatively with human perception in the cases we have examined.

(A. Watson and A. Ahumada, Ext. 6584/6290)

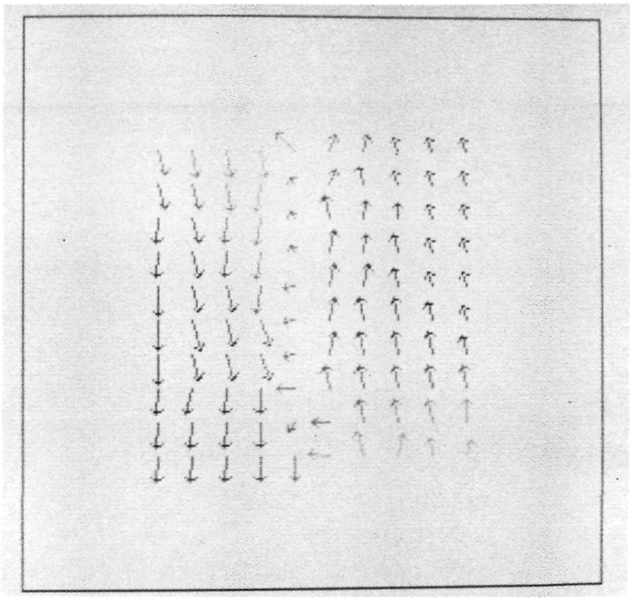
Watson/Ahumada

Motion sensor output vector field at a scale of 4 cycles/picture width

Watson/Ahumada

An input to the motion sensor

Investigating Growth Factors to Alleviate Muscle Atrophy in Spaceflight

In weightlessness, significant atrophy occurs in the little-used postural and leg muscles. This is because the body requires less structural support against the force of gravity. In the long flights required for an operational human-tended space station, muscle loss may be a serious problem.

The results of muscle atrophy were observed during the lengthy Skylab flights of the mid-1970s, and during short-term flights of Gemini, Apollo, and Soyuz spacecraft. Experiments flown on the Soviet Cosmos biosatellites have provided U.S. and U.S.S.R. scientists with a clearer understanding of the detailed effects of muscle atrophy caused by spaceflight.

Ground-based research (sponsored by NASA's Office of Space Science and Applications) allows investigators to examine the biochemical process

of muscle atrophy prior to the testing of hypotheses during actual spaceflight experiments. Muscle mass was found to increase in the presence of certain proteins, such as insulin growth factor, as well as other growth factors as yet unidentified. During stretch of a chicken muscle, an intrinsic growth factor increased, resulting in cell division and muscle growth. Upon release of the muscle, the concentration of growth factor returned to normal. These biochemical and biomechanical findings may eventually lead to more effective exercise or drug countermeasures to alleviate spaceflight muscle wasting.

(S. Ellis, Ext. 5757)

Simulated Weightlessness and Female Astronauts

Because the presence of female astronauts in space is becoming routine, their physiological response to the stresses of spaceflight must be understood. The Human Research Facility at Ames conducted an unprecedented study on female subjects undergoing -6° head-down bedrest to simulate the cardiovascular effects of weightlessness as accurately as it is possible to do on Earth. Their reactions were similar to those of males in previous studies. Contributing to reduced acceleration tolerance following weightlessness, a lower release of norepinephrine (NE) was found in subjects prone to fainting. On the other hand, nonfainters showed an exaggerated NE response, apparently to compensate for fluid and vascular changes resulting from the bedrest simulation of weightlessness.

(J. Danellis, Ext. 5552)

Psychophysiology Facility for Biofeedback Training and the Study of Motion Sickness

Foremost among the medical problems identified by NASA's Office of Space Science and Applications is the anorexia, vomiting, and malaise during the first few days of adaptation to weightless flight. Some of the most promising research toward a medical countermeasure has been conducted by scientists from Ames Biomedical Research Division with collaborators from the University of California's Langley Porter Neuropsychiatric Institute and the Rockefeller University of New York.

Motion sickness was reduced or prevented entirely in subjects who voluntarily controlled their physiological activity by monitoring electronic biofeedback signals to inform them of real-time changes in their bodily functions. Autogenic Feedback Training (AFT), an autogenic or self-training technique, was developed at Ames to control the symptoms of motion sickness. AFT aided some subjects in controlling their symptoms on Earth for up to two years after only six hours of training. Presently, researchers at Ames and Johnson Space Center are preparing a series of *Shuttle* experiments to investigate the use of AFT in the space environment.

Psychophysiological studies at Ames demonstrated a relationship between motion sickness

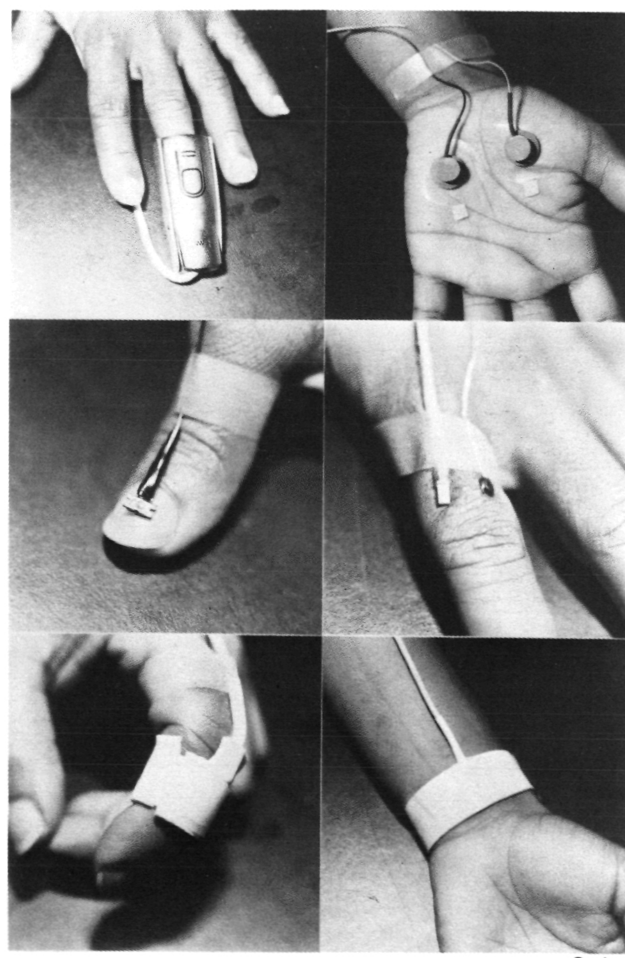

Cowings

Variety of biofeedback sensors used to examine the psychophysiology of motion sickness

and various physiological measurements, such as heart rate, respiration, skin resistance, and peripheral vasoconstriction as measured by finger pulse volume. Most recently in tests using more than 100 subjects, those disposed to motion sickness showed a higher heart rate and peripheral blood volume compared to less susceptible subjects. Also, electrical activity of the stomach recorded as an electrogastrogram (EGG) was highly correlated to motion sickness in a study of 20 subjects. Thus EGG may be an effective biofeedback signal for learning to control motion sickness.

(P. Cowings, Ext. 5724)

Echocardiography for Shuttle Crews

Weightlessness in spaceflight induces cardiovascular deconditioning, which may be reflected in a weakening of the cardiac muscle and may create possible problems for some members of flight crews during reentry and return to terrestrial gravity levels. To monitor and understand cardiac changes, as well as to assess potential countermeasures, echocardiograms were performed before and after flight on 17 Shuttle crewmen in a cooperative study with Johnson Space Center under sponsorship of NASA's Office of Space Science and Applications.

Goldwater

Ultrasonoscope used in echocardiographic studies of the heart in Shuttle astronauts

Echocardiography produces real-time images of the heart and its function using high-frequency sound waves, or ultrasound. A portable ultrasonoscope was modified for the preflight and postflight measurements, and for future use aboard the Shuttle to evaluate cardiac changes during flight. To analyze echocardiograms, extensive software was developed in collaboration with Stanford University. The software was validated in tests on subjects during ground-based bedrest simulations of spaceflight at Ames' Human Research Facility. The software is now being applied to actual crew data. Also, thousands of echo measurements were taken of subjects during simulations of Shuttle reentry (lower-body negative pressure following bedrest) to permit a controlled evaluation of potential drug countermeasures.

(D. Goldwater, Ext. 5749)

Student Shuttle Involvement Project (SSIP)

Dan Webber, a student at Cornell University who was sponsored by Pfizer, Inc., developed the experiment selected for this program. The experiment was taken on STS-41B. Webber hypothesized that the development of adjuvant-induced arthritis has a gravity component. Studies on an animal model simulating some aspects of spaceflight (unloading or rear limbs, fluid shift toward the head) suggested that unloading of the limbs, and/or fluid shifts contributed to the onset of the disease process. Data collected immediately postflight suggested that gravity did not contribute to the development of the arthritic process. However, gnotobiotic animals were used for flight and specific pathogen free (SPF) animals had been used for all ground-based studies. The flight experiment was based on a time course of the disease process found in SPF animals (about 10 days for apparent systemic disease), whereas the onset of systemic disease required about 14 days in the gnotobiotic rats. Reentry, at the time the systemic disease occurred, may have significantly impacted the data.

(E. Holton, Ext. 5471)

Hot Atom Chemistry and the Production of Organic Compounds in Planetary Atmospheres

The atmospheres of the outer planets in our solar system are complex mixtures of hydrogen, helium, methane, and ammonia, with trace amounts of other gases including simple hydrocarbons and organic nitriles. Simple equilibrium cooling of the presolar nebula can account for the first four of these gases, but the others imply the occurrence, past or present, of active organic chemistry in the atmospheres.

Several chemical processes have been proposed to explain the presence of these compounds. On Jupiter, for example, the upper atmosphere is exposed to the entire solar spectrum, and thus, photolysis of methane can produce the observed hydrocarbons. In the lower regions where the colored clouds exist, lightning and thermochemistry may be responsible for the production of organic molecules. In the middle regions, however, where the ammonia is frozen out to form the white clouds, direct photolysis of methane cannot occur. Here "hot" atom chemistry may be responsible for organic synthesis. Hot hydrogen atoms, formed from the photolysis of ammonia, have kinetic energies greater than the thermal background and can react with each other to form hydrocarbons, or with amino radicals from ammonia to form organic nitrogen compounds.

To model the hot atom process in the laboratory, photolysis experiments using methane labeled with a deuterium tracer have been carried out. The results show that the efficiency of the process is low, from 1 to 5%, but that it persists even in the large excesses of hydrogen found in outer planet atmospheres. Thermalization of the hot atoms, which renders them unreactive, does occur, but not at levels high enough to stop the

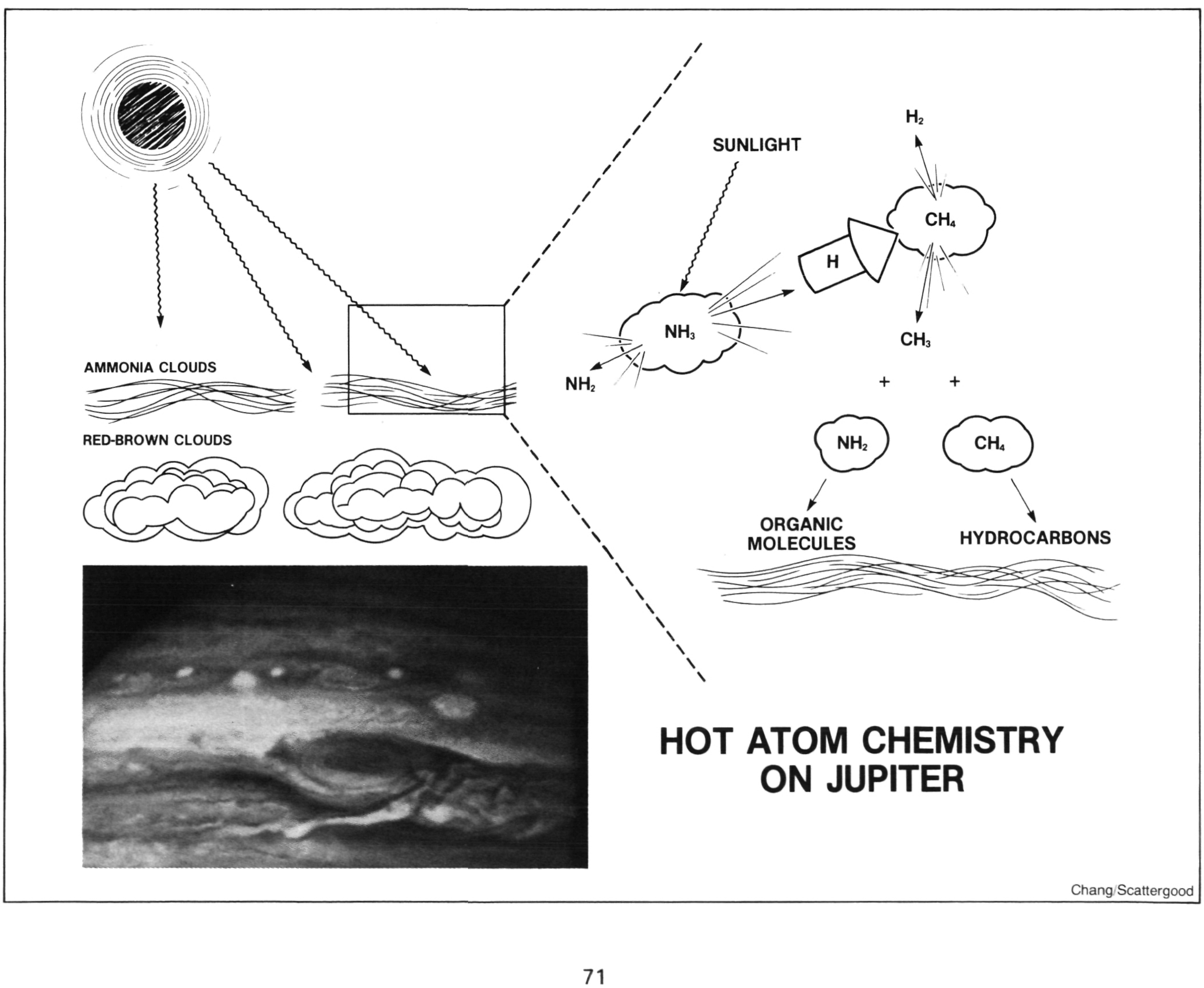

hot atom process. Since no other chemical process may be occurring in the vicinity of the ammonia clouds, hot atom chemistry may be the dominant source of organic species found there.

(S. Chang and T. Scattergood, Ext. 6206/6164)

Satellite Estimation of Forest-Leaf Area

Transfers of energy, water, carbon, and nutrients in forest ecosystems occur largely in the forest canopy. Measurement by NASA remote sensing satellites of foliar mass, surface area, and biochemistry can help determine the role of forests in global biogeochemical cycling.

An empirical investigation using an airborne instrument simulating the Thematic Mapper (Landsat 4 and 5) predicted the one-sided leaf area per unit ground area, called leaf area index (LAI), for temperate coniferous forests. Radiative theory predicts that visible red solar radiation is strongly absorbed by chlorophyll in the leaves while near infrared (IR) (760-900 nm) radiation is strongly scattered and weakly absorbed. Thus, as LAI increases, the reflection of IR steadily increases while the red absorption quickly reaches saturation. To compensate for various radiative effects, the ratio of IR to red is related to LAI. The forests of Oregon were studied having LAI values from one to twenty. This ratio, corresponding to bands 4 and 3 of the satellite, does predict LAI, the first time this was demonstrated for forests. In addition, all of the species studied (12 communities in Oregon) fall on the same curve, which is encouraging results for global studies.

Gases, particulates, and aerosols in the atmosphere absorb and scatter solar radiation to varying degrees in the spectrum. The satellite perceives this as reduced transmittance and additive path radiance to the reflected radiation from the canopy. Comparisons of reflectance just above the canopy (by helicopter instruments) with the satellite show additive radiance of nearly 60% for red radiation while the absolute effect is nearly constant for IR and red. This effect greatly reduces sensitivity . The effect is more pronounced for dark objects like forests. A reliable technique for systematically removing this effect from terrestrial data has yet to be developed.

(D. Peterson, Ext. 5899)

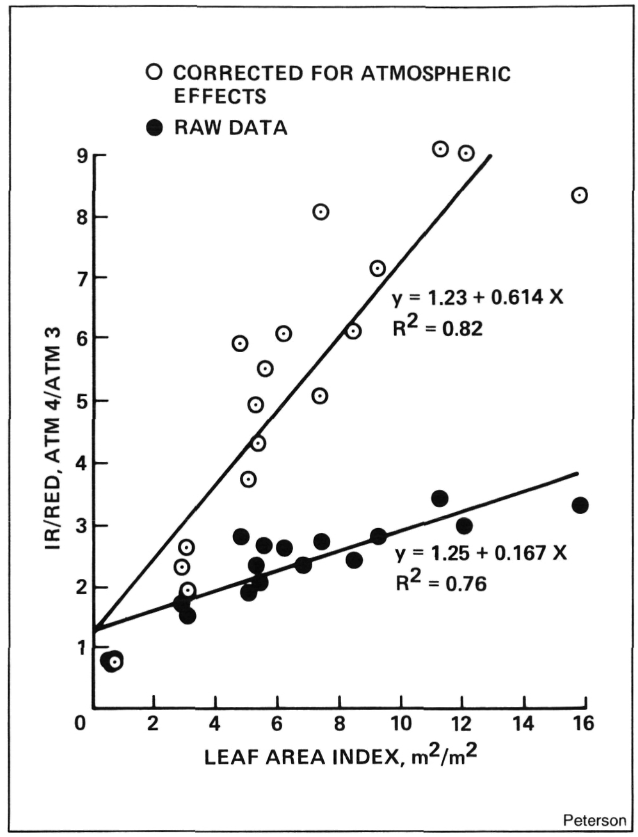

Predictive equations of forest leaf area index using satellite remote sensing data; comparison of uncorrected data to that corrected for atmospheric effects

Remote Sensing Techniques for Waste Disposal Impact Assessment

One potential impact of hazardous waste disposal is the contamination of nearby surface water. Remotely sensed data may be effective in monitoring water quality or in identifying pollutant outfalls. A recently completed study was one of the first to evaluate Landsat Thematic Mapper (TM) data for the assessment of water quality.

Water quality samples were collected at 25 sites concurrent with a TM Simulator (TMS) overflight. Regression analysis was conducted to develop equations for mapping water quality constituents using TMS data. A multiple regression, using TM channels 1 through 7, was developed for mapping suspended solids. Nosier channels, 5 and 7, were omitted from the multiple regression developed for mapping the logarithm of conductivity. The best turbidity regression was a multiple regression using the first four TM principal components.

(E. Horn, Ext. 5896)

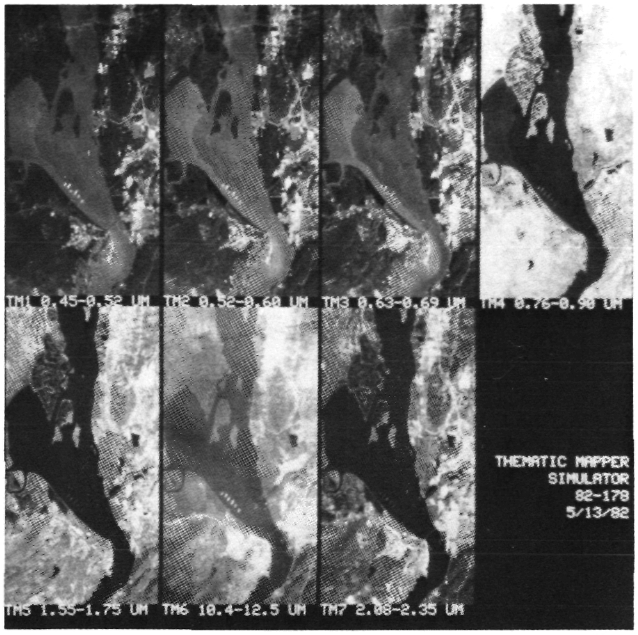

Horn

Seven Landsat Thematic Mapper channels (simulated) for the Carquinez Straits-Suisun Bay, California, study site

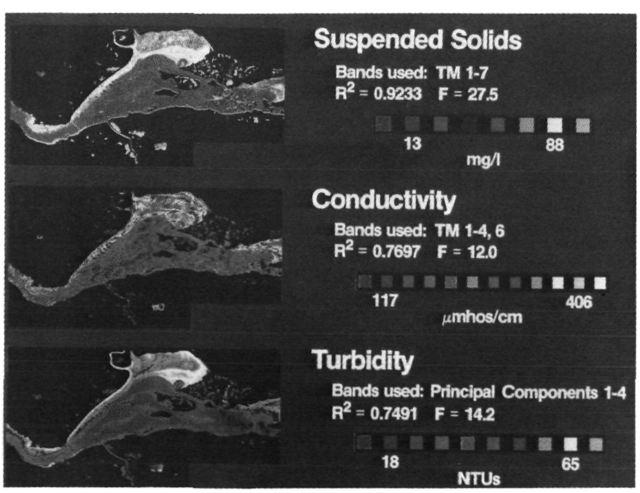

Horn

Suspended solids, conductivity, and turbidity maps produced by application of regression equations to the Thematic Mapper digital data

Gas Chromatographic Separations of Atmospheric Gases Using Custom-Made Porous Polymers

Gas chromatography is the technique best suited to obtain definitive results in probes of the atmospheric composition of extraterrestrial bodies. Separation of certain gases is, however, often difficult. Depending on the complexity of the gaseous mixture, consideration must be given to using more than one column in the gas chromatograph.

Previous work developed an improved microporous polymer column packing which separates the permanent gas group (Ne, H_2, N_2, O_2, Ar, CO, Kr, CH_4). Further work has led to the development of a porous polymer which is capable of separating air, methane, carbon dioxide, ethylene, ethane, acetylene, propane (propene), propadiene, propyne, isobutane, and n-butane. Another porous polymer was synthesized which has the capability of separating certain polar molecules such as sulfur dioxide, acetaldehyde, methanol, water, formaldehyde, and acetonitrile without interference from the previously mentioned gases.

Work is continuing on these last two polymer types to study variations which may improve separations and to include more gases and compounds of cosmological interest.

(G. Pollack, Ext. 6165)

Simple and Effective Modulator for Multiplex Gas Chromatography

Simplification and miniaturization are desirable in the design of any instrument component intended for NASA flight operations. Obtaining improved performance at the same time is a desirable bonus.

A new and simple chemical modulator for multiplex gas chromatography has been demonstrated. The modulator is constructed simply by painting the first few centimeters of a commercially available fused silica capillary column with an electrically conductive paint. An electric current, on command from a microprocessor, rapidly heats the painted section of the column, driving any adsorbed substances out of the stationary phase and into the rest of the column. A continuously flowing sample stream, passing through the modulator and column, is modulated in concentration as the microprocessor repeatedly pulses the temperature of the modulator. The modulator has very little mass and, therefore, can change temperature rapidly. The chromatogram of the sample stream is computed from the complex signal observed at the end of the column. This modulator is simpler than the mechanical valves used for conventional gas chromatographic sampling. It is also much smaller and lighter in weight and has no moving parts.

Using this thermal modulator, hydrocarbons have been detected by multiplex gas chromatography at concentrations three orders of magnitude below what can be detected by conventional instruments. The resolution is also better, and less restrictions are placed on the composition and volume of the sample.

(J. Phillips, Ext. 5766)

The Multichannel Spectrum Analyzer

The NASA Search for Extraterrestrial Intelligence (SETI) program will hunt for signals in the microwave window from about 1 to 10 GHz. The signals may be narrowband carriers or pulses whose spectrum is as narrow as their duration permits. For this purpose, we need a high resolution, wideband radio frequency spectroscope — a receiver that looks at a large number of narrow channels simultaneously. Such a device, called a multichannel spectrum analyzer (MCSA), is nearing completion at Stanford University under a NASA grant.

The prototype unit has 74,000 channels, each 1 Hz wide, but the design is capable of expansion to over 8 million channels. This will permit the examination of 8 MHz of spectrum at a time. The device operates in real time, delivering a complete spectrum once per second.

The algorithms are stored in RAM and so are down-loadable from a disk file. Thus, the MCSA can be made to furnish a spectrum with 2 Hz wide channels, twice a second, or one with 4 Hz wide channels every quarter second, and so on, up to channels 512 Hz wide. Simultaneously, spectra with 1024 Hz, and 74 kHz wide channels are available. All outputs are available as complex amplitudes or as power.

The real time capability and flexibility of the MCSA suggest that it may be useful in other applications besides SETI.

(B. Oliver, Ext. 5166)

Space Science and Applications

Testing of Cryogenically Cooled Silica Mirror Mounts

Testing of a newly-developed, mount concept for cryogenically cooled silica mirrors for infrared telescopes has been successfully completed at ARC. The mount concept, developed for ARC under a grant to the University of Arizona, Optical Sciences Center, utilizes three symmetrically-located, parallel-spring-guide flexure and clamp assemblies attached to the back of a lightweight, fused-silica mirror. The mirror and its mount were installed in the ARC Cryogenic Optical Test Facility, and cooled to 7 K using liquid helium in the nitrogen-shrouded facility Dewar.

With the mounted mirror at low temperature, interferograms were taken using a Shack interferometer with an optical path through a small window in the Dewar. Processing of the interferograms using FRINGE, an optical analysis computer program, provided a quantitative assessment of the figure of the mirror before cool-down at 7 K, and the difference in figure between the extreme temperatures. This figure difference is a combination of cryogenic distortion due to the mirror material itself and any stresses induced by the mounts. The mounts must attach to both the low expansion silica of the mirror and the relatively high expansion aluminum of the structure and must prevent stresses due to differential expansion of the materials from distorting the mirror beyond acceptable limits.

At room temperature the mounted mirror had a surface figure error of 0.05 wave rms at a wavelength of 0.633 micron. At 7 K the mirror figure changed to 0.10 wave rms. The point-by-point subtraction of the surface measurements yielded a figure difference of 0.09 wave rms. Previous tests of the unmounted mirror produced a difference of 0.07 wave rms, attributed to the mirror material. On a root-sum-square basis, this result indicates that the figure change due to the cryogenic distortion caused by the mounts was less than 0.06 wave rms. Although the mounts tested are not a flight-qualified design, this amount of mount-induced distortion is well within a reasonable error budget allocation for the telescope planned for the Space Infrared Telescope Facility (SIRTF)

(R. Melugin, Ext. 6530)

Silica mirror and mount cryogenic distortion in waves at 0.633 micron

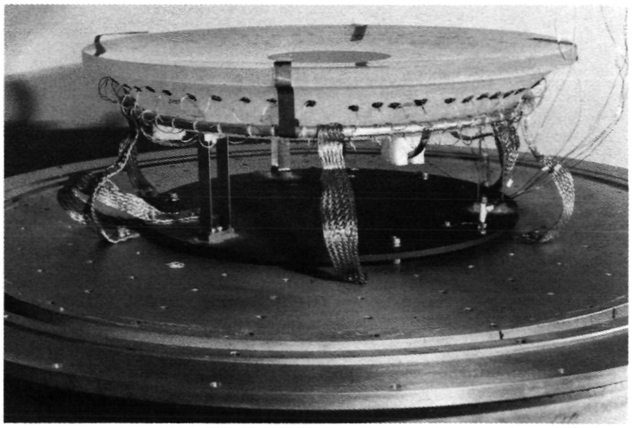

Fused silica mirror and mounts Melugin

Development of Lightweight Mirrors for Space

Space missions of the future, such as the Large Deployable Reflector (LDR), will require a large, segmented primary mirror on the order of 20 m in diameter. The segments must necessarily be lightweight to make the launch into space practical. An important problem to overcome is the cost to make the segments in sufficient quantity (over 300 m^2) and of sufficient quality to enable diffraction-limited imaging at an infrared wavelength in the range of 30 to 50 microns.

A process has been developed at the University of Arizona, Steward Observatory, to fabricate lightweight, honeycomb-core, sandwich mirrors from low-cost borosilicate glasses. The process utilizes a unique concept to make the honeycomb core and to fuse it to the segment face and back plates. The process begins with thinwall glass tubing cut to uniform lengths and close-packed between two glass plates in a furnace. The furnace temperature is raised to the softening point of the glass to fuse the ends of the tubing to the plates. After the initial fusion and while the assembly is still hot, air under pressure is introduced into the glass tubes through holes in the back plate. Since the plates are constrained between two flat surfaces, the tubes expand radially outward, press against each other and form hexagons which also fuse together at the elevated temperature. When cooled, the result is a high stiffness, plano-plano segment blank which can then be slumped in a second furnace cycle over a suitable convex form to produce a concave blank with the approximate figure desired. Final grinding and polishing produces the finished surface.

Plano-plano blanks finished as flat mirrors at 0.75 m^2 have been produced with cores 7.62 cm thick, using stock tubing with a wall thickness of 0.24 cm, and 1.27 cm thick plates. The areal density of this construction is approximately 80 kg/m^2. Lighter blanks may be made by thinning the plates and by using thinner wall tubing in the core. Though no practical lower limit for areal density has been established for this technology, a 38 cm diameter, f/2, concave sphere with 0.63 cm thick plates has been fabricated using an older technique to get 55 kg/m^2. This indicates that further reduction to near 30 kg/m^2 should be possible.

(R. Melugin, Ext. 6530)

Bolometers Cooled by Adiabatic Demagnetization

Presently, bolometers are the most sensitive infrared detectors at wavelengths longer than 200 microns. The noise intrinsic to these devices decreases rapidly with decreasing operating temperature; thus, bolometers operating at low temperatures are desirable in low infrared background environments. Such environments will be attained in cooled orbiting space infrared telescopes such as the Space Infrared Telescope Facility. The most promising refrigeration technique for cooling bolometers to temperatures below 1 K in space is the adiabatic demagnetization of a paramagnetic salt. This technique is compact, low-power, gravity independent, and capable of achieving temperatures well below 100 mK. We have developed a cryogenic system utilizing this technique that, coupled with optimized bolometer detectors we also developed, can be used as a development test bed for this type of detector system. The system is compact, capable of achieving temperatures below 50 mK, and is able to be mounted on the 200″ Hale telescope at Mount Palomar for test observations at a wavelength of 1 mm. Tests in the laboratory have shown that this is presently the most sensitive bolometer system in the world. Portions of this work were accomplished with consortium agreements with Stanford University and The California Institute of Technology.

(T. Roellig, Ext. 6426)

Passive Orbital Disconnect Strut

One of the biggest parasitic heat loads on a space-based cryogenic system is the support system. These supports must provide low thermal conductance yet have sufficient strength to withstand launch. A new type of support has been developed in conjunction with the Lockheed Palo Alto Research Laboratory. These are the passive orbital disconnect struts (PODS). The struts are variable conductance, variable strength devices. In orbit the loads are taken by a thin wall, low-thermal conductance graphite-epoxy tube. When launch loads are applied, this thin tube stretches elastically until it bottoms against a stop. The loads are then taken by a larger, higher strength glass-epoxy tube. The PODS have

several advantages over conventional supports: (1) for the same launch strength, the orbital conductance is an order of magnitude smaller; and (2) the launch and orbital components can be designed independently rather than having to design only for the launch conditions.

A single strut has been built and extensively tested. These tests include: (1) measurement of the thermal conductance, (2) measurement of the load required to change from the orbital to launch configuration, (3) measurement of resistance to side loads, (4) measurement of ultimate strength, and (5) fatigue testing at launch loads for more than 500,000 cycles. These tests have shown that the PODS meet or exceed their expected performance, proving the usefulness of the concept.

(P. Kittel, Ext. 6525)

Astronomical Demonstration of Infrared CID Technology

To demonstrate the applicability of integrated detector array technology for future space astronomy missions such as the Space Infrared Telescope Facility (SIRTF), a 256-element array and an ARC-developed data system were used in two telescope demonstrations. The 16 x 16 bismuth-doped silicon IR array, developed under contract by Aerojet ElectroSystems Company, was previously characterized in our laboratory, where it exhibited low readout noise and good uniformity. For the demonstration, the array was mounted in an astronomical dewar which included two circular variable filter wheels for spectral imaging. The portable microcomputer-based data system allows real-time digital integration of large numbers of array frames, and processing software to concatenate and smooth images.

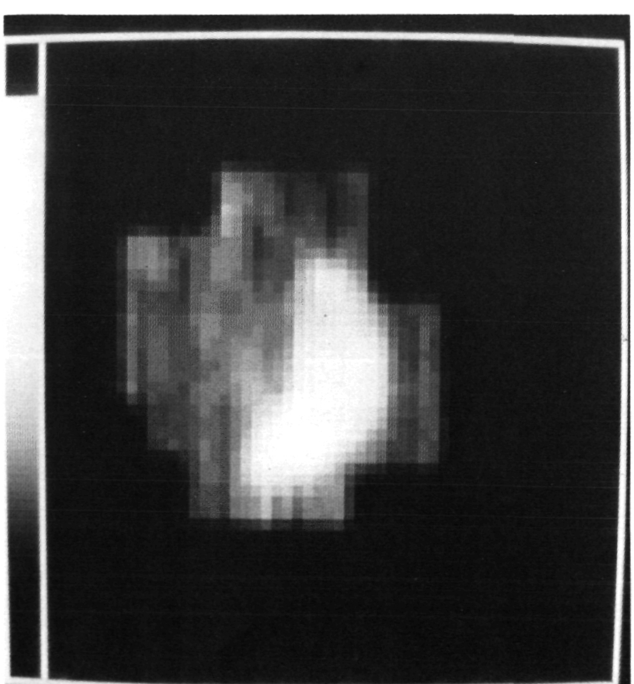

Goebel/McCreight

Collage of images of Venus taken at 3.0 μm with a 1.8 arc sec pixel size. Five fields comprise this collage

In October 1983 and January 1984, the system was successfully operated on the 60-inch NASA/ University of Arizona infrared telescope at Mt. Lemmon, Arizona. A number of objects were imaged with 1.8 arcsec per pixel resolution. A 3μ image of the crescent of Venus was obtained with the array system; an averaging filter routine has been used to smooth the data. The test dewar and electronics systems were recently upgraded, and in October 1984 a follow-on observing run in the 10 μm region was carried out.

(J. Goebel and C. McCreight, Ext. 6525/6549)

Optical Information Processing

A key technological bottleneck for the field of optical information processing has been the lack of a programmable mask. The mask is required to produce spatial patterns suitable for modifying optically produced images. Mathematical transformations of the image are then possible in a truly optical manner, i.e., without an electronic computer. Such a programmable mask can be realized by suitable implementation of a liquid crystal display (LCD).

We have used an LCD as a programmable mask (LCDPM), and we have successfully demonstrated its capability to perform mathematical operations. The LCDPM has been used as a Hadamard Image Encoder (HIE), and a reconstructed encoded image is shown in the accompanying figure. The comparison is quite favorable in details that are too subtle to be revealed on the printed page.

A similar mask will soon be incorporated into a matrix-matrix multiplier for a fast 32-bit processor.

(J. Goebel, Ext. 6525)

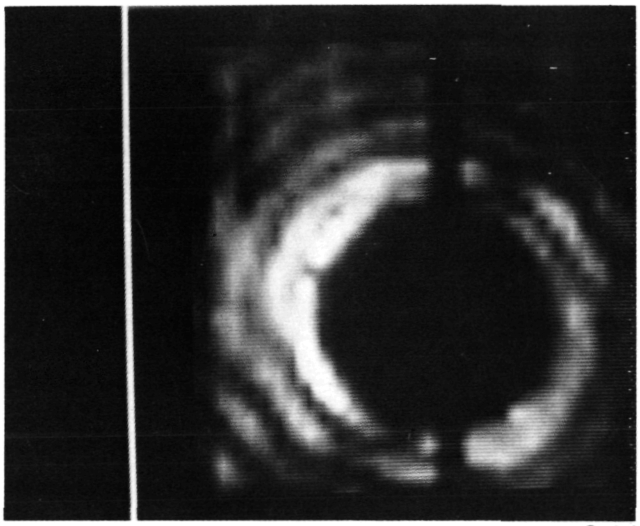

Goebel

Decoded Hadamard image of a diffraction pattern. The laser beam passed through a pinhole, and the central peak was blocked with an opaque mask. The thread supporting the mask is clearly discernible

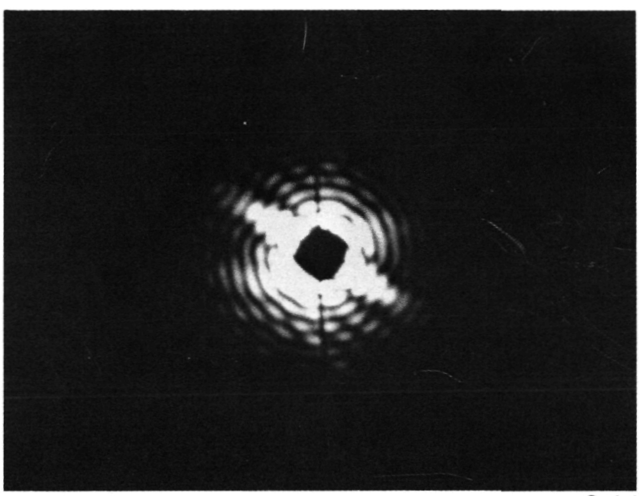

Goebel

Photo of diffraction. Pattern encoded in accompanying figure. Note larger field of view

Study of the Radiative Effects of the Arctic Haze

The Arctic, which lies far from most major sources of pollution, has been traditionally considered a remote region where the air and water are still clean and pure. However, during the last 25 yr, each winter-early spring season has seen a remarkable increase in the concentration of man-made pollutant particles (haze) in the Arctic atmosphere. An important component of the Arctic haze is black carbon, which is an efficient absorber of solar radiation. The solar energy absorbed is converted into heat and results in an increase in the temperature of the atmosphere. A consequence of this temperature increase is the alteration of the local climate with potential for global climatic changes that may be forthcoming as the result of a steady buildup of light-absorbing haze over the northern polar cap of the Arctic. These effects are enhanced during the early spring, when both the carbon concentration is high and the Sun elevation is sufficient for a considerable amount of solar radiation to reach the Arctic.

In order to determine for the first time the magnitude of the radiative effects of the Arctic haze, we flew repeatedly over the Arctic during March-April 1983. We found the haze to be much denser and more extensive than expected (comparable to urban areas in its black carbon content). The analysis of our experiments shows that the heating of the atmosphere by the Arctic haze-absorbed sunlight is 2 to 3 times larger than normal.

The measured values during this period were on the order of 1.5 K/day in a layer extending from the surface to 5 km. Due to the complicated interaction of ice physics and atmospheric dynamics, it is difficult to assess the climatic impact of this additional heating, although enhancement of the melting rate of the pack ice is likely. Analysis of the data is continuing and plans are underway for a second flight series to be conducted in Spring 1986.

(F. Valero and T. Ackerman, Ext. 5510/5233)

El Chichon Aerosol Evolution

Stratospheric aerosol perturbations caused by El Chichon's 1982 eruption are being studied with a number of airborne samplers, under the management of NASA's Climate Program Office. One such sampling approach is a wire impactor flown on U-2 aircraft. Data obtained with this method reveal that stratospheric aerosols collected over the western United States from late 1982 to mid-1984 continue to show strong effects of El Chichon's eruption. Although mineral particles have disappeared, large ($>$0.9

microns in diameter) acid droplets are common. These have never been seen in prevolcanic, background-level collections, and result from increased droplet growth made possible by the unusual abundance of sulfate. Aerosol size distributions show a wide variety of multimodal curves, owing to mixtures of air containing aerosols of various ages. Towards the end of the study period there are fewer large aerosols, because of gravitational settling and poleward transport. These effects reduce sulfate, as most aerosol mass is concentrated in a small number of large droplets. Even the lower sulfate levels are, however, two to four times typical prevolcanic background contents. The influence of El Chichon on high-altitude air is still considerable two years after the eruption. Monitoring of the study area continues, to further document aerosol changes.

(K. Snetsinger, Ext. 5494)

Models of Venus' Atmosphere Structure from the Surface to 100 Kilometers Altitude

Models of the thermal structure of the atmosphere of Venus have been generated based on a synthesis of data from six spacecraft experiments. The major data base was from four experiments on the Pioneer Venus Entry Probes and Orbiter, with supplementary data from the USSR Venera 10, 12, 13, and 14 landers. The data were compared, and differences, which were generally moderate, were critically evaluated. The model was selected to represent those data believed to be most valid in given altitude intervals. The resulting atmospheric model is believed to be the best available representation of the atmosphere of Venus. Mean temperatures are probably correct to within a few degrees K, although it is known that there is some variability present. Temperature, density, and pressure are tabulated as functions of altitude, along with auxilliary parameters.

This work was a contribution to the COSPAR Venus International Reference Atmosphere, and will be published by COSPAR. It includes contributions from co-authors in the USSR, from Oxford University, the University of Wisconsin, and the Jet Propulsion Laboratory.

(A. Seiff, Ext. 5685)

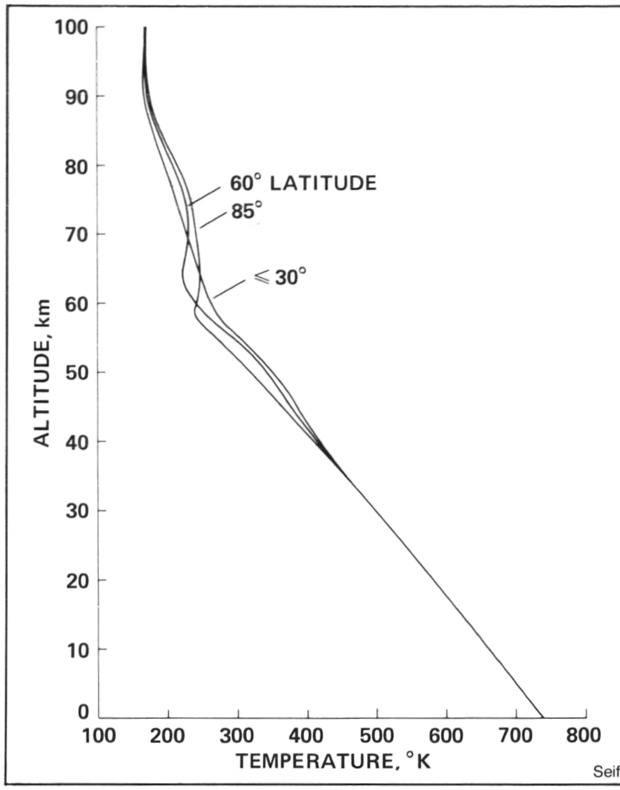

Models of the temperature structure of the atmosphere of Venus

Dynamics of the Venus Ionosphere

In order to investigate the dynamics of the Venus ionosphere, Ames and Santa Clara University scientists have constructed a preliminary two-dimensional model of the Venus ionosphere. This axially symmetric model, which extends from the subsolar to the antisolar point has for the first time successfully predicted the horizontal plasma velocity at altitudes of between 150 and 500 km above the surface. (By "successfully" we mean that the computed velocities agree very well with the values measured by the retarding potential analyzer experiment carried by Pioneer Venus Orbiter.) These results appear in the November 1984 issue of *Icarus.* More recently, a simple two-dimensional "spectral" model of the plasma temperature has been developed. The preliminary model, which is run on an IBM personal computer, has demonstrated that plasma advection is sufficient to account for the observed broad features of the nocturnal ion temperature, but not for the corresponding electron temperature.

(R. Whitten, Ext. 5498)

Planetary Lightning Studies

Spacecraft observations have shown that lightning activity is not confined to the terrestrial atmosphere, but is also found in the atmospheres of Venus, Jupiter, and possibly Saturn. The high temperatures produced by lightning discharges in atmospheres containing nitrogen, carbon, and hydrogen cause the formation of molecules that are precursors to those found in living organisms. Ames scientists are studying the formation of prebiological molecules and optical radiation by lightning in the primitive-Earth atmosphere as well as in the atmospheres of other planets and moons. Experiments conducted at Ames during 1984 have shown that the incidence of production of some prebiological molecules by lightning discharges is 1000 times larger than expected. A paper describing these results is being presented at the Division of Planetary Studies Meeting in Kona, Hawaii. Theoretical work is underway to understand the high production rates and to predict the impact of such rates in the Earth's primitive atmosphere and the atmospheres of other planets and moons. Recent calculations done at Ames have shown that lightning on Titan could form substantial amounts of trace gases and aerosols in that atmosphere. These calculations are in agreement with spacecraft observations of Titan that have shown HCN and C_2N_2 at such high concentrations that some, as yet unidentified, process must be actively producing them.

(W. Borucki, Ext. 6492)

Photometric Search for Other Solar Systems

Photometric methods of searching for planets around stars depend on observing the decrease in light flux, or the change in the color of the light flux produced by the transit of a planet across a stellar disk. The magnitude of the flux reduction is proportional to the ratio of the planet's area to that of the star. The color change is a function of the area ratio and the wavelength separation and width of the filters. For the solar system, the decrease in light amounts to 1.0 percent for Earth-sized planets. The color changes are approximately 1/5 of the flux changes. The photometric method works only for planets whose orbital plane includes the Earth. Consequently, many stars must be monitored on a nearly-continuous basis to obtain a substantial discovery rate. Ames scientists are developing the techniques and instrumentation that are required to make simutaneous, high-precision photometric measurements on many stars so that other planetary systems can be detected.

During 1984, a workshop attended by the world's experts on photometry was held to discuss ways to increase the precision of the measurements to the point that planets could be detected. In the course of the deliberations it was discovered that an unidentified phenomenon was limiting the day-to-day precision to 0.3 percent even though the instrumentation and techniques should have been sufficient to do much better. Efforts at Ames, the National Bureau of Standards, California State University at San Diego, and at the Lowell Observatory are underway to identify and understand the phenomenon.

(W. Borucki, J. Scargle, and D. Black, Ext. 6492)

Atmospheric Evolution Studies

Photochemical modeling of the primitive (e.g., low-O_2) Earth atmosphere has shown the importance of rainout of soluble trace gases in the past. The previous existence of high CO_2 concentrations in the Earth's primitive atmosphere are predicted on the basis of a variety of geochemical and climatological arguments. Photochemical reactions in such a high-CO_2 atmosphere should have resulted in production of large amounts of formaldehyde (H_2CO) and hydrogen peroxide (H_2O_2). Rainout of H_2CO would have constituted a drain on atmospheric H_2 and may also have been an important source of biological precursor molecules; that is, molecules which can serve as the basic building blocks for life. Rainout of H_2O_2 would have been an effective H_2 source, since the extra oxygen atom it contains (relative to water) would presumably have reacted with dissolved ferrous iron in the early oceans. Rainout of H_2O_2 would have continued to be important as the atmospheric O_2 level rose to its present value. Model calculations indicate that H_2O_2 would have been the dominant oxidant in rain-

water at O_2 levels below one percent of present. This fact must be taken into account when trying to interpret the Precambrian rock record.

(J. Kasting, Ext. 5233)

Cryogenic Grating Spectrometer

NASA's Gerard P. Kuiper Airborne Observatory (KAO), a 91-cm diam telescope mounted in a modified C-141 jet aircraft, permits routine observations of astronomical sources at infrared wavelengths which are inaccessible from ground-based sites. Airborne astronomy has led to the discovery and study of a wide variety of far infrared spectral lines, originating primarily in the interstellar medium, which characterize the composition and condition of the emitting gas. To exploit the potential of the KAO for measuring far infrared lines, a grating spectrometer is being developed as a facility for the observatory. The entire optical system of the spectrometer is cooled with liquid helium to a temperature of -270° C to minimize the thermal background radiation falling on the detectors, thereby maximizing their sensitivity. The first observations with the spectrometer have provided a number of interesting scientific results: new information regarding the photoionization structure around hot stars has been obtained by mapping the Orion nebula in lines of ionized oxygen and nitrogen, suggesting significant corrections to earlier determinations of elemental abundance gradients in the galaxy. A previously undetected line of neon, which should be an important diagnostic of conditions in ionized galactic clouds, was observed in the Omega nebula. Measurements of oxygen lines from the galaxy M82 have provided new estimates of the density and mass of ionized gas in its nucleus. The first detection of a rotational transition of the phosphine (PH_3) molecules in Saturn's atmosphere demonstrate that these bands will be valuable probes of the atmospheric chemistry and conditions on the giant planet. Further development of the spectrometer will emphasize improvements in reliability, sensitivity, and wavelength coverage.

(E. Erickson, Ext. 5508)

Reflecting-Layer Model of Thick Rough Films Developed for SIRTF

A reflecting-layer model of the specular reflectance of rough, thick dielectric films has been developed and successfully applied to far-infrared spectra obtained at Ames a few years ago. Seven different spectra of optical-black coatings were fitted by the model at wavelengths between 12 and 500 μm. The coatings, which are commonly used at visual wavelengths to reduce stray light in optical instruments, were quite different; their reflectance varied by a factor of nearly 10^3 at 100 μm. Fitting the model to these spectra determined important surface parameters, such as the rms surface roughness and slope, and the refractive indices of the coating materials. Because the model indicates which parameters control reflectance in the far-infrared, it will be useful in designing infrared-opaque coatings for the Space Infrared Telescope Facility (SIRTF).

(S. Smith, Ext. 6264)

Planetary Detection Studies

Most astronomers believe it likely that many stars have planetary systems like our solar system. But it is a difficult observational problem to detect such objects, and there is currently no evidence for the existence of any planets outside the solar system.

Researchers in the Space Science Division at NASA Ames are developing two new observational techniques for detecting planets around other stars. One is a method that combines the ancient concept of a transit telescope with modern high-speed electronics and light detectors. The star images are moved past an array of detectors that can time the passages of the images to a high precision which results in accurate measurements of the star positions. This may enable the tiny "wobble" in the star's motion caused by a planet to be detected. Ground-based observations are being obtained as part of a study of possible application to space astrometry.

(J. Scargle, Ext. 6330)

Secondary Mirror Chopper for the Space Infrared Telescope Facility (SIRTF)

Future cryogenically cooled spaceborne telescopes such as SIRTF will enable sensitive observations in the infrared limited only by the natural background from 2 to 200 μm. The secondary mirror in the SIRTF concept must be articulated to compensate for line-of-sight errors due to system jitter and to allow chopping of the signal from 1 to 20 Hz with throws up to 30 arc minutes. To maintain the sensitivity, the power introduced into the secondary mirror to accomplish this articulation must be minimized.

A design has been developed which utilizes a flex pivot and voice coil actuators to drive the secondary mirror. A capacitive sensor which utilizes the back of the mirror as one of the plates is used to sense mirror position. A diode bridge circuit operating at the low temperatures is used to read out the signal.

A brassboard one-dimensional chopper assembly simulating the expected mirror mass and moment of inertia (0.13 Kg, 1.8e-4 Kg-m^2) has been successfully operated at 8 K. The drop in resistance of the copper coils resulted in significantly lower power dissipation at cryogenic temperatures and the cold electronics performed well.

(M. Dix and L. Salerno, Ext. 6525)

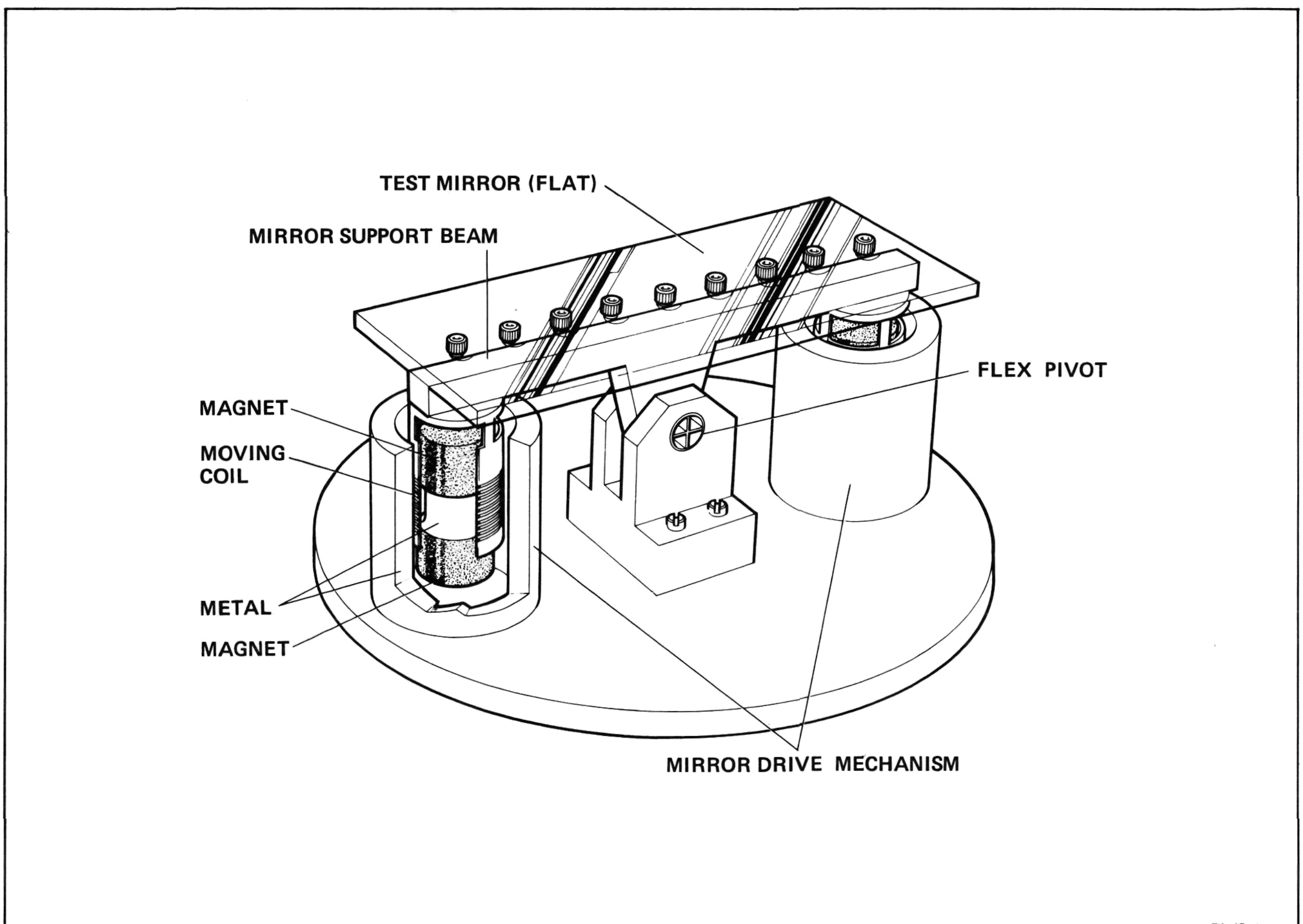

Secondary mirror chopping mechanism (ARC)

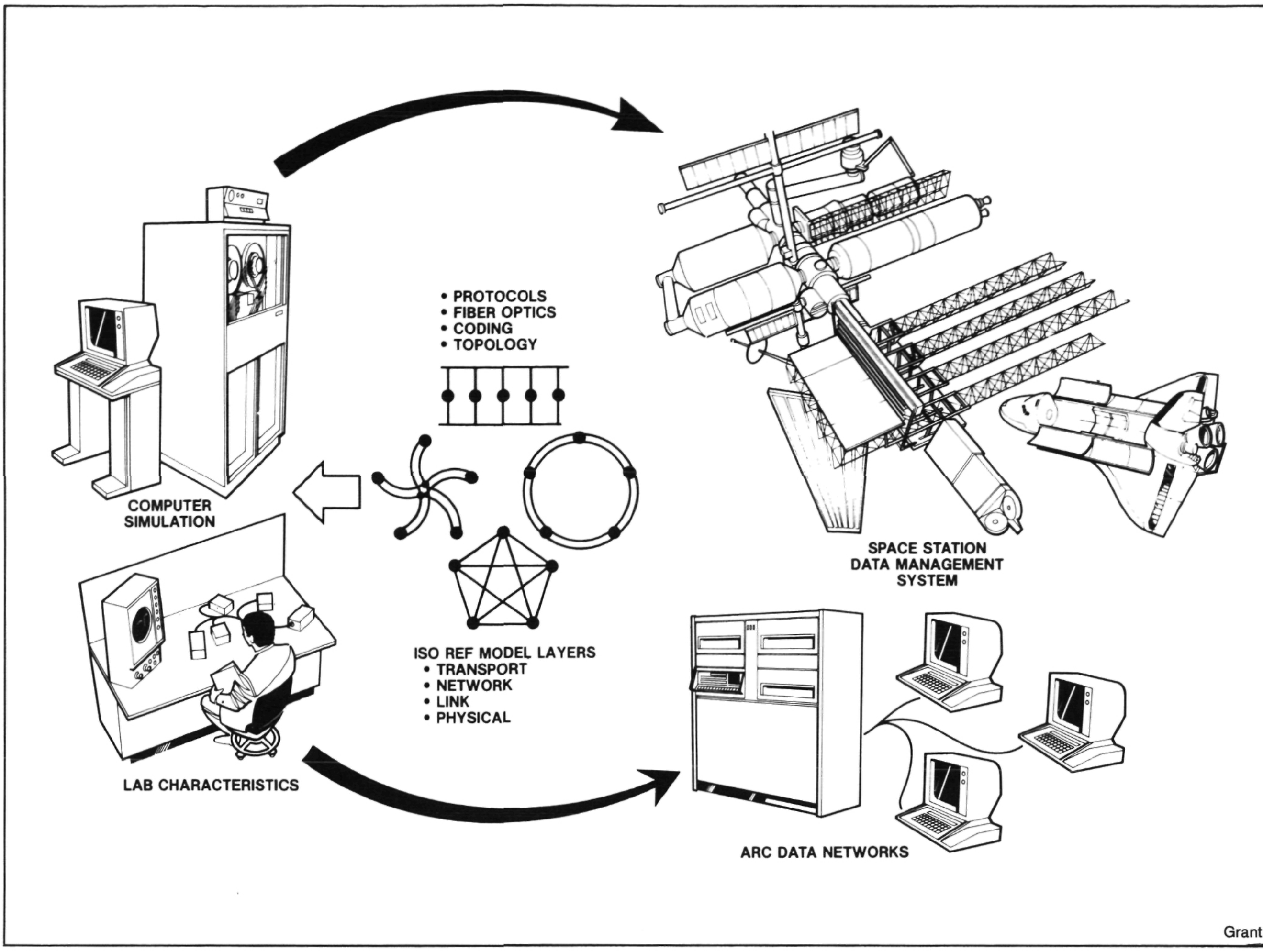

Future data systems concepts network simulation and analysis

Future Data Systems Concepts (Network Simulation and Analysis)

The requirements for an advanced spaceborne data network applicable to the Space Station have been defined through intercenter working group contacts, technology reviews, and the monitoring of the initial reports from the contracted "Space Station Data System Architecture" studies. Software simulation of data networks has advanced with the following major accomplishments:

1. A preliminary intercenter design review of the network simulation functional specifications and top-level design features.
2. The installation of the "Distributed System Simulator" language applicable to high-level network models.
3. The installation of Slam II simulation language and Ingres relational data base for the initial simulation of the low four layers of data networks.
4. The production verification and distribution of a prototype model for Carrier Sense Multiple Access-Collision Avoidance (CSMA-CA) protocol with an optional bus or star topology.
5. The production and initial in-house testing of the first version of the Local Area Network Extensible Simulator (LANES1).

The major analytic reports for data network concepts are:

1. An introductory report by Dr. Mark Herro, University of Notre Dame, on "Coding Considerations for Fiber Optic Data Networks."
2. Dr. Donald DuBois, consultant on "Characterizing Workload Models for Local Area Network Simulators."
3. An introductory report by Dr. Marjory J. Johnson, RIACS, on "Network Control."

(T. Grant, Ext. 6526)

Spatial, Spectral and Radiometric Resolution Affect Classification Accuracy of Satellite Imagery

The Landsat Multispectral Scanner (MSS) has proven to be a useful tool to categorize the land surface into various cover types using multispectral classification techniques, although it suffers from a number of first-generation disadvantages. The second-generation Landsat Thematic Mapper (TM) was designed specifically to categorize land cover types, incorporating 30-meter spatial resolution, higher radiometric resolution, and several spectral bands featuring better placement in the spectrum and including the middle and thermal infrared regions. An experiment was designed to determine how well TM categories land cover types in comparison to MSS, and how the various TM improvements contribute to any differences in capability.

The factorial experiment used Airborne Thematic Mapper data to simulate the spatial, spectral, and radiometric characteristics of both TM and MSS. Eight data sets represented all possible combinations of the three factors. Multispectral classification techniques converted each data set into land cover categories. The classification accuracy of each data set at a detailed level of information was used to test the effects of each factor by averaging out the effects of the other factors.

The results showed that the improved spectral and radiometric characteristics of TM aided classification accuracy, but that TM's improved spatial resolution actually decreased the classification accuracy and that it had the largest effect. The net effect of all the TM characteristics combined was a small increase in classification accuracy. The decrease due to spatial resolution was interpreted to mean that the greater spectral heterogeneity of high spatial-resolution data created problems with the multispectral classification techniques currently in use. Improved algorithms need to be developed to take advantage of the spatial content of TM data. Texture, per-field classifiers, and contextual classifiers have been suggested as candidate approaches.

(R. Wrigley, Ext. 6060)

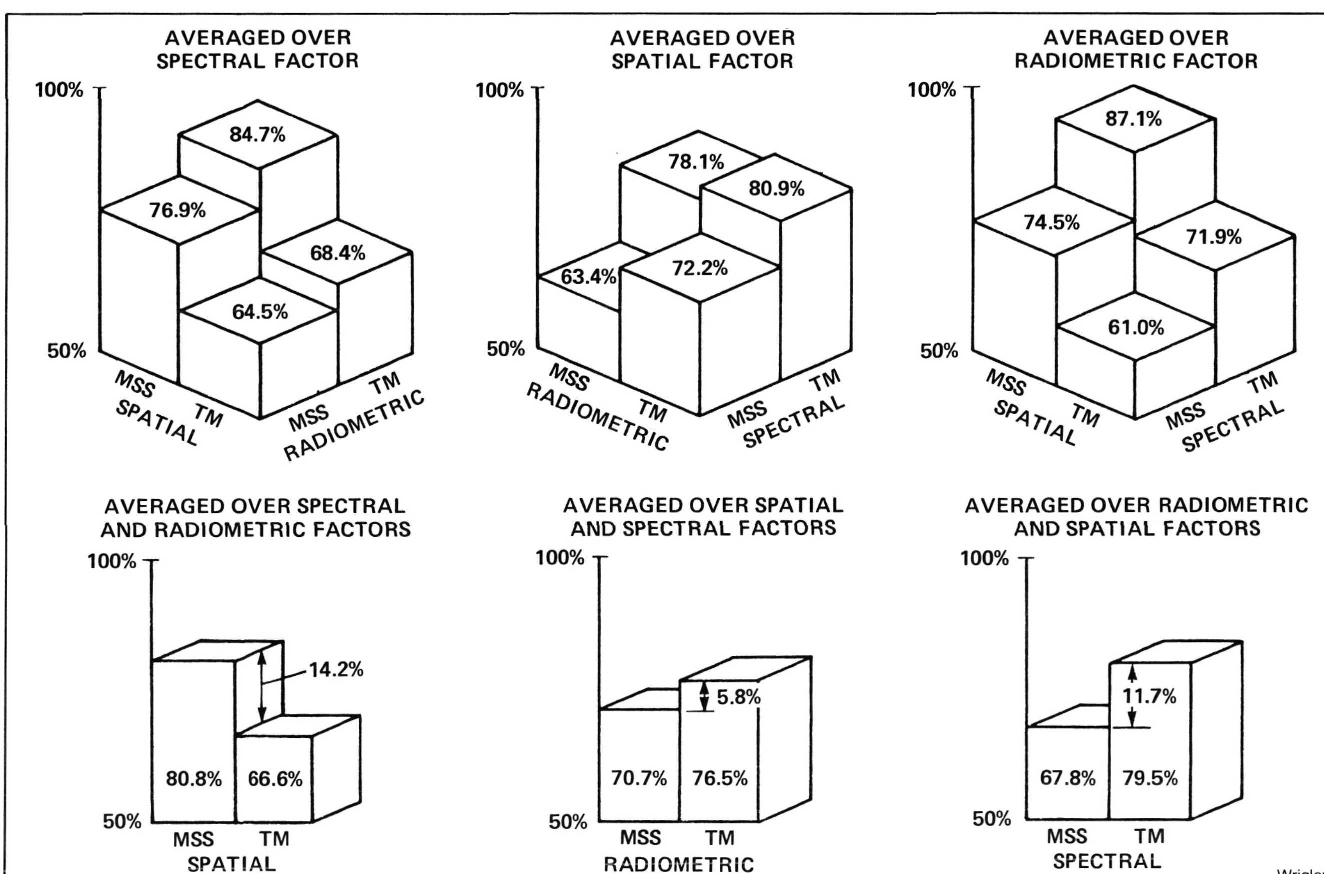

Level II/III overall classification accuracies averaged over one and two factors

1. Report No. NASA TM-86662	2. Government Accession No.	3. Recipient's Catalog No.
4. Title and Subtitle RESEARCH AND TECHNOLOGY ANNUAL REPORT-1984		5. Report Date March 1985
		6. Performing Organization Code
7. Author(s)		8. Performing Organization Report No. 85045
		10. Work Unit No. G-1000
9. Performing Organization Name and Address NASA Ames Research Center Moffett Field, CA 94035		11. Contract or Grant No.
		13. Type of Report and Period Covered Technical Memorandum
12. Sponsoring Agency Name and Address National Aeronautics and Space Administration Washington, D.C. 20545		14. Sponsoring Agency Code

15. Supplementary Notes

Point of contact: Dr. J. N. Nielsen, Chief Scientist, Ames Research Center MS 200-1A, Moffett Field, CA 94035 (415)694-5500 or FTS 464-5500.

16. Abstract

This report describes various research and technology activities at Ames Moffett and Ames Dryden. Highlights of these accomplishments indicate the Center's varied and highly productive research efforts for 1984.

17. Key Words (Suggested by Author(s))	18. Distribution Statement
Space science Life science Space and terrestrial applications Aeronautics Space technology	Unlimited Subject category: 99

19. Security Classif. (of this report)	20. Security Classif. (of this page)	21. No. of Pages	22. Price*
Unclassified	Unclassified	91	A05

*For sale by the National Technical Information Service, Springfield, Virginia 22161

1/21/86 Glen Peters 341/2705E/37051

Ql

18 FEB 86

NASA

National Aeronautics and
Space Administration

Washington, D.C
20546

Postage and Fees Paid
National Aeronautics and
Space Administration
NASA-451

Official Business
Penalty for Private Use $300

U.S.MAIL ®

Mr. Hershel Sams
Vice President-Engineering Technologies
McDonnell-Douglas Corporation
Dept. 330, Bldg. 33, Rm 463
P.O. Box 516
St. Louis, MO 63166

NHQ FORM 150A NOV 81